DESIGN, SIMULATION ,CONSTRUCTION AND TESTING OF A THERMOSYPHON SOLAR WATER HEATER FOR A BLOCK IN POSTGRADUATE HOSTEL IN AHMADU BELLO UNIVERSITY, ZARIA

M.Sc. (INTERNAL DEFENCE SEMINAR)

PRESENTED BY:

SAYYADI SANDA

MSc/ENG/14006/11-12

MECHANICAL ENGINEERING DEPARTMENT

AHMADU BELLO UNIVERSITY ZARIA

NIGERIA

MARCH, 2016

DESIGN, SIMULATION CONSTRUCTION AND TESTING OF A THERMOSYPHON SOLAR WATER HEATER FOR A BLOCK IN POSTGRADUATE HOSTEL IN AHMADU BELLO UNIVERSITY, ZARIA

BY

Sayyadi SANDA, B.eng(abu) 2010

M.Sc/ENG/14006/2011-2012

A DISSERTATION SUBMITTED TO THE SCHOOL OF POSTGRADUATE STUDIES, AHMADU BELLO UNIVERSITY IN PARTIAL FULFILLMENT FOR THE AWARD OF A MASTER DEGREE IN MECHANICAL ENGINEERING

DEPARTMENT OF MECHANICAL ENGINEERING

FACULTY OF ENGINEERING

AHMADU BELLO UNIVERSITY, ZARIA, NIGERIA

MAY, 2016

DECLARATION

I declare that the work in this dissertation entitled **Design, Construction, Testing and Simulation of a Thermosyphon Solar Water Heater for a block in postgraduate Hostel** has been carried out by me in the Department of Mechanical Engineering. The information derived from the literature has been duly acknowledged in the text and a list of references provided. No part of this thesis was previously presented for another degree or diploma at this or any other Institution.

Sayyadi SANDA	_____	_____
Name of student	Signature	Date

CERTIFICATION

This dissertation entitled **DESIGN, CONSTRUCTION, TESTING AND SIMULATION OF A THERMOSYPHON SOLAR WATER HEATER FOR A BLOCK IN POSTGRADUATE HOSTEL** by Sayyadi SANDA meets the regulations governing the award of the degree of (Masters of Engineering Mechanical Engineering) of the Ahmadu Bello University Zaria and is approved for its contribution of knowledge and literary presentation.

Dr. F.O. ANAFI (Signature) ----------

Chairman Supervisory Committee Date ----------

Dr. G.Y. PAM (Signature) ----------

Member Supervisory Committee Date ----------

Dr. M. Dauda (Signature) ----------

Head of Department Date ----------

Prof. Kabir Bala (Signature) ----------

Deen, School of Postgraduate Studies Date ----------

DEDICATION

This dissertation is dedicated to God Almighty for giving me the power to carry out this research despite the seemingly insurmountable challenges faced in the course of the research and also to my late father (Umar Sanda Isah) for all his encouragement and his believe in my ability,

ACKNOWLEDGEMENT

I must appreciate my supervisors Engr. Dr. F.O. Anafi and Engr. Dr. G.Y. Pam, for patiently guiding and encouraging me to ensure that this research is successfully carried out.

I am also indebted to the entire staff of the Department of Mechanical Engineering Ahmadu Bello University, Zaria for the training and moral support given to me during my course work and this research.

ABSTRACT

All nations of the world depend on fossil fuels for their energy needs. However the obligation to reduce Carbon dioxide and other gaseous emissions is the reason behind which countries turn to non-polluting renewable energy sources. Hot water heated by the sun is used in many ways, in residential settings to provide domestic hot water, also has industrial applications, e.g. to generate electricity. Designs suitable for hot climates can be much simpler and cheaper, and can be considered an appropriate technology for these places. Hot water use represents a large proportion of energy needs in hostels. This energy need accounts for a large portion of the total annual energy consumption in hostels and therefore a reasonable amount of the university income is spent on electricity bills used for heating water for bathing in hostels. A solar water heater was designed, simulated, fabricated and tested. The design, simulation, fabrication and performance tests of a thermosyphon solar water heater were carried out successfully for a block in Postgraduate hostel of Ahmadu Bello University Zaria. the fabrication was carried out using locally available materials. The solar water heater has the ability to heat 200 liters of water from a temperature of 25^{o}C to a temperature of 50^{0}C,. The design was purposely for students to use the water for bathing in order to totally discourage the use of electric heating devices in the hostel which on several occasions has been the reason of fire outbreaks in the hostel. The system factors such as costs and sizing were taken into consideration which assisted in the choice of materials and the design. The average solar radiation data was obtained from typical meteorological year (TMY) of Zaria which was used to determined the month with the least solar radiation. From the analysis of the typical meteorological year (TMY) data of Zaria the month of August has the least energy ratio which point it out as the month with the least solar radiation and it was used as the design month.The optimization of the system components was also carried out using MATLAB to determine the optimum system size. After the fabrication of the system the performance was evaluated by comparing the simulation results obtained from the model (solar data processor, Type 109 of TRNSYS) and the results obtained from the experiment using Microsoft Excel and standard deviation, Nash-Sutcliff coefficient statistical tools were used to validate the predictive power of the model. From the result obtained from the research it can be concluded that the thermosyphon solar water heater of collector area of 2.6m^2 has the ability to heat 200 litre of water to a temperature of 50^{0}C in the month that has the least solar radiation in Ahmadu Bello University Samaru, Zaria.The statistical tools used for the validation of the simulation model confirm that the model is valid and can be used in the estimation of the actual characteristics of a real system. The relative error is very minimal for all the measured parameters and Nash-Sutcliff coefficient shows that the degree of fitting is very high which shows that the simulation model has high accuracy, also the standard deviation shows that the deviation of the experimental parameters from the simulated is very low and therefore it is negligible.The results show little deviation of predicted values from actual values with a good level of fit, thereby validating the model used for simulating the solar water heating system.

TABLE OF CONTENTS

DECLARATION iii
CERTIFICATION iv
DEDICATION v
ACKNOWLEDGEMENT vi
ABSTRACT vii
LIST OF FIGURES xi
LIST OF TABLES xii
LIST OF APPENDICES xiii
NOMENCLATURE xiv
CHAPTER ONE 1
INTRODUCTION 1
1.1 Background to the Study 1
1.2 Statement of the Problem 2
1.3 The Present Work 3
1.4 Aim and Objectives of the Work 4
1.5 Significance of the Research 4
CHAPTER TWO 6
LITERATURE REVIEW 6
2.2 Passive and Active Solar Water Heater 6
2.2.1 Passive solar water heater 6
2.2.2 Active solar water heater 8
2.3 Components of a Solar Water Heater 10
2.3.1 Hot water storage tanks 10
2.3.2 Solar collector 11
2.3.2.1 Types of solar collectors used for domestic water heating 12
2.3.2.2 Solar collector orientation 16
2.3.3 Absorber plate 18
2.3.4 Transparent cover 19
2.3.5 Collector casing 19
2.3.6 Insulation 19
2.4 Application of Solar Heated Water 20
2.5 Selecting and Sizing a Solar Heating System 20
2.6 Siting Your Solar Water Heating System 22

2.7 Review of Past Research Work 22
2.8 Theoretical Background 28
2.8.1 Thermal radiation 28
2.8.2 Optical Analysis 28
2.8.3 Estimation of Absorptance of Absorber Plate 33
CHAPTER THREE 36
MATERIAL AND METHOD 36
3.1 Solar Water Heater Description and Operation 36
3.2 Working Principle of the Solar Water Heater 37
3.3 Solar Resources and Weather Data 37
3.4 Material Selection 37
3.5 Design Analysis 39
3.5.1.1 Total Radiation on Tilted Surfaces 39
3.5.1.2 Absorbed Solar Radiation 41
3.5.1. 3 Extraterrestrial solar radiation 41
3.5.1.4 Terrestrial irradiation 42
3.5.1. 5 Declination (δ) 43
3.5.1.8 Collector energy losses 44
3.5.1.12 Collector useful energy 47
3.5.1.13 Heat Removal Factor 48
3.5.2 Determination of the Design Month 50
3.5.3 Optimum Geometrical Parameters 51
3.5.3.2 *Optimum tube to tube distance and collector tube diameter* 52
3.5.3.3 Orientation angle of tilt 52
3.5.3.4 Absorber plate thickness 53
3.5.3.5 Number of glass cover 53
3.5.3.6 Collector absorber plate distance from the glazing material 53
3.5.3.7 Shading 54
3.6 Design Consideration 54
3.7 Design Assumptions 55
3.8.1 Determination of total solar radiation absorbed by the collector 55
3.8.2 Design calculation of heat loss in the collector 57
3.8.3 Heat transfer through the storage tank component 58
3.8.3 Heat transfer through the storage tank component 59

3.9 Simulation and Validation of the Solar Water Heater..... 59
3.10 Fabrication, Costing and Testing. 64
3.10.1 Fabrication..... 65
3.10.2 Cost of Solar Water Heater..... 67
3.10.3 Testing of solar water heater..... 69
CHAPTER FOUR 72
4.0 RESULTS AND DISCUSSION 72
4.1 Meteorological and Simulated Solar Data for Zaria and Solar Water Heater Design Parameter 72
4.2 Collector Tilt Angle ($\boldsymbol{\beta}$) 76
4.3 Collector Tube Diameter and Centre to Centre Distance. 77
4.4 Collector Absorber Plate Thickness 78
4.5 Collector Number of Glazing 79
4.6 System Optimum Parameters and Simulation 80
4.8 Comparison of experimental results with result obtain from simulation and determining the Authenticity of the simulation software (TRNSYS 16)..... 84
4.8.1 Comparison and Validation of simulated ambient temperature with experimental ambient temperature 84
4.8.2 Comparism and Validation of simulated Solar Radiation with experimental Solar Radiation 87
4.8.3 Comparism and Validation of simulated Collector outlet Temperature with experimental Collector outlet Temperature. 91
4.8.4 Comparison and Validation of simulated Collector Inlet Temperatures with experimental Collector Inlet Temperatures..... 94
CHAPTER FIVE..... 99
5.0 SUMMARY, CONCLUSION AND RECOMMENDATIONS..... 99
5.1 Summary 99
5.2 Conclusion..... 100
5.3 Recommendations..... 101
REFERENCES..... 102
20,2012 from http//:www.redscreen.net 103
APPENDIX B 109

LIST OF FIGURES

Figure. 2.1: passive solar water heater system - - - - - - 7

Figure. 2.2: Active solar water heater system - - - - - - 8

Figure. 2.3 Integrated Collector storage- - - - - - - -12

Figure. 2.4 Cross section of plat plate solar collector- - - - - -14

Figure. 2.5 Cross section of evacuated tube collector - - - - -15

Figure. 2.6 Collector tilts at an angle equal to the latitude - - - - -17

Figure. 2.7 Refractive index - - - - - - - - -30

Figure. 3.1 Front view of the proposed thermosyphon water heating system. - -36

Figure. 3.2. Beam radiation on horizontal and tilted surfaces - - - -39

Figure. 3.3. Schematic model of simulation studio - - - - - -60

Figure. 3.4: Information flow diagram for the simulation of the solar water - -

Figure. 3.5. Experimental setup of the solar water heater - - - - -69

Figure. 4.1 The variation of collectors tilt angle on the absorption - - - -77

Figure.4.2. The variation of the center to center distance - - - - -78

Figure. 4.3.The variation of the Absorber Plate Thickness of the collector - - -79

Figure. 4.4. The effect of varying the number of glazing with the system efficiency. -80

Figure. 4.5a. Annual variation of hourly Solar Radiation on a tilted surface - -81

Figure 4.5b: Comparison of solar collector efficiency. - - - - -84

Figure 4.6: Comparison of hourly Ambient Temperature (28 August 2015) - -85

Figure 4.7: Comparison of hourly Ambient Temperature (29 August, 2015) - -86

Figure 4.8: Comparison of hourly Ambient Temperature (30 August, 2015) - -86

Figure 4.9: Comparison of hourly solar radiation (28 August, 2015) - - -89

Figure 4.10: Comparison of hourly solar radiation. (29 August, 2015) - - -89

Figure 4.11: Comparison of hourly solar radiation. (30 August, 2015.) - - -90

Figure 4.12: Comparison of hourly Collector outlet Temperature (28 August, 2015) -92

Figure 4.13: Comparison of hourly Collector inlet Temperatures (29 August, 2015) -93

Figure 4.14: Comparison of hourly Collector outlet Temperature (30 August, 2015) -94

Figure 4.15: Comparison of hourly Collector inlet Temperatures (28 August, 2015). -96

Figure 4.16: Comparison of hourly Collector inlet Temperatures (29 August, 2015) -97

Figure 4.17: Comparison of hourly Collector intlet Temperature (30 August, 2015)- -97

LIST OF TABLES

Table 2.1: Domestic water usage data - - - - - - -21

Table 2.2: Dimensioning of domestic hot water solar systems - - - -21

Table 3.1: Materials Selected and their properties - - - - - -38

Table 3.2 Recommended average days for the month and values of n by month. - -43

Table 3.3 Monthly average absorbed solar radiation - - - - - -56

Table 3.4: Heat loss in the collector - - - - - - - -57

Table 3.5: Heat transfer through the storage Tank - - - - - - -59

Table 3.6: Parameters for the Collector - - - - - - -62

Table 3.7: Connection of the weather data with input of collector - - - -63

Table 3.8: Connections of the output of collector with the plotter. - - - -64

Table 3.9: Details of costs of material used in fabricating the solar water heater - -67

Table 4.1 Zaria Meteorological data - - - - - - -72

Table 4.2 Simulated Solar Data for Zaria - - - - - - -73

Table 4.3 Monthly average daily system design for determination of design month - 74

Table 4.4 Monthly average daily system design for Determination of Collector Area - 75

Table 4.5 System design parameters - - - - - - - - 76

Table 4.6: System characteristics - - - - - - - -81

Table 4.7: System final optimum design parameters and components size. - -82

Table 4.8: Validation of simulated Ambient Temperature 28 of August 2015 - - -86

Table 4. 9: Validation of simulated Solar Radiation of 28 August 2015. - - -90

Table 4.10: Validation of simulated Collector outlet Temperature of 28 August 2015- -93

Table 4.11: Validation of simulated Collector inlet temperature on 29 August 2015. - -97

LIST OF APPENDICES

Appendix A: Calculation Of Radiation On Tilted Surface Design Programme Codes Developed Using Matlab- - - - - -105

Appendix B: Solar Water Heater Collector Design Programme Codes Developed Using Matlab - - - - - - -109

Appendix C: Removal Fraction Design Programme Codes Develop Using Matlab - - - - - - - -110

Appendix D: Calculation Daily Tank Lost Coefficient Design Programme Codes Developed Using Matlab - - - - -112

Appendix E: Tilt Angle Optimisation Design Programme Codes Developed Using Matlab - - - - - - - -113

Appendix F: Optimisation Of Collector Tube Diameter And Tube Centre To Centre Distance. - - - - - -114

Appendix G: Optimisation Of Absorber Plate Thickness Design Programme Codes - - - - - - -115

Appendix H: Optimisation Of Number Of Glass Covers Design Programme Codes Developed Using Matlab - - - - -116

:

Appendix I : Optimisation Of Number Of Glass Covers Design Programme Codes Developed Using Matlab - - - - -118

:

Appendix J: Photographs Of Construction And The Assembly Of The System Components - - - - - -119

Appendix K: The Assembly And Working Drawings Of Solar Water Heater - - - - - - - -126

NOMENCLATURE

Ac	Collector area (m^2)
A_i	Anisotropic index
A_e	Edge insulation area (m^2)
A_{st}	Tank surface area (m^2)
b_o	Incidence angle modifier constant
C_b	Contact resistance (KJ/hr.m.K).
C_p	Fluid specific heat (KJ/kgK)
d_o	Outer diameter of collector outlet pipe (m)
d_R	Riser diameter (m)
d_i	Diameter of collector inlet pipe (m)
d_o	Diameter of collector outlet piping (m)
Di	Inner tube diameter (m)
D	Outer tube diameter (m)
f	Square root of ratio of beam to total radiation
F_R	Heat removal factor
F'	Collector efficiency factor
F	Standard fin efficiency for straight fins with rectangular profile
F''	Collector flow factor
F	Solar fraction over a specified time horizon
H_d	Header diameter (m)
H_L	Header length (m)
h_c	Horizontal distance between collector outlet and inlet (m)
h_o	Horizontal distance between outlet of tank and inlet of collector (m)
H_t	Tank height (if vertical) or diameter (if horizontal) (m)

H_R Height of collector return to tank above bottom of tank (m)

$\bar{H}$ Monthly average daily radiation on a horizontal surface (kJ/hr.m^2)

$\bar{H}_0$ Monthly average extraterrestrial daily radiation on a horizontal surface

$\bar{H}_T$ Monthly average total radiation on tilted surface (kJ/hr.m^2)

H_b Total beam radiation on horizontal surface (kJ/hr.m^2)

H_d Total diffuse radiation on horizontal surface (kJ/hr.m^2)

h_{fi} Internal fluid heat transfer coefficient (KJ/hr.m^2.K).

h_w Wind heat transfer coefficient (KJ/hr.m^2.K).

KL Product of extinction coefficient and the thickness of each cover plate

k_f Thermal conductivity of fluid in the tank (kJ/h m ^{o}C)

k_{ins} Thermal conductivity of insulation material (kJ/hr m ^{o}K)

$\bar{K}_T$ Monthly average clearness index,

k Plate conductivity (kJ/hr m ^{o}K)

K_{ei} Thermal conductivity of edge insulation materials (kJ/hr m ^{o}K)

L Length of each pipe (m)

L_i Length of collector inlet pipe form the storage tank (m)

L_o Length of collector outlet pipe to the tank inlet (m

NB_1 Number of right angle bends (or equivalent) in inlet pipe 2

NB_2 Number of right angle bends (or equivalent) in collector outlet piping

N_g Number of glass covers

N_R Number of parallel collector risers

N_x Number of collector nodes for thermal head calculations

$\dot{m}$ Collector fluid mass flow rate (kg/hr.m^2)

$\dot{m}_L$ Desired load mass flow rate, kg/s

$\dot{m}$ Mass flow rate of fluid in the collector (kg/s)

N Number of turns

N_g Number of glass covers

Q_u Useful energy gain per unit time (kJ/hr m^2)

Q_L Quantity of heat required to meet load (kJ/hr)

Q_{aux} Auxiliary energy requirement to meet the desired load (kJ/hr)

Q_{Ls} Load met by solar energy (kJ/hr)

R_b Monthly average ratio of beam radiation on a tilted to horizontal surface

R Index of refraction of cover material

Re Reynolds number

T_{pm} Mean plate temperature (K)

T_{ci} Collector fluid inlet temperature (K)

Ta Ambient temperatures (K)

T_{co} Collector fluid outlet temperature (K)

T_L Desired load (hot water) temperature, ^oC

t_{ins} Thickness of insulation material (m)

T_{ci} Fluid inlet temperature (^oc)

T_{st} Storage temperature (^oc)

T_{fm} Collector means fluid temperature (k)

T_{ci} Collector inlet fluid temperature (^oc)

T_{sti} Storage tank inlet temperature (^oc)

t_p Plate thickness (m)

U_e Loss coefficient edge of collector per unit aperture area (kJ/hr-m^2-K)

U_o Loss coefficient of collector outlet pipe plus insulation (kJ/hr m^2 ^oK)

V_t Tank volume (m^3)

U_L Overall collector Loss Coefficient (kJ/ m^2hr.k)

U_t Collector top loss coefficient (KJ/hr.m^2.K).

U_b Back loss coefficient (KJ/hr.m^2.K).

U_{st} Tank loss coefficient (KJ/hr.m^2.K).

W Tube spacing (m)

x_{ei} Insulation thickness at the edge (m)

ε_p Absorber plate emittance

α_p Absorptance of absorber plate

β Collector slope (degrees)

ρ_{fs} Fluid density at standard conditions (kg/m^3)

θ_T Incident angle of beam radiation on tilted surface (degrees)

θ_z Zennit angle (degrees)

δ Declination (Degrees)

$\emptyset$ Latitude of the location (Degrees)

ω Solar angle hour (Degrees).

$\bar{\theta}_b$ Monthly average (equivalent) beam incident angle (degrees)

ω_s Sunset hour angle (Degrees).

$\overline{\tau\alpha}$ Monthly average daily transmittance-absorptance product

ρ_d Reflectance of the cover system for diffuse radiation

$(\tau\alpha)_b$ Transmittance-absorptance product of beam radiation

$(\tau\alpha)_d$ Transmittance-absorptance product of diffuse radiation

$(\tau\alpha)_g$ Transmittance-absorptance product of ground reflected radiation

ρ_g Diffuse reflectance of the ground

δ_t Absorber plate thickness (m)

ε_g Emittance of glass (0.88)

ε_P Emittance of plate

μ	Dynamic viscosity, (kg/m s)
ρ	Density of water (kg/m^3)
υ	Kinematic viscosity (m^2/s)
β'	Thermal cubic expansion coefficient
η_C	Collector efficiency over a specified time horizon

CHAPTER ONE

INTRODUCTION

1.1 Background to the Study

The sun has produced energy for thousands of years. Solar energy is the sun's rays (solar radiation) that reach the earth. This energy can be converted into other forms of energy, such as heat and electricity. Radiant energy from the sun has powered life on earth for thousands of years. In the 1830s, the British astronomer, John Herschel, famously used a solar thermal collector box (a device that absorbs sunlight to generate heat) to cook food during an expedition to Africa (Soteris, 2004).

Solar energy is the most capable of the renewable energy sources. Despite this hopeful evaluation of the potential of solar energy, considerable technical and economic problems must be solved before utilisation of solar energy can occur (Ahmad, 2010). The solar power development will depend on how a number of serious constraints are dealt with, including scientific and technological problems, marketing, financial limitations and political challenges. In addition, the education of engineers will have to change its focus from non-renewable fossil-fuel technology to renewable power sources. There has been a general agreement that the most significant of the renewable energy sources is solar radiation (Ahmad, 2010).

When a dark surface is placed in sunshine, it absorbs solar energy and heats up. A solar energy collector working with sun facing surfaces will transfer energy to the water that flows through it. To reduce heat loss to the atmosphere and to improve its efficiency, one or two sheets of glass are usually placed over the absorber surface. This type of thermal collector suffers from heat losses due to radiation and convection. Such losses increase rapidly as the temperature of the working fluid increases. Improvement such as the use of

selective surfaces, evacuation of the collector to reduce heat losses, and the special glass is used to increase the efficiency of the collector.

Solar water heating (SWH) is a proven and famous renewable energy technology and has been used in many countries of the world. The SWH system consists of mainly three parts, namely a solar collector, a storage tank and a circulating pump. A solar water heating system has been the famous application that uses solar radiation as an energy source that uses thermal conversion.

Hot water heated by the sun is used in many ways, in residential settings to provide domestic hot water, also has industrial applications, e.g. to generate electricity. Designs suitable for hot climates can be much simpler and cheaper, and can be considered an appropriate technology for these places. The global solar thermal market is dominated by China, Europe, Japan and India (Dobson, 2008). Water heating accounts for a substantial portion of energy use in many residential, commercial, institutional and federal facilities. Worldwide, approximately 18% of energy use in residential buildings and 4% in commercial buildings are for water heating. Solar water heating systems, which use the sun's energy rather than electricity or gas to heat water, can efficiently serve up to 80% of hot water needs—with no fuel cost or pollution and with minimal operation and maintenance (O&M) expense. (Walker, 2012).

1.2 Statement of the Problem

It is now widely accepted that human activities have contributed to a noticeable average global warming in the twentieth century. However, there are differential impacts of this global trend on regional climate, agriculture, storm damage, and other effects in different parts of the world. This complicates both the assessment of global effects of atmospheric emissions and international negotiations over requisite changes in fossil fuel use.

Burning fossil fuels for the generation of energy, especially coal is a dirty process. Incomplete combustion of coal and oil produces particulate matter. Heavier particulates produce an annoying dirty grit, and lighter particulates can be inhaled deeply and become a health hazard. In addition, impurities such as sulphur also burn and produce potentially dangerous oxides. Since the air is made about 80% nitrogen, nitrogen is combusted along with the fuel at high temperatures, releasing nitrogen oxides (Christopher, 2010). Since fossil fuels are composed mainly of carbon by weight. All fossil fuels produce carbon dioxide when burned. In the atmosphere, the sulphur and nitrogen oxides produce sulphuric acid and nitric acid, respectively, which can lead to acid rain. The carbon dioxide helps trap heat in the atmosphere contributing to the warming of the earth's atmosphere.

Hot water use represents a large proportion of energy needs in hostels. This energy need accounts for a large portion of the total annual energy consumption in hostels and therefore a reasonable amount of the university income is spent on electricity bills used for heating water for bathing in hostels. Also students are involved in all kinds of illegal electrical connections of electrical boiling rings, which had resulted in many fire outbreaks in the hostels all in the quest of warming bathing water.

1.3 The Present Work

This research involves design, simulation, construction and performance tests of a solar domestic hot water heating thermosyphon system for Ahmadu Bello University Samaru, Zaria, Nigeria, located on latitude 11.2^{o} N and longitude 7.8^{o}N to generate 200liter hot water at 50^{0}C using passive single glazed solar water heater for a block of postgraduate hostel in Ahmadu Bello University Zaria, When the preliminary viability was established, system performance was evaluated and generate more precise engineering data, optimal system parameter. The system was simulated using hourly simulation software, for this

task ***Transient system simulation (Trnsys) software*** was used. The system was constructed based on the final optimal result of the system parameters obtained from the optimisation result and the system performance test was carried out based on standard test procedure of ISO 9806-3:1995 (ISO, 1995b) to validate the simulation results.

1.4 Aim and Objectives of the Work

The aim of the study is to design, construct, test and simulate a solar water heater for the postgraduate hostel in Ahmadu Bello University, Zaria.

The specific objectives of the study are:

i. to determine the optimal system size, through a design analysis
ii. to construct the solar water heater
iii. to test and simulate the performance of the system.
iv. to estimate the cost of the solar water heating system.

1.5 Significance of the Research

i. Installation of solar water heater in the hostels is economically very paramount because it will reduce the cost of electricity and maintenance charges on the university income.

ii. The use of solar water heating systems in the hostel will dramatically lead to decrease in frequent fire outbreaks in the hostels and illegal electrical connections.

iii. Solar water heater use renewable energy, as it is renewable, it will never run out.

iv. Solar water heater produces little or no waste products such as carbon dioxide or other chemical pollutants, so has minimal negative impact on the environment.

v. Solar heater systems can easily operate 20 years or more without needing any serious maintenance. Very little service or maintenance is required for the life of the system.

vi. Simple and Easy Installation. Once installed, the system is fully automated.

vii. High return on investment, compared to all other alternative energy options, solar energy is the most economical renewable energy (Ahmed 2010).

CHAPTER TWO

LITERATURE REVIEW

2.1 Preamble

Solar water heaters also called solar domestic hot water systems can be a cost-effective way to generate hot water for domestic use. They can be used in any climate, and the fuel they use, sunshine, is free (Gulland, 2012).

2.2 Passive and Active Solar Water Heater

Residential solar thermal installations fall into two groups: passive (sometimes called "compact") and active (sometimes called "pumped") systems. Both typically include an auxiliary energy source (electric heating element or connection to a gas or fuel oil central heating system) which is activated when the water in the tank falls below a minimum temperature setting such as 55 °C. Hence, hot water is always available. Solar water heating systems include storage tanks and solar collectors (Walker, 2012).

2.2.1 Passive solar water heater

Systems rely on heat-driven convection or heat pipes to circulate water or heating fluid in the system as shown in figure 2.1. Passive solar water heating systems cost less and have extremely low or no maintenance, but the efficiency of a passive system is significantly lower than that of an active system, and overheating and freezing are major concerns.

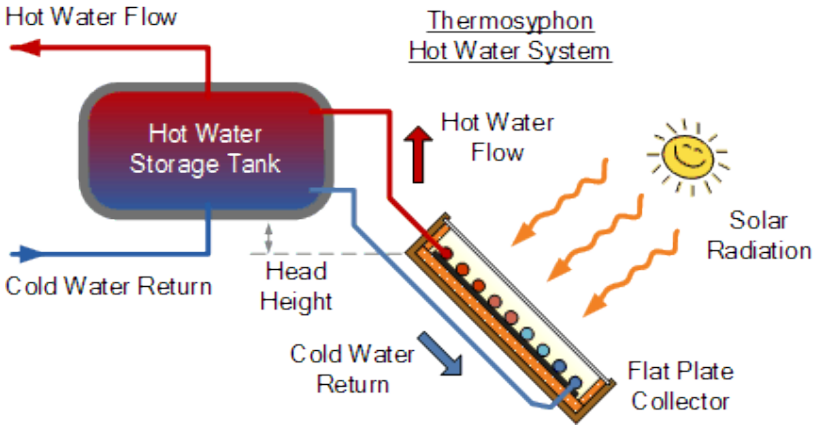


Figure. 2.1: Passive solar water heater system (Alternative energy tutorials, 2012)

However, passive systems can be more reliable and may last longer. There are two basic types of passive systems (Walker, 2012).

i. **Integral collector-storage passive solar water heater**

It's simple; it is an insulated box with a black-painted tank inside and a glass cover that faces the sun. The use of Integrated Collector storage systems in mild climates transcends more than a century of fairly wide popularity (Norton, 2013). In places where freezing temperatures are common Integrated Collector storage units can be used seasonally, and bypassed and drained when winter weather comes. These work best in areas where temperatures rarely fall below freezing. They also work well in households with significant daytime and evening hot-water needs.

ii. **Thermosyphon solar water heater**

Water flows through the system when warm water rises as cooler water sinks. The collector must be installed below the storage tank so that warm water will rise into the tank. These systems are reliable. They are usually more expensive than integral collector-storage passive systems.

2.2.2 Active solar water heater

Systems use one or more pumps to circulate water and/or heating fluid in the system, as shown in figure 2.2

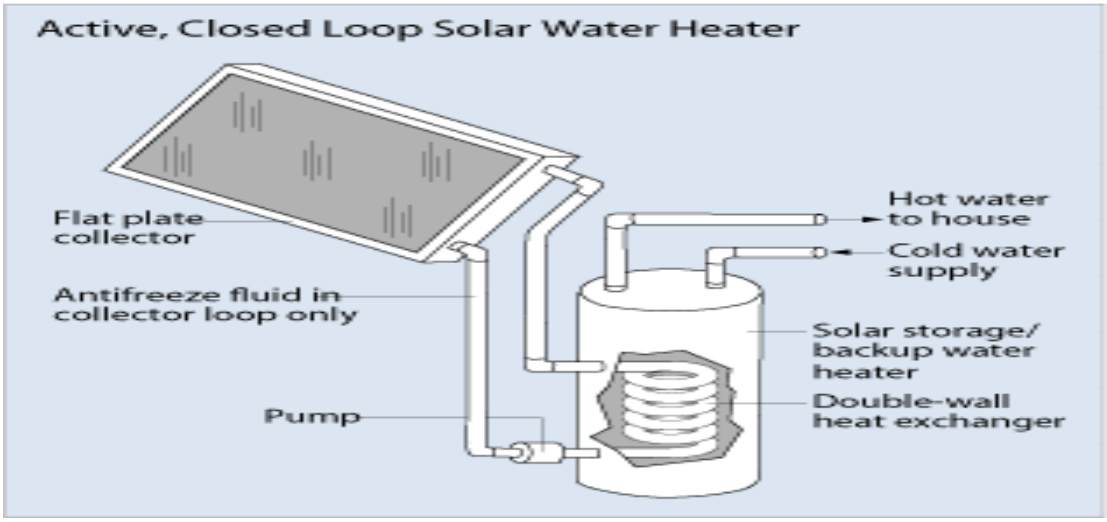


Figure. 2.2: Active solar water heater system (Alternative energy tutorials, 2012)

Though slightly more expensive, active systems offer several advantages (Walker, 2012):

i. The storage tank can be situated lower than the collectors, allowing increased freedom in system design and allowing pre-existing storage tanks to be used.
ii. The storage tank can always be hidden from view.
iii. The storage tank can be placed in conditioned or semi-conditioned space, reducing heat loss.
iv. Drain back tanks can be used.
v. Superior efficiency.
vi. Increased control over the system.

Controls for solar heating systems are usually more complex than those of a conventional heating system, because they have to analyse more signals and control more devices

(including the conventional back-up heating system). Solar controls use sensors, switches, and/or motors to operate the system. The system uses other controls to prevent freezing or extremely high temperatures in the collectors. The heart of the control system is a differential thermostat, which measures the difference in temperature between the collectors and storage unit. When the collectors are 10° to 20°F (5.6° to 11°C) warmer than the storage unit, the thermostat turns on a pump or fan to circulate water or air through the collector to heat the storage medium or the house (Soteris, 2012).

The operation, performance, and cost of these controls vary. Some control systems monitor the temperature in different parts of the system to help determine how it is operating. The most sophisticated systems use microprocessors to control and optimise heat transfer and delivery to storage and zones of the house.

There are two types of active solar water heating systems (Walker, 2012):

i. **Direct circulation solar water heater**

   Pumps circulate household water through the collectors and into the home. They work well in climates where water rarely freezes.

ii. **Indirect circulation solar water heater**

   Pumps circulate a non-freezing, heat-transfer fluid through the collectors and a heat exchanger. This heats the water that flows into the home. They are popular in climates proned to freezing temperatures (Markens, 2009).

2.3 Components of a Solar Water Heater

2.3.1 Hot water storage tanks

Storage tanks are basically of two types; stratified storage and well-mixed storage tanks. When heated fluid returns from the collector and does not mix with fluid near the collector inlet port, the storage is called stratified storage. In the case of well-mixed storage tank both cold and warm water are well mixed. The storage in this system is known as well-mixed storage and it is designed only for liquid as working fluid. Water tanks will stratify automatically if they are constructed like ordinary hot water tanks with a height greater than the tank diameter, because large diameter results in laminar flow rather than turbulent flow, that will develop swirl and eddy which will make both warm and cold water to mix together as the case may be in well mixed storage systems (Young et al, 2012).

Most solar water heaters require a well-insulated storage tank. Solar storage tanks have an additional outlet and inlet connected to and from the collector. In two-tank systems, the solar water heater preheats water before it enters the conventional water heater. In one-tank systems, the back-up heater is combined with the solar storage in one tank.

Solar water heating systems almost always require a backup system for cloudy days and times of increased demand. Conventional storage water heaters usually provide backup and may already be part of the solar system package. A backup system may also be part of the solar collector, such as rooftop tanks with thermosyphon systems. Since an integral-collector storage system already stores hot water in addition to collecting solar heat, it may be packaged without a tank or demand-type water heater for backup (Markens, 2009).

2.3.2 Solar collector

Solar thermal collectors capture and retain heat from the sun and use it to heat a liquid. Two important physical principles governing the technology of solar thermal collectors (Soteris, 2004):

i. Any hot object ultimately returns to thermal equilibrium with its environment, due to heat loss from the hot object. The processes that result in this heat loss are conduction, convection and radiation. The efficiency of a solar thermal collector is directly related to heat losses from the collector surface (efficiency being defined as the proportion of heat energy that can be retained for a predefined period of time). Within the context of a solar collector, convection and radiation are the most important sources of heat loss. Thermal insulation is used to slow down heat loss from a hot object to its environment. This is actually a direct manifestation of the Second law of thermodynamics.

ii. Heat is lost more rapidly if the temperature difference between a hot object and its environment is larger. Heat loss is predominantly governed by the thermal gradient between the temperature of the collector surface and the ambient temperature. Conduction, convection, and radiation all occur more rapidly over large thermal gradients.

The simplest approach to solar heating of water is to simply mount a metal tank filled with water in a sunny place. The heat from the sun would then heat the metal tank and the water inside. Indeed, this was how the very first Solar Water Heater systems worked more than a century ago (Soteris 2004). However, this setup would be inefficient due to an oversight of the equilibrium effect, as soon as heating of the tank and water stops, the heat gained starts to be lost back into the environment, and this continues until the water in the tank reaches

the ambient temperature. The challenge is therefore to limit the heat loss from the tank, thus delaying the time when thermal equilibrium is regained (Dobson, 2008).

2.3.2.1 Types of solar collectors used for domestic water heating

1. **Integrated Collector Storage (ICS) or batch collectors**: are collectors which reduce heat loss by placing the water tank in a thermally insulated box. This is achieved by encasing the water tank in a glass-topped box that allows heat from the sun to reach the water tank However, the other walls of the box are thermally insulated, reducing convection as well as radiation to the environment, In addition, the box can also have a reflective surface on the inside. This reflects heat lost from the tank back towards the tank. In a simple way one could consider an ICS as a water tank that has been enclosed in a type of 'oven' that retains heat from the sun as well as heat of the water in the tank as shown in figure 2.3.

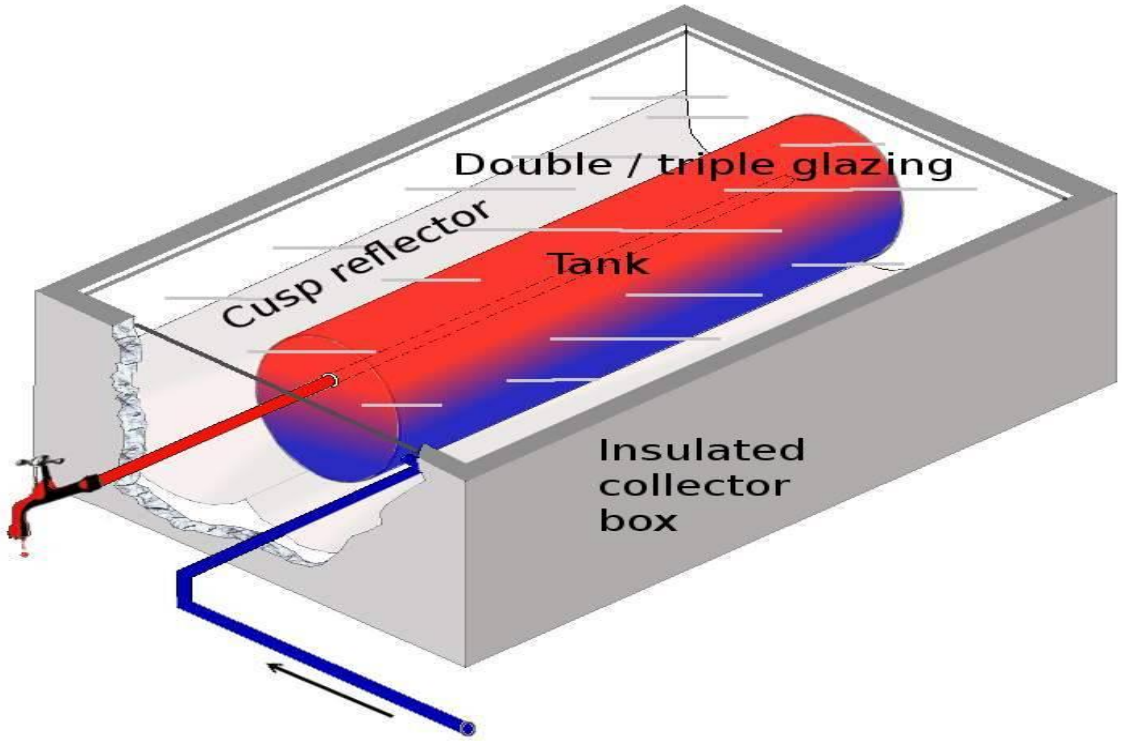


Figure. 2.3: Integrated Collector Storage (Alternative energy tutorials, 2012)

Using a box does not eliminate heat loss from the tank to the environment, but it largely reduces this loss (Rai, 2008). Standard ICS collectors have a characteristic that strongly limits the efficiency of the collector: a small surface-to-volume ratio. Since the amount of heat that a tank can absorb from the sun is largely dependent on the surface of the tank directly exposed to the sun, it follows that a small surface would limit the degree to which the water can be heated by the sun. Cylindrical objects such as the tank in an ICS collector inherently have a small surface-to-volume ratio and most modern collectors attempt to increase this ratio for efficient warming of the water in the tank. There are many variations on this basic design, with some ICS collectors comprising several smaller water containers and even including evacuated glass tube technology, a type of ICS system known as an Evacuated Tube Batch (ETB) collector (Rai, 2008).

2. **Flat plate collectors:** are an extension of the basic idea to place a collector in an 'oven'-like box with glass in the direction of the Sun Most flat plate collectors have two horizontal pipes at the top and bottom, called headers, and many smaller vertical pipes connecting them, called risers(Rai, 2008). The risers are welded (or similarly connected) to thin absorber fins. Heat-transfer fluid (water or water/antifreeze mix) is pumped from the hot water storage tank (direct system) or heat exchanger (indirect system) into the collectors' bottom header, and it travels up the risers, collecting heat from the absorber fins, and then exits the collector out of the top header as shown in figure 3.4

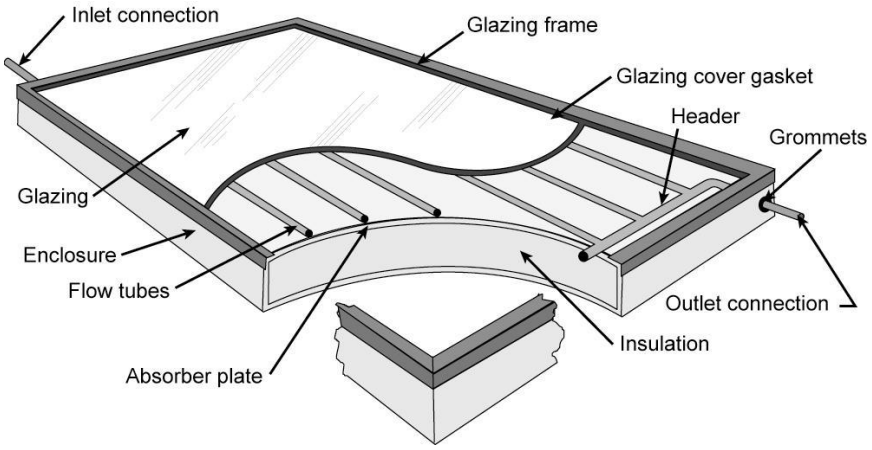


Figure 2.4 Cross sections of flat plate solar collector (Alternative Energy Tutorials, 2012)

Serpentine flat plate collectors differ slightly from this "harp" design, and instead use a single pipe that travels up and down the collector. However, since they cannot be properly drained of water, serpentine flat plate collectors cannot be used in drain back systems (Walker, 2012).

The type of glass used in flat plate collectors is almost always low-iron, tempered glass. Being tempered, the glass can withstand significant hail without breaking, which is one of the reasons that flat-plate collectors are considered the most durable collector type (Markens, 2009).

3. Unglazed or formed collectors are similar to flat-plate collectors, except they are not thermally insulated nor physically protected by a glass panel. Consequently these types of collectors are much less efficient for domestic water heating. For pool heating applications, however, the water being heated is often colder than the ambient roof temperature, at which point the lack of thermal insulation allows additional heat to be drawn from the surrounding environment (Markens, 2009).

4. Evacuated tube collectors (ETC) are collectors in which heat loss to the environment, inherent in flat plates, has been reduced. Since heat loss due to convection cannot cross a vacuum, it forms an efficient isolation mechanism to keep heat inside the collector pipes. Since two flat sheets of glass are normally not strong enough to withstand a vacuum, the vacuum is rather created between two concentric tubes (Markens,2009). Typically, the water piping in an ETC is therefore surrounded by two concentric tubes of glass with a vacuum in between that admits heat from the sun (to heat the pipe) but which limits heat loss back to the environment. The inner tube is coated with a thermal absorbent. Life of the vacuum varies from collector to collector.

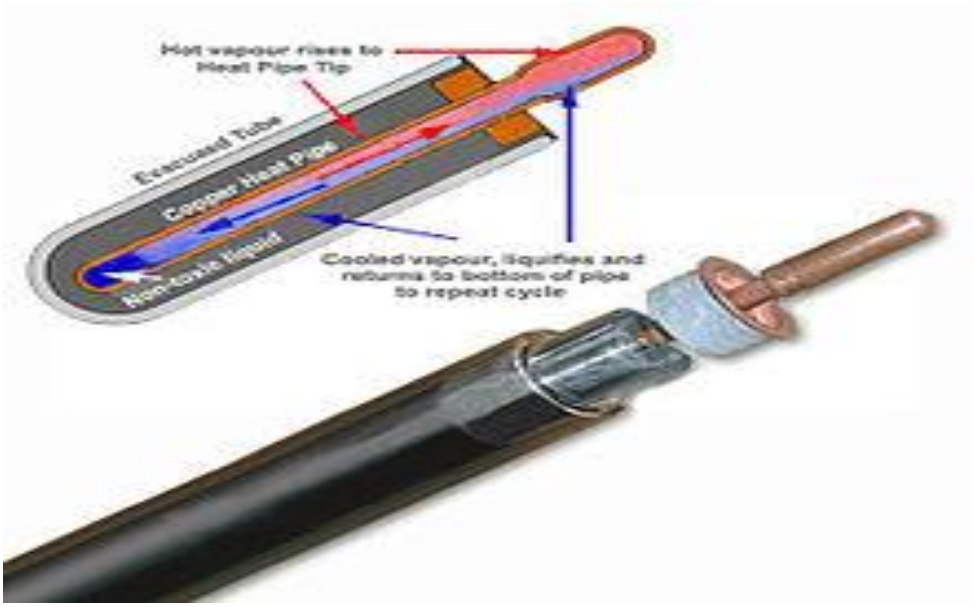


Figure 3.5 cross sections of Evacuated tube collectors.(Norton, 2013).

Flat plate collectors are generally more efficient than ETC in full sunshine conditions. However, the energy output of flat plate collectors is reduced slightly more than evacuated tube collectors in cloudy or extremely cold conditions. Most ETCs are made out of annealed glass, which is susceptible to hail, breaking in roughly golf ball -sized hail. ETCs made from "coke glass," which has a green tint, are stronger and less likely to lose their

vacuum, but efficiency is slightly reduced due to reduced transparency (Crawford *et al.*, 2003).

Solar water heating systems use heat exchangers to transfer solar energy absorbed in solar collectors to the liquid or air used to heat water or a space. Heat exchangers can be made of copper, bronze, stainless steel, aluminum, or cast iron. Solar heating systems usually use copper, because it is a good thermal conductor and has greater resistance to corrosion (Crawford *et al.*, 2003). When the daily hot water demand is known the collector area can be determined. The required collector area depends on several factors such as:

· Collector type

· Size of the solar storage tank

· Location, tilt, and orientation of the collectors

· Local climatic conditions

2.3.2.2 Solar collector orientation

Solar water heater collectors should be oriented geographically to maximise the amount of daily and seasonal solar energy that it can receive. In general, the optimum orientation for a solar collector in the northern hemisphere is true south. However, recent studies have shown that, depending on the location and collector tilt, collector can face up to 90º east or west of true south without significantly decreasing its performance (Markens, 2009).

Although the optimal tilt angle for the collector is an angle equal to the latitude as shown in figure 2.5, fixing the collector flat on an angled roof will not result in a big decrease in system performance, however, the roof angle should be considered when sizing the system

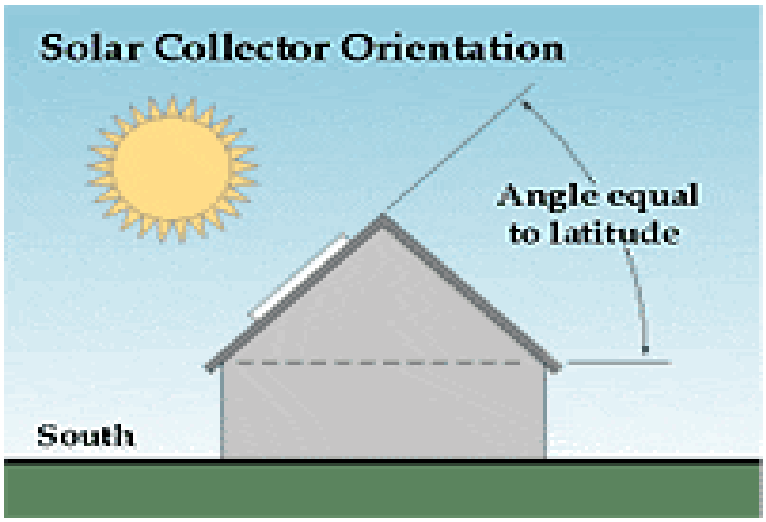


Figure. 2.6 Collector tilts at an angle equal to the latitude (Retscreen International, 2004)

The most usual place to install collectors is the roof area. If it is not possible to mount the collectors on the roof, they can also be mounted on a suitable frame near the house, they can be integrated into an earth bank, or mounted on a flat roof. However, in each case attention should be paid to keeping the pipes to and from the tank as short as possible.

As a general rule, the collector should be aligned to the equator. That means in the southern hemisphere facing north and in the northern hemisphere facing south. A deviation of 40° to the east or west is nevertheless possible, as it does not reduce the yield significantly (Koffi *et al.*, 2008).

In addition, care should be taken that the collectors are not shaded at any time of the year, either by trees or buildings, if possible. Apart from the effect of the characteristics of the collector itself, the output of the solar system is strongly dependent on the inclination angle of the collector to the sun. The largest yield is obtained when the collector is always orientated perpendicular to the sun. However, the optimal tilt angle for the collectors varies according to the season, as the sun is higher in the sky in summer than in winter. As a

general rule, *the optimum angle of tilt is equal to the degree of latitude of the site.* But the minimum angle of the collector should be 15 degree (Walker, 2012).

2.3.3 Absorber plate

The function of the absorber is to effectively convert solar radiation into heat. The absorber surface is often coated to maximise this energy collection. The absorber coating is thus designed with a high absorption coefficient, α, for the sun's radiation spectrum (typically α = 0.92 to 0.96) (Walker, 2012).

Absorptivity is the fraction of incident sunlight captured (not reflected) by the absorber. The reflectance is the complement of the absorption and is given by: $\rho = 1 - \alpha$. For best performance, the absorber should have a low emission coefficient ε (typically, ε = 0.05 to 0.1) for infrared radiation to keep the losses from long wave radiation emission low as the collector heats up (Mudansir, 2008).

Emissivity is the ratio of radiant heat loss off the absorber relative to that of a perfectly black surface ("blackbody"). Most common materials, such as black paint, have an absorptivity equal to the emissivity, and the second law of thermodynamics requires that all materials have absorptivity=emissivity at a given wavelength of incident light. However, special surface treatments (semiconductor coatings, blackened nickel layer) have absorptivity in the short-wavelength solar spectrum that is much higher than emissivity in the long-wavelength infrared radiant heat loss spectrum. Such surfaces are called "selective surfaces" and improve the performance of solar collectors, especially when operating at elevated temperatures where radiant heat loss is more important.

Absorber coatings that possess high absorptivity and low reflectance are called "selective absorbers (Christopher,2010).

2.3.4 Transparent cover

The purpose of the transparent cover is to reduce the convection losses from the absorber, while allowing the maximum amount of radiation to reach the absorber. The cover must also provide the mechanical strength to protect the absorber from the environment.

Special solar glass with low iron content is used. It is occasionally called "water white glass" and its typical transmittance is $\tau = 0.89$ to 0.91 for the wavelength range of the solar radiation. This can be enhanced to $\tau = 0.94$ to 0.96 when anti reflective coatings are applied. This glass should be tempered to reduce breakage by impact (Mudashir, 2008).

2.3.5 Collector casing

The housing of a collector must provide the necessary mechanical strength to protect the absorber and the insulation to minimize heat loss to the environment. It must withstand wind and snow loads that occur in the area where the collector is installed. It also must be tight enough against rain penetration. These features need to be ensured over the entire lifetime of the system.

Housings are typically made from aluminum sheet stock or extruded sections, galvanized and painted steel, molded or extruded plastic parts, composite or wood products.

2.3.6 Insulation

Insulation is added behind the absorber plate and on the sides of the collector to reduce thermal heat losses. The insulation must use a minimum of binders because it is intended for high temperatures; otherwise, the binders will outgas and form a film on the underside of the collector glazing blocking solar radiation.

Common insulating materials include, for example, mineral fibre, ceramic fibre, fibreglass, and plastic foams. Sometimes polyurethane foam is used, though its resistance to temperature and moisture is limited so it should not be allowed to contact the absorber

plate inside the collector. The insulation provides low heat conductivity, some mechanical strength, and temperature and fire resistance (Dobson, 2008).

2.4 Application of Solar Heated Water

Hot water finds many applications in our everyday lives such as in our homes (catering, bathing etc), public institutions such as hospitals which require hot water for sterilisation of the equipment, hotels, laundries etc.

2.5 Selecting and Sizing a Solar Heating System

Selecting the appropriate size of solar energy system depends on factors such as the site, design, and heating needs of your house. Local covenants may restrict your options. The local climate, the type and efficiency of the collector(s), and the collector area determine how much heat a solar heating system can provide. A well-designed and insulated home that incorporates passive solar heating techniques will require a smaller and less costly heating system of any type, and may need very little supplemental heat other than solar (Tripanagnostopoulos, 1999).

The hot water demand in a household is decisive for the dimensioning of a domestic hot water (DHW) solar system. However, this depends on the users' habits. For example, if a family is used to have a shower rather than a bath, the daily hot water demand is significantly lower than if a bath is frequently taken. The daily hot water demand can be estimated as shown in table 2.1.

Table 2.1: Hot water demand for different users at a hot water temperature of 60 °C.

		Low demand . (litres)	Medium demand . (litres)	High demand (litres)
Residential buildings	per person and day	30	50	60
Sport facilities	Per shower	20	30	50
Accommodation	Per bed	20	40	60

(Source: Institute for sustainable Technologies, 2001).

The dimensioning indicated in tables 2.2, is to be understood as guidelines for West Africa conditions. In order to gain exact information, a calculation based on the system site characteristics in question is recommended.

Such calculations can be performed with the help of simulation programmes. These give exact predictions of the solar fraction and the system efficiency for the planned system as well as information on the additional energy needed during the rainy season. Table 2.2 indicates the estimated dimension of the domestic hot water solar systems for West African weather condition.

Table 2.2: Dimensioning of domestic hot water solar systems for West African conditions.

Daily hot water demand [litres]	Solar storage capacity [litres]	Collector area* SV [m^2]	Collector area* SC [m^2]
50	50-75	1.0-1.5	0.9-1.3
100	100-150	2.0-3.0	1.5-2.5
200	200-300	3.5-4.5	3.0-4.0
300	300-450	4.5-6.0	4.0-5.0
500	500-750	7.5-10	6.0-8.5

(Source: Institute for sustainable Technologies, 2001)

SV= coating of solar Varnish

SC= selective coating

2.6 Siting Your Solar Water Heating System

Before the installation of a solar water heating system, there is need to first consider the site's solar resource, as well as the optimal orientation and tilt of the solar collector . The efficiency and design of a solar water heating system depends on how much of the sun's energy reaches the building site (Christopher, 2010). Both the orientation and tilt of the collector will affect the solar water heating system's performance.

2.7 Review of Past Research Work

Rhushi *et al.* (2011) studied and simulated with a computer programme in C-language the performance of a solar water heater using a flat plate collector. The Program calculates instantaneous beam and diffuse radiations for the given location of the collector, number of days for the given date, angle of incidence of beam radiation on the collector, total solar flux incident on the collector, transmissivity – absorbtivity product for beam and diffuse radiations, incident flux absorbed by the absorber plate, collector heat removal factor, overall loss coefficient, water outlet temperature and the instantaneous efficiency. The developed simulation program not only predicts performance of a given solar collector system, but also could be used to size the solar hot water systems for different applications. Comparison between simulated results and the collector test results, showed that generalised program predicts the values very near to the experimental values and hence the approach of design analysis based upon mathematical modeling is cheap and efficient compared to the analysis of physical models, which in some cases may become very tedious

Ityona (2003) designed a compact solar water heater for domestic and small scale industrial applications it is a modification of the convectional flat plate collector for the solar water heater with use of plane reflectors to increase the energy input and the collector and improving the thermal efficiency.

Ahmed (2010) investigated solar water heating system in terms of mathematical theory to produce a mathematical model of solar water heating system. The analysis done by using a mathematical model developed to obtain data on temperature by varying flat plate collector area, storage tank insulation volume, piping size and mass flow rate of water. Efficiency of flat plate collector and storage tank insulation was calculated for any changes in size and volume. Solar fraction was calculated for any changes in the size of a flat plate collector and storage tank insulation in the consideration of changes in temperature and mass flow rate of water. Analysis showed the water temperature will increase with increasing area of flat plate collector, decreased with the increasing volume of insulated storage tank, and decreased with increasing size of the pipe. These studies can provide data for the optimum design with high capacity and the mathematical models will facilitate the future study.

Jae-Mo (1999): carried out a very detailed thermal analysis of a flat-plate solar collector to predict the thermal performance. This analysis was based on the established theory about flat-plate solar collector: the radiation absorption, heat loss from the collector, and temperature distribution on the plate. The calculation of useful energy and top heat loss from the collector is based on the aperture area to make a more accurate prediction of collector performance. The correlation for natural convection heat transfer between the covers and between the plate and cover was selected with the consideration of the low conductivity of plastics. The semi-gray radiation model was adopted to determine the optical properties of the collector cover and absorber plate. Comparison of the results between calculated with experimental showed good agreement. The collector tests were performed by Florida Solar Energy Centre. The calculations based on the information from test reports yielded an accurate prediction of the thermal performance of flat-plate solar collectors. Based on the analysis, a flat-plate solar collector design programme (CoDePro) has been developed.

Young-Deuk Kim (2012) optimized the long-term performance of an existing active-indirect solar hot water plant (SHWP), which supplies hot water at 65 C for use in a flight kitchen, using a micro genetic algorithm in conjunction with a relatively detailed model of each component in the plant and solar radiation model based on the measured data.

Taherian (2011) studied the dynamic simulation of thermosyphon solar water heater collector considering the weather conditions of a city in north of Iran. The simulation was done for clear and partly cloudy days. The useful energy, the efficiency diagrams, the inlet and the outlet of collector, center of the absorber and center of the glass cover temperatures, were obtained. The simulation results were then compared with the experimental results in fall and showed a good agreement.

Soteris (2004) surveyed the various types of solar thermal collectors and applications, initially, an analysis of the environmental problems related to the use of conventional sources of energy is presented and the benefits offered by renewable energy systems are outlined. A historical introduction into the uses of solar energy is attempted followed by a description of the various types of collectors including flat-plate, compound parabolic, evacuated tube, parabolic trough, Fresnel lens, parabolic dish and heliostat field collectors. This is followed by an optical, thermal and thermodynamic analysis of the collectors and a description of the methods used to evaluate their performance. Typical applications of the various types of collectors are presented in order to show to the reader the extent of their applicability. These include solar water heating, which comprise thermosyphon, integrated collector storage, direct and indirect systems and air systems, space heating and cooling, which comprise, space heating and service hot water, air and water systems and heat pumps, refrigeration, industrial process heat, which comprise air and water systems and steam generation systems, desalination, thermal power systems, which comprise the parabolic trough, power tower and dish systems, solar furnaces, and chemistry

applications. As can be seen solar energy systems can be used for a wide range of applications and provide significant benefits, therefore, they should be used whenever possible.

Zhani(2011) presented the modeling and the experimental validation of air and water solar collectors used in humidification and dehumidification (HDH) solar desalination unit. The solar desalination process is currently operating under the climatological conditions of Sfax (34 N, 10 E), Tunisia. To numerically Simulate the air and water solar collectors; we have developed dynamic mathematical models of the solar collectors. The resulting distributed parametric systems of equations are transformed into a system of ordinary differential equations (ODEs) using the orthogonal collocation method (OCM). A comparison between numerical and experimental data was conducted. It was found that the two-temperature mathematical model describes more precisely the real behavior of the water solar collector than the one-temperature mathematical model. It was also shown that the developed mathematical models are able to predict accurately the trends of the thermal characteristic of the water and air solar collectors. As a result, the proposed models can be used to size and test the behaviour of such a type of water and air solar collectors.

Papamarcou(2000) studied thermosyphon solar water heater consisting of two plate collectors of total aperture area of 2.7 m^2 and 150 liter storage tank is modeled using TRNSYS. Simple experiments were conducted in order to validate the model. During the experiments weather conditions were measured every 10 min and integrated over an hour. The temperature of the water in the storage tank was also measured at the beginning and at the end of the day. The storage tank temperature rise was used to validate the model by using the actual weather data as input to the program. Validation tests were performed for 25 days spread over 6 months and the mean deviation between the predicted and the actual values of water temperature rise is 4.7% which is very satisfactory. Subsequently, long

term system performance is estimated by using TRNSYS model run with the weather values of TMY for Nicosia, Cyprus. The annual solar fraction obtained was 79% and the system could cover all the hot water needs of a house of four people during the three summer months. The maximum auxiliary energy was needed during the months of December and January (about 280 MJ/month). In addition, an economic analysis of the system was carried out. The pay-back time of the system was found to be 8 years and the present worth of life cycle savings was found equal to C£ 161.

Rodríguez (2010) Thermosyphon solar heaters are considered as an interesting chance in domestic hot water applications being widely used. The complexity of analysis of these systems, due to the strongly coupling between their different components (solar collectors, storage tanks, heat exchangers, connecting pipes,) and their operation principle (thermosyphon effect), makes the numerical simulation of these systems a useful tool on the their necessary optimization. Based on the numerical solution of the energy and momentum equations for the different parts of the thermosyphon systems; two levels of modelization have been considered:

i) simple models allowing global system simulation for real long term operating conditions; ii) CFD models (Computational Fluid Dynamics), as a design tool for the different components of the system, and as a source of information to feed simpler models. The aim of this work is to present numerical simulations of thermosyphon solar heaters, using a system modelization fed by numerical data obtained from CFD computations when this necessity has been considered. A special emphasis on the friction factors evaluation for connecting pipes and its influence in the overall performance of system is focused. The numerical results obtained are compared with those obtained with the TRNSYS commercial code.

Zwalnan (2015) designed, simulated, constructed and tested a thermosyphon solar water heater. The system was designed to supply a daily hot water capacity of $0.1m^3$ at a minimum temperature of 70^oC for domestic use. The design approach was in three parts; firstly, since solar radiation and weather data which are driving function for solar systems design vary randomly with time, the monthly average daily solar radiation and weather data obtained from the typical meteorological year (TMY) solar data of Zaria were used to determine the design month as the month (August) with the least monthly average daily solar energy ratio.. The results of this research led to the conclusion that a thermosyphon solar system with collector area of 2.24 m^2 operated under the weather condition of Zaria, would be capable of supplying a daily domestic water of $0.1m^3$ at temperature ranging from 59^oC for the worst month (August) to 81^oC for the best month (April).The computed Nash-Sutcliffe Coefficient of Efficiency (NSE) values of 0.663, 0.956 and 0.885 and the low RMSE values of 8.09^oC, 3.65^oC and 5.31^oC between the modeled tank inlet temperature and the observed tank inlet temperature for the three days tests conducted indicated that the model formulated using TRNSYS software was valid and closely agreed, capable of predicting the performance of the system with a 66.3 %, 95.6% and 88.5 % degree of accuracy for the 3 days that the experiments were conducted respectively.

From the literature reviewed it is obvious that all the solar water heater design simulated in Nigerian university are models which are discarded after the research work and later turn to garbage in the workshops, there is need for engineers to solved the immediate problem of their community and also to implement the solutions to serve humanity which will make an impact to the society. Also from the previous research work done in the department, (Zwalnan, 2015) recommended the need to investigated the effect of placing the copper tubes above the absorber plate on the system performances.

2.8 Theoretical Background

2.8.1 Thermal radiation

Thermal radiation is a form of energy emission and transmission that depends entirely on the temperature characteristics of the emissive surface. There is no intervening carrier, as in the other modes of heat transmission, i.e., conduction and convection. Thermal radiation is in fact an electromagnetic wave that travels at the speed of light (C = 300,000 km/s in a vacuum). This speed is related to the wavelength (λ) and frequency (v) of the radiation as given by the equation (Soteris, 2009):

$$C=\lambda v \tag{2.1}$$

2.8.2 Optical Analysis

When radiation strikes a body, a fraction of it is absorbed, another fraction is reflected and a third fraction is transmitted. The fraction of the incident radiation that is absorbed is known as absorptance (α), the fraction that is reflected is known as reflectance (ρ) and the fraction that is transmitted is known as transmittance (τ).

$$\alpha + \rho + \tau_{r} = 1 \tag{2.2}$$

For a transparent material like glass, there exists a value for transmittance, absorptance and reflectance even though the transmittance might be very high. On the other hand, for an opaque surface like a metal plate, the transmittance is zero (Duffie and Beckman, 1991).

The input to the Solar Collector system is the total radiation incident on the glass cover, but it is of interest to know the quantity of radiation absorbed by the absorber plate, of the total incident radiation on the glass cover.

- only a part (of the incident radiation) is transmitted through the glass, while the remaining is either reflected to atmosphere or absorbed by the glass and

- of the transmitted radiation striking the absorber plate a part is absorbed and the remaining is reflected.

To estimate the radiation absorbed by the absorber plate the following information should be known the incident global radiation on the collector (glass) surface, the transmittance of the glass to the incident radiation and the absorptance of the absorber plate (of the incident radiation).

In order to estimate the transmittance of the glass cover, it is necessary to know the reflectance and the absorptance of the cover because these materials possess the ability to reflect as well as absorb the radiation.

2.8.2.1 Reflectance (ρ)

When a beam of radiation strikes the surface of a transparent plate at angle θ_1, called the *incidence angle*, as shown in Figure 2.1, part of the incident radiation is reflected and the remainder is refracted, or bent, to angle θ_2, called the *refraction angle*, as it passes through the interface. Angle θ_1 is also equal to the angle at which the beam is specularly reflected from the surface. Angles θ_1 and θ_2 are not equal when the density of the plane is different from that of the medium through which the radiation travels. Additionally, refraction causes the transmitted beam to be bent toward the perpendicular to the surface of higher density. The two angles are related by the Snell's law

$$n=\frac{n_1}{n_2}=\frac{Sin\theta_2}{Sin\theta_1} \qquad (2.3)$$

where n_1 and n_2 are the refraction indices and n is the ratio of refraction index for the two media forming the interface. The refraction index is the determining factor for the reflection losses at the interface. A typical value of the refraction index is 1.000 for air,

1.526 for glass, and 1.33 for water. Where n_1, n_2 are the refractive indices of medium 1 (usually air) and medium 2 (usually glass) respectively.

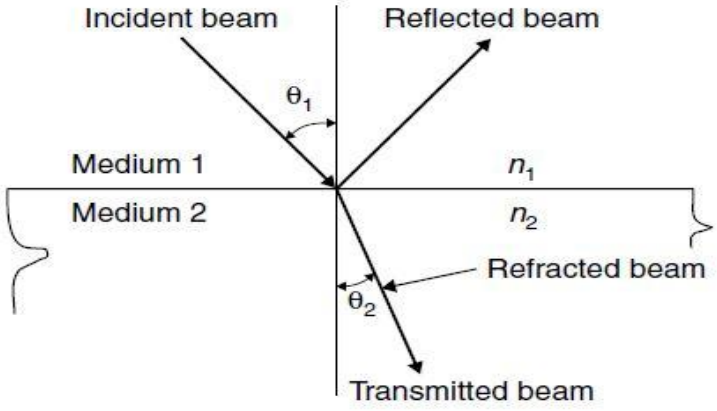


Fig. 2.7 Refractive index

Expressions for perpendicular and parallel components of radiation for smooth surfaces were derived by Fresnel as

$$r_{\rho ar} = \frac{\tan^2(\theta_2 - \theta_1)}{\tan^2(\theta_2 - \theta_1)} \qquad (2.4)$$

$$r_{per} = \frac{Sin^2(\theta_2 - \theta_1)}{Sin^2(\theta_2 - \theta_1)} \qquad (2.5)$$

Equation (2.4) represents the perpendicular component of unpolarized radiation and Equation (2.5) represents the parallel one. It should be noted that *parallel* and *perpendicular* refer to the plane defined by the incident beam and the surface normal. Properties are evaluated by calculating the average of these two components as

$$r = \frac{1}{2}(r_{par} + r_{per}) \qquad (2.6)$$

If the incident radiation is in a direction normal to the surface (i.e.) $\theta = 0$, then for a single surface, and Equation (2.6) can be combined with Equation. (2.3) to yield

$$r(0) = \left[\frac{n_1 - n_2}{n_1 + n_2}\right]^2 \qquad (2.7)$$

If one medium is air (n=1.0), then Eq. (2.7) becomes

$$r(0) = \left[\frac{n-1}{n+1}\right]^2 \tag{2.8}$$

In case of a single glass cover [(n_2 = 1.526) and for air (n_1 = 1)], r = 0.44. Meaning that about 4.4% of the incident radiation is reflected from one surface. Thus, for single glass plate, the loss due to reflection of the incident radiation will be about 8.8% (4.4 % for each surface - top and bottom). (Soteris, 2009)

Similarly, the transmittance, τr (subscript r indicates that only reflection losses are considered), can be calculated from the average transmittance of the two components as follows:

$$Tr = \frac{1}{2}\left(\frac{1-r_{\rho er}+1-r_{\rho er}}{1+r_{\rho er}+1+r_{\rho er}}\right) \tag{2.9}$$

Normally, a flat plate collector has only one or a maximum of two glass covers. For a system of N covers of the same material neglecting absorption by the material, the reflectance is given by

$$\text{Tr}_{\text{t}} = 1-\frac{1}{2}\left[\frac{1-r_{\rho er}}{1+(2N-1)r_{\rho er}}+\frac{1-r_{\rho ar}}{1+(2N-1)r_{\rho ar}}\right] \tag{2.10}$$

It should be noted that the discussion on reflectance of cover material has been done by not considering absorption by cover material.

2.8.2.2 Absorptance (α)

While considering reflectance, it was assumed that the absorptance of glass of the incident solar radiation is zero. But in reality, the absorptance is given by Bouguer's law, which states that the absorbed radiation is proportional to the intensity in the medium and the distance the radiation has travelled in the medium. Mathematically, the fraction that is absorbed over a path length L in a medium of extinction coefficient K is given by

$$1-\alpha = e^{-KL} \tag{2.11}$$

If θ is the angle between the normal surface and the direction of light ray in a slab of thickeness '*d*' then

$$L=d/Cos\theta \tag{2.12}$$

The transmittance, $\tau\alpha$ (subscript α indicates that only absorption losses are considered), can be calculated from

$$\tau\alpha = e^{(\frac{-KL}{COS\theta})} \tag{2.13a}$$

Where *K* is the extinction coefficient, which can vary from 4 m^{-1} (for low-quality glass) to 32 m^{-1} (for high-quality glass), and *L* is the thickness of the glass cover

In glass, it is iron oxide that controls the color and the absorptive of glass. Low iron glass containing about 0.05% iron oxide has an absorptance of about 2.5%, while ordinary window glass has an absorptivity of nearly 15% at normal incidence and these values will be higher at other incidence angles (Soteris 2009).

It should be noted that the discussion on absorptance of cover material has been done by neglecting reflectance of cover material. both the refractive indices and the extraction coefficient are dependent on wavelength. However, we consider that glass has its optical properties constant over the narrow range of solar wavelengths of interest.

2.8.2.3 Transmittance (τ)

The equation for the transmittance of a collector cover can be simplified for solar collector with cover materials and angles of practical interest as

$$\tau = \tau \alpha \tau_r \quad \textbf{(2.13b)}$$

As the transmittance (total) is a Function of wavelength, the transmitted heat flux in each wavelength has to be added in the entire wavelength range and the ratio of this quantity to the total incident heat flux gives the total transmittance.

2.8.3 Estimation of Absorptance of Absorber Plate

The absorptance of the absorber plate should be estimated accurately because if the radiation incident on an absorber plate is H and the plate has an absorptance A then the solar radiation absorbed by the plate is HA, which s the actual input energy to the collector. The absorptance of radiation by a surface mainly depends on wavelength of radiation and the incidence angle. Monochromatic absorptance (al) is the fraction of the incident radiation at a specified wavelength (I) that is absorbed. Then, the total absorptance for this surface for the given spectral radiation is found by integration over the entire wavelength (Soteris, 2009).

$$\alpha = \frac{\int_0^{\alpha} \alpha_2 1_2 d_2}{\int_0^{\alpha} 1_2 d_2} \quad (2.14)$$

This clearly indicates that absorptance not only depends on the surface, but also on the incident radial spectral distribution.

The absorptance of the surface for the terrestrial solar ‘spectrum can be calculated by dividing the incident radiation into increments and the contributions of these increments

are summed to obtain the absorptance liar that incident radiation. For example, for an increment in incident radiation D fi, the contribution to a is a i D fi Adding,

$$\alpha = \frac{1}{n}\sum_{i=1}^{n}\alpha_N = 1 - \frac{1}{n}\sum_{i=1}^{n}\rho_n \qquad (2.15)$$

Absorptance is also a function of the angle of incidence of the radiation striking the surface and is of course maximum when it strikes in a normal direction (ic) incidence angle is zero. The dependance of absorptance on the angle of incidence given in equational form

$$\frac{\alpha}{\alpha_n} = 1 + 2.0345\,x10^{-3}\theta - 1.99\,x10^{-4}\theta^2 + 5.324\,x10^{-6}\theta^3 - 4.799\,x10^{-8}\theta^4 \qquad (2.16)$$

where, a is the absorptance

a_n is the absorptance at normal incidence

θ is the incidence angle in degrees

The above fit is, however, valid only between $0< \theta <80^0$ (Duffie and Beckman, 1991).

2.8.4 Transmittance - absorptance product ($\tau\alpha$)

To consider the radiation absorbed by a plate, it is necessary to know the transmitted radiation through the cover (τ) as well as the absorptivity of the plate (α). In this case, we define transmittance absorptance product ($\tau\alpha$) which combines the individual properties.

The monthly average daily transmittance-absorptance products are determined by finding independently the angular dependence of the transmittance τ and absorptance α and the transmittance-absorptance product obtained as (Rai, 2008):

$$(\overline{\tau\alpha})_{eff} = \frac{\overline{\tau\alpha}}{1-(1-\alpha)\rho_d} \qquad (2.17)$$

For practical solar collector applications, we can use

$$\tau\alpha = 1.01\,\tau\alpha \qquad (2.\ 18)$$

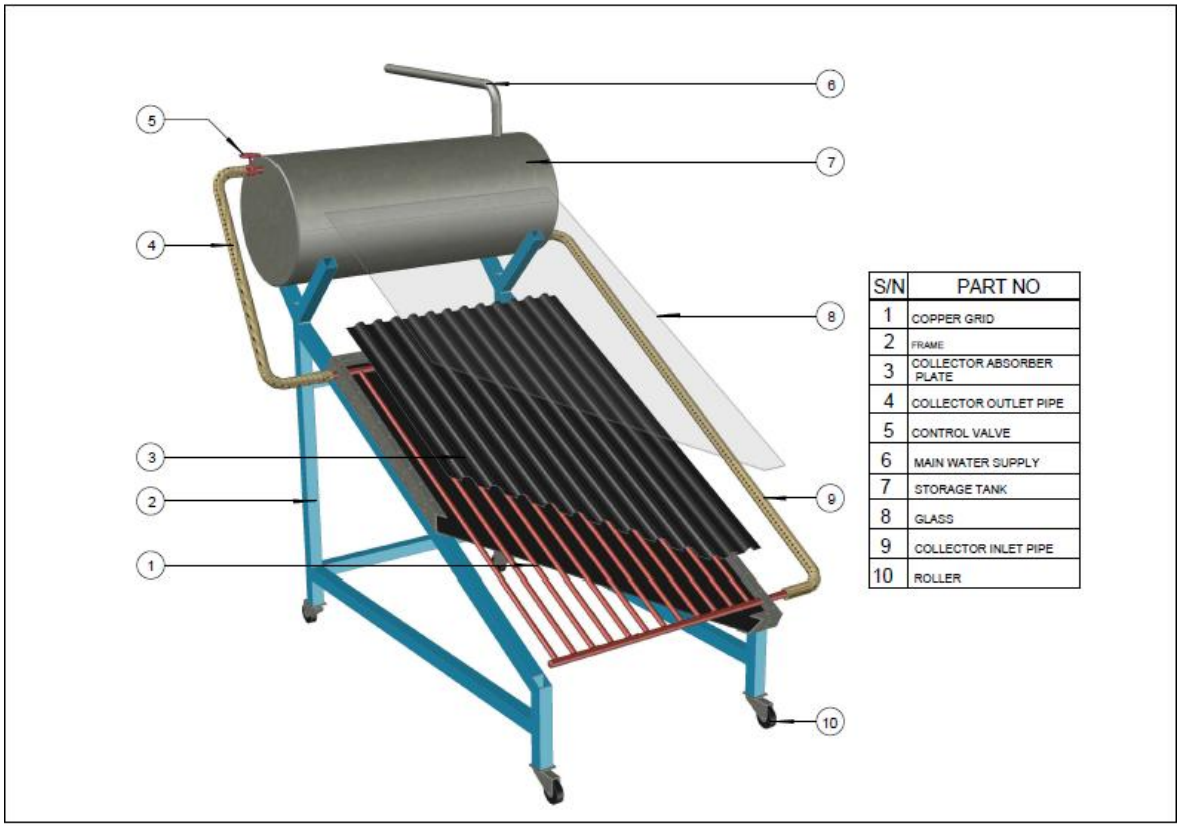
As the absorptance and transmittance are dependent on the incidence angle, typical ($\tau\alpha$) / ($\tau\alpha$)n values for different covers are given for glass (refractive index = 1 .526). This is similar to the result obtained by considering the angular dependance of τ and α separately.

CHAPTER THREE

MATERIAL AND METHOD

3.1 Solar Water Heater Description and Operation

The flat plate solar collector of the system was made of mainly an air tight rectangular wooden cased box inclined at an elevation (tilt angle), to maximise absorption of radiant energy as shown in figure 3.1. Its upper part (covering) is made of glass as glazing material. Inside the box is a flat aluminium absorber plate painted black to enhance absorbance of solar energy followed by copper pipe fittings which serve as the fluid tubes.



S/N	PART NO
1	COPPER GRID
2	FRAME
3	COLLECTOR ABSORBER PLATE
4	COLLECTOR OUTLET PIPE
5	CONTROL VALVE
6	MAIN WATER SUPPLY
7	STORAGE TANK
8	GLASS
9	COLLECTOR INLET PIPE
10	ROLLER

Figure 3.1 Sketch of the thermosyphon water heating system.

Water heating takes places as heat is transferred from the aluminium absorber plate to the fluid tubes. Everything in the box (collector) is painted black to maximise absorption of solar energy. The box is well insulated using fibre glass wool as material to minimise heat

loss. The fluid tubes that transport water from the storage tank to the collector and back to the storage tank are made of PVC water pipes well insulated to minimise heat loss.

3.2 Working Principle of the Solar Water Heater

The density of the hot fluid is less than the density of the cold fluid. The force of attraction to the earth of the hot fluid is less than for the cold fluid. As a result of this force imbalance, cold fluid sinks and the hot fluid rises and the fluid circulates around the loop. The denser or heavier fluid package sinks and pushes the less-dense or lighter fluid up (Dobson, 2008).

3.3 Solar Resources and Weather Data

Meteorological data which are very important driving functions for all solar system design often seem to be highly random and irregular. However, long-term statistical analysis indicates that these variables are predictable to some degree. Therefore, the dynamic nature of solar data can be smoothed out by formulating a representative data, which characterises the mean-value behaviour of any location over a long period (Qin, 1998). Solar radiation, Temperature and Air velocity meteorological data of Zaria were obtained from www.solaranalytical.com was processed to obtain the monthly average daily solar resources of Zaria using the solar radiation and weather data processor TYPE 109 component of TRNSYS 16 software. The Meteorological data and the system calculated parameters are presented in Tables 4.1 and 4.2 to 4.5 respectively.

3.4 Material Selection

The choice of the components for the Solar collector were made based on different criteria, such as strength, corrosion resistance, availability, design specifications and their respective prices as determined from market survey.

Effective materials used for the different component of the solar collector, their description and comments which explain why these materials were chosen are tabulated in table 3.1

Table 3.1: Materials Selected and their properties

S/NO	*Component*	*Material*	*Description and Comments*
1	*Glazing Material*	*Glass*	➢ *Transparent to short wave radiation* ➢ *Withstands the effects of weather, rain, wind, sunshine, dust etc.* ➢ *Low water absorbance* ➢ *Low iron content*
2	*Absorber plate*	*Alluminium Plate*	➢ *High reflectivity* ➢ *High radiation obsorptivity* ➢ *High thermal conductivity(211W/m^{2}K* ➢ *Ability to withstand corrosion* ➢ *Cheap and readily available*
3	*Tube*	*Copper*	➢ *High thermal conductivity* ➢ *Light in weight* ➢ *High corrosion resistance* ➢ *Ductile and Tough*
4	*Collector frame*	*plywood*	➢ *Readily available* ➢ *Good insulator*
5	*Insulator*	*Fibreglass*	➢ *Low thermal conductivity(Good insulator)* ➢ *Poor radiator of heat* ➢ *Very cheap and suitable for insulation*
6	*Drain pipe*	*Polyvinyl Chloride(PVC) pipe*	➢ *High tensile strength* ➢ *Cheap and readily available*
7	*Support structure*	*Ferrous metal*	➢ *High tensile strength* ➢ *Cheap and available*

3.5 Design Analysis

3.5.1 Design theories

3.5.1.1 Total Radiation on Tilted Surfaces

Usually, collectors are not installed horizontally but at an angle to increase the amount of radiation intercepted and reduce reflection and cosine losses.

Therefore, system designers need data about solar radiation on such titled surfaces; measured or estimated radiation data, however, are mostly available either for normal incidence or for horizontal surfaces. Therefore, there is a need to convert these data to radiation on tilted surfaces.

The amount of insolation on a terrestrial surface at a given location for a given time depends on the orientation and slope of the surface.

A flat surface absorbs beam (H_b), diffuse (H_d), and ground-reflected (H_g) solar radiation; that is,

$$H_T=H_b+H_d+H_g \tag{3.1}$$

As shown in figure 3.2, the beam radiation on a tilted surface is



Fig 3.2. Beam radiation on horizontal and tilted surfaces.

$$H_b= H_{bn}cos(\Phi) \tag{3.2}$$

and on a horizontal surface,

$$H_T=H_{bn}cos(\theta) \tag{3.3}$$

where

H_T= beam radiation on a tilted surface (W/m2).

H_b = beam radiation on a horizontal surface (W/m2).

It follows that (Soteris, 2009).

$$R_b = \frac{H_T}{H_b} = \frac{\cos(\emptyset+\beta)\cos\delta\sin\omega_s{}^1 + (\frac{\pi}{180})\omega_s{}^1\sin(\emptyset+\beta)\sin\delta}{\cos\emptyset\cos\delta\sin\omega_s + \frac{\pi}{180}\omega_s\sin\emptyset\sin\delta} \quad (3.4)$$

Where: $$\omega_s{}^1 = min\begin{pmatrix}\cos^{-1}(-\tan\emptyset\tan\delta)\\ \cos^{-1}(-\tan(\emptyset+\beta)\tan\delta)\end{pmatrix} \quad (3.5)$$

And

δ is the declination (Degrees)

$\omega_s$is the sunset angle in degrees

∅is the latitude of the location in degrees

Where "min" means the smaller of the two in the bracket.

Where R_b is called the *beam radiation tilt factor*. So the beam radiation component for any surface is

$H=H_bR_b$ (3.6)

Many models give the solar radiation on a tilted surface. The first one is the isotropic sky model developed originally by Hottel and Woertz (1942) and refined by Liu and Jordan (1960) (Soteris 2009). According to this model, radiation is calculated as follows.

Diffuse radiation on a horizontal surface,

$$H_T = (H_b)R_b + H_d\left(\frac{1+Cos\beta}{2}\right) + H\rho_g\left(\frac{1-Cos\beta}{2}\right) \quad (3.7)$$

Where :

H_b is the total beam radiation on horizontal surface

H_d is the total diffused radiation on horizontal surface

3.5.1.2 Absorbed Solar Radiation

The prediction of collector performance requires information on the solar energy absorbed by the collector absorber plate, the incident radiation has three special components: beam, diffuse, and ground-reflected radiation. This calculation depends on the radiation model employed. Using the isotropic model on an hourly basis,

$$S = (H_b)(\tau\alpha)_b R_b + H_d(\tau\alpha)_d \left(\frac{1+Cos\beta}{2}\right) + H\rho_g(\tau\alpha)_g \left(\frac{1-cos\beta}{2}\right) \quad (3.8)$$

$\bar{H}$= monthly average daily radiation on a horizontal surface in MJ/m^2

H_b = monthly average daily beam radiation on a horizontal surface in MJ/m^2

H_d = monthly average daily diffused radiation on a horizontal surface in MJ/m^2

R_b= monthly average ratio of beam radiation on a tilted to horizontal surface

$(\tau\alpha)_b$= monthly average transmittance-absorptance product of beam radiation

$(\tau\alpha)_d$= monthly average transmittance-absorptance product of diffuse radiation

$(\tau\alpha)_g$= monthly average transmittance-absorptance product of ground reflected radiation

β = is the collector slope in degrees

ρ_g= is the diffuse reflectance of ground (0.2)

Where the terms [1 + cos(β)]/2 and [1 – cos(β)]/2 are the view factors from the collector to the sky and from the collector to the ground, respectively. The same equation can be used to estimate the monthly average absorbed solar radiation, *S*, by replacing the hourly direct and diffuse radiation values with the appropriate monthly average values, H_b and H_d, H_g with R_b, and various $(\tau\alpha)$ values with monthly average values (Soteris, 2009).

3.5.1. 3 Extraterrestrial solar radiation

The amount of solar energy per unit time, at the mean distance of the earth from the sun, received on a unit area of a surface normal to the sun (perpendicular to the direction of propagation of the radiation) outside the atmosphere is called the *solar constant*, *G*sc. This

quantity is difficult to measure from the surface of the earth because of the effect of the atmosphere. A method for the determination of the solar constant was first given in 1881 by Langley (Garg, 1982), who had given his name to the units of measurement as Langleys per minute (calories per square centimeter per minute). This was changed by the SI system to Watts per square meter (W/m2) (Soteris, 2009)

$$H_0 = \frac{86400\, G_{sc}}{\pi}\left(1 + 0.033cos\left(360\frac{n}{365}\right)\right)(cos\emptyset \cos\delta\, sin\omega_s + \frac{\pi}{180}\omega_s \sin\emptyset \sin\delta) \quad (3.9)$$

where:

G_{sc} is the solar constant equal to 1,367 W/m^2

3.5.1.4 Terrestrial irradiation

A solar system frequently needs to be judged on its long-term performance. Therefore, knowledge of long-term monthly average daily insolation data for the locality under consideration is required. Daily mean total solar radiation (beam plus diffuse) incident on a horizontal surface for each month of the year is available from various sources, such as radiation maps or a country's meteorological service. In these sources, data, such as 24 h average temperature, monthly average daily radiation on a horizontal surface H (MJ/m2-d), and monthly average clearness index, K_T, are given together with other parameters(Soteris, 2009).

The monthly average clearness index, K_T, is defined as

$$\overline{K}_T = \frac{\overline{H}}{\overline{H}_0} \quad (3.10)$$

where

$\overline{H}$ =monthly average total insolation on a terrestrial horizontal surface (MJ/m2-d).

Ho = monthly average daily total insolation on an extraterrestrial horizontal surface (MJ/m2).

3.5.1. 5 Declination (δ)

The earth axis of rotation (the polar axis) is always inclined at an angle of 23.45° from the ecliptic axis, which is normal to the ecliptic plane. The ecliptic plane is the plane of orbit of the earth around the sun. As the earth rotates around the sun it is as if the polar axis is moving with respect to the sun. The solar declination is the angular distance of the sun's rays north (or south) of the equator, north declination designated as positive.

Declination is the angle between the sun-earth center line and the projection of this line on the equatorial plane. Declinations north of the equator (summer in the Northern Hemisphere) are positive, and those south are negative.

The declination during the equinoxes and the solstices ranges from 0° at the spring equinox to +23.45° at the summer solstice, 0° at the fall equinox, and -23.45° at the winter solstice(Duffie and Beckman, 1991).

$$\delta = \left(23.45 sin\left(2\pi \frac{n+284}{365}\right)\right) \quad (3.11)$$

The solar declination during any given day can be considered constant in engineering calculations (Duffie and Beckman, 1991).

Table 3.2: Recommended average days for each month of the year and values of *n* by month.

Average day of the month			
Month	Date	n, Day of the Year	Declination.
January	17	17	-20.9
February	16	47	-13
March	16	75	-2.4
April	15	105	9.4
May	15	135	18.8
June	11	162	23.1
July	17	198	21.2
August	16	228	13.5
September	15	258	2.2
October	15	288	-9.6
November	14	318	-18.9
December	10	344	-23

Source: Duffie and Beckman (1991).

3.5.1.6 Angle of incidence of beam radiation

This is defined as the angle between the beam radiation to a surface and the normal to that surface. The angle of incidence θ_T of beam radiation for fixed flat plate collectors surfaces in the northern hemisphere sloped to the north or south relating to other angles which describe the direction of beam radiation is given by the equation (Duffie and Beckman, 1991)

$$\theta_T = Cos^{-1}[Cos(\emptyset - \beta)\,\mathrm{Cos}\,\delta Cos\omega + \mathrm{Sin}(\emptyset - \beta)\,\mathrm{Sin}\,\delta] \quad (3.12)$$

The solar incidence angle, θ_T, is the angle between the sun's rays and the normal on a surface. For a horizontal plane, the incidence angle θ_T, and the zenith angle, θ_z, are the same. (Duffie and Beckman, 1991):

3.5.1.7 Angle of incidence of the diffused and ground-reflected radiation

For a given collector tilt angle, ∅, the following empirical relations, derived by Brandemuehl and Beckman (1980), can be used to find the effective incidence angle for diffuse radiation from sky, θ_d and ground-reflected radiation, θ_g

$$\theta_d = 59.7 - 0.1388\emptyset + 0.001479\emptyset^2 \quad (3.13)$$

$$\theta_g = 90 - 0.578\emptyset + 0.002693\emptyset^2 \quad (3.14)$$

where ∅ = collector slope angle in degrees.

3.5.1.8 Collector energy losses

When a certain amount of solar radiation falls on the surface of a collector, most of it is absorbed and delivered to the transport fluid, and it is carried away as useful energy. However, as in all thermal systems, heat losses to the environment by various modes of heat transfer are inevitable. The overall heat loss coefficient is a complicated function of the collector construction and its operating conditions, given by the following expression:

$$U_L = U_t + U_b + U_e \quad (3.15)$$

where

U_t =top loss coefficient (W/m2-K).

U_b =bottom heat loss coefficient (W/m2-K).

U_e =heat loss coefficient form the collector edges (W/m2-K).

2.5.1.9 Collector Top Loss(U_t)

Iterations are required for the calculation of the top heat loss coefficient, U_t, since the air properties are functions of operating temperature. Because the iterations required are tedious and time consuming, especially for the case of multiple-cover systems, straightforward evaluation of U_t is given by the following empirical equation with sufficient accuracy for design purposes (Klein, 1975):

$$U_t = \frac{1}{\frac{N_G}{\frac{C}{T_{pm}}\left[\frac{T_{pm}-T_a}{N_G+f}\right]^e}+\frac{1}{h_w}} + \frac{[\sigma(T_{pm}{}^2+T_a{}^2)][T_a+T_{pm}]}{\frac{1}{\varepsilon_p+0.00591\,N_G h_w}+\frac{2N_G+f-1+0.133\,\varepsilon_p}{\varepsilon_g}-N_G} \quad (3.16)$$

Where:

$$f = \left(1+0.089h_w-0.1166h_w\varepsilon_p\right)(1+0.07866N_G) \quad (3.17)$$

$$C = 520[1-0.000051\beta^2] \quad (3.18)$$

$$e = 0.430\left(1-\frac{100}{T_{pm}}\right) \quad (3.19)$$

Where:

N_G = number of glass covers

β=collector tilt (degrees)

ε_g = emittance of glass (0.88)

ε_P = emittance of plate

Ta = ambient temperature (K)

T_{pm}= mean plate temperature (K)

h_w= wind heat transfer coefficient (W/m^2.C)

2.5.1.10 Collector back loss (U_b)

The energy loss through the bottom of the collector is made up of conductive loss to heat flow through the insulation and convection and radiation resistance to the environment. The energy loss from the bottom of the collector is first conducted through the insulation and then by a combined convection and infrared radiation transfer to the surrounding ambient air. Because the temperature of the bottom part of the casing is low, the magnitude of the conduction and radiation loss compared to the radiation loss is such that the radiation is negligible (Duffie& Beckman, 1991). Thus the back loss coefficient is estimated as (Duffie& Beckman, 1991).

$$U_b = \frac{K_{bi}}{x_{bi}} \tag{3.20}$$

Where:

K_{bi} is the thermal conductivity of material

x_{bi} is the thickness of material.

2.5.1.11 Collector edge loss (U_e)

The edge loss coefficient is the ratio of the thermal conductivity of the insulation at edge to it thickness; times the ratio of the area of edge to the collector effective aperture area. Tabor (1958) recommends edge insulation of about the same thickness as the bottom insulation. The edge loss estimated by assuming one-dimensional sideway heat flow around the perimeter of the collector system is (Rai, 2008).

$$U_e = \frac{K_{ei}}{x_{ei}} \frac{A_e}{A_C} \tag{3.21}$$

Where:

K_{ei} is the thermal conductivity of edge insulation materials.,

A_c is the collector area.

A_e is the edge insulation area.

x_{ei} is the insulation thickness at the edge

The conduction resistance of the insulation behind the collector plate governs the heat loss from the collector plate through the back of the collector casing.The heat loss from the back of the plate rarely exceeds 10% of the upward loss. Typical values of the back surface heat loss coefficient are 0.3–0.6 W/m2-K. In a similar way, the heat transfer coefficient for the heat loss from the collector edges can be obtained from typical values of the edge heat loss coefficient are 1.5–2.0 W/m2-K (Brandemuehl, 1980).

3.5.1.12 Collector useful energy

In steady state, the performance of a flat-plate solar collector can be described by the useful gain from the collector, Q_u, which is defined as the difference between the thermal loss and the absorbed solar radiation .Duffie and Beckman, (1991) expresses the useful energy gain by a solar collector as:

$$Q_u = A_C\left[S - U_L\left(T_{pm} - T_a\right)\right]^+ \tag{3.22}$$

$$Q_u = F_R[S - U_L(T_i - T_a)]^+ \tag{3.23}$$

where:

Q_u is the useful energy gain per unit time,

A_c (m^2) is the collector area,

F_R is the collector heat removal factor,

U_L is the overall loss coefficient of the collector.

S is the absorbed solar radiation.

T_i ,T_a are the collector fluid inlet and ambient temperatures, respectively.

The collector useful energy can also be defined as the quantity of energy absorbed by a fluid moving in the tubes of a solar collector to raise the fluid temperature from the fluid inlet temperature T_i to fluid outlet temperatureT_o. It is expressed as:

$$Q_u = \dot{m}C_p(T_o - T_i) \tag{3.24}$$

From equation (2.22) and equation (2.23) the collector area can be derived

$$A_C = \frac{\dot{m} C_p (T_L - T_i)}{[S - U_L (T_{pm} - T_a)]^+} \quad (3.25)$$

3.5.1.13 Heat Removal Factor

Heat removal factor represents the ratio of the actual useful energy gain that would result if the collector absorbing surface had been at the local fluid temperature.

3.5.1.14 Collector heat removal factor

The collector heat removal factor, F_R, is the ratio of actual useful energy gain of a collector to the useful gain if the whole collector surface were at the fluid inlet temperature, $F_R$is analogous to the heat exchanger effectiveness. For a header-riser flat-plate collector, the collector heat removal factor can be expressed as (Duffie and Beckman, 1991).

$$F_R = \frac{\dot{m} C_p}{A_c U_L} \left[1 - exp \left(- \frac{A_c U_L F'}{\dot{m} C_p} \right) \right] \quad (3.26)$$

Where:

$F_R$is the heat removal factor

$\dot{m}$is the collector fluid mass flow rate(kg/hr.m^2)

$C_p$is the fluid specific heat (KJ/kgK)

$A_c$is the collector area

$U_L$is the overall collector Loss Coefficient (kJ/h.k)

Where *F'* is the collector efficiency factor expressed as.

$$F' = \frac{1/U_L}{W \left[\frac{1}{U_L [D_i + (W - D_i) F]} + \frac{1}{C_b} + \frac{1}{\pi D_i h_{fi}} \right]} \quad (3.27)$$

Where

W (m) represents tube spacing,

C_b(W/m.K) is the contact resistance, $\frac{1}{C_b} = 0$

$C_p$specific heat (4200J/Kg)

h_{fi}(W/m^2.K) is the internal fluid heat transfer coefficient and

*F*is the standard fin efficiency for straight fins with rectangular profile, given as:

$$F = \frac{\tanh\left[\frac{m(W-D_i)}{2}\right]}{\frac{m(W-D_i)}{2}} \quad (3.28)$$

Where :

$$m = \sqrt{\frac{U_L}{K\delta}} \quad (3.29)$$

U_L is the overall heat transfer coefficient

$k\delta$ is the plate thermal conductivity and thickness product.

D_i is the internal diameter of tube.

3.5.1.15 Flow Factor, and Thermal Efficiency

Another parameter usually used in the analysis of collectors is the flow factor.

This is defined as the ratio of FR toF', given by

$$F_f = \frac{F_R}{F'}$$

$$F_f = \frac{\dot{m}C_p}{A_c U_L F'}\left[1 - exp\left(-\frac{A_c U_L F'}{\dot{m}C_p}\right)\right] \quad (3.30)$$

3.5.1.16 Collector efficiency

The Hottel-Whillier equation defines the efficiency for a solar collector in terms of the collector heat removal factor F_R, given in equation form as (Govind *et al*., 2008):

$$\eta_C = \frac{Q_u}{H_T A_c} = \frac{F_R[S - U_L(T_i - T_a)]^+}{H_T} \quad (3.31)$$

The + superscript indicates that only positive values of the terms in the square brackets are to be used.

3.5.1.17 Heat transfer through the storage tank component

Coefficient of Heat Loss through insulation of the surfaces (U_s), given by

$$U_s = \frac{1}{R} = \frac{K}{L} \quad (3.32)$$

Resistance due to convection Between Outer cylinder and the sky (R_2)

$$R_2 = \frac{1}{h_w} \tag{3.33}$$

Top loss from cylinder U_t is given by

$$U_t = \left\{ \frac{1}{\frac{1}{R_2} + \frac{1}{R_3}} \right\}^{-1} \tag{3.34}$$

Total heat loss from the storage Tank is the Heat loss through Curved Surfaces and the Heat loss through bottom or top surface.

Total heat loss through insulation of the storage tank

$$U_T = U_t + U_s \tag{3.35}$$

3.5.2 Determination of the Design Month

It is of paramount importance to determine the design month so that the system will be designed in such a way that it can be valid throughout the year. In determining the design month, the month with the lowest clearness index was considered. The monthly average clearness index, $\bar{K}_T$ is defined as: The ratio of the monthly average daily radiation on a horizontal surface to the monthly average daily extraterrestrial radiation. Written as:

$$\bar{K}_T = \frac{\bar{H}}{\bar{H}_0} \tag{3.36}$$

Where:

$\bar{H}$ is the monthly average daily solar radiation on a horizontal surface and

$\bar{H}_0$ is the monthly average extraterrestrial daily solar radiation on a horizontal surface.

Another factor considered was the month with the least energy ratio, R_e, defined as the ratio of monthly average daily solar radiation on the tilted collector surface to the monthly average daily load. Written as

$$R_e = \frac{H_T}{Q_L} \tag{3.37}$$

Where:

H_T is the monthly average daily solar radiation on the tilted collector surface (KJ/day)

Q_L is the monthly average daily load. (KJ/day).

To determine the design month, the weather data processor (type 109 component) of TRNSYS 16 software was used to generated the monthly average daily weather data and solar radiations on the surface of the collector for all months which was used as input into MATLAB programme codes as shown in appendix (A) to calculate the clearness index, $\overline{K}_T$ from (equation 3.36) and energy ratio, E_R, from (equation 3.37). The month with the least clearness index $\overline{K}_T$ and energy ratio, E_R, is considered the design month. The results obtained were tabulated and shown in Table 4.3.

3.5.3 Optimum Geometrical Parameters

To assure maximum performance, the appropriate sizing of each component in the system and operating conditions are important parameters and need to be accounted for.

The study of optimum geometrical parameters is very important in order to design for efficiency and low cost. The parameters considered in this report are optimum collector area, tube spacing, tilt angle, absorber-plate and glass cover distance, absorber plate thickness and number of glass covers.

3.5.3.1 Collector area

The amount of solar radiation received by a flat plate collector is also dependent on the area of the collector. The optimisation analysis was carried out and the optimum collector area is calculated from the programme codes developed in MATLAB programming

language (appendix B) from equations (3.15) to equation (3.25) and the results is shown in table 4.4.

3.5.3.2 *Optimum tube to tube distance and collector tube diameter*

This is an important parameter in any solar water heater collector because when the pipes are close or far apart, efficiency is affected. The optimum tube spacing (pitch) and the optimum tube diameter were determined by varying the diameter of the absorber tubes and the distance between the tubes to ascertain how it affect the efficiency of the system. The calculation is shown in appendix E which was computed using a software known as Matlab. The sort code was generated from equation(3.26) to equation (3.29).and the variation of tube diameter and the distance between the tube on the efficiency of the system is shown in figure 4.2.

3.5.3.3 Orientation angle of tilt

The amount of solar radiation received by a flat plate collector is also dependent on the orientation of the collector. A flat plate collector inclined at an angle does not only receive direct and diffused radiation but also reflection from the ground. However it was analysed on two components; diffused and direct radiation from the sky. It is to be noted here that the tilted surface does not see part of the sky and the reflection from the ground balances out the loss from that effect. Jagadash (2006) in his research carried out experiment for four different locations in India and from his result; he concluded that for maximum output which is constant throughout the life of the collector could be at an angle equal to latitude of that location. The optimisation analysis was carried out and the optimum tilt angle was calculated from the programme codes developed in MATLAB programming language (appendix E) from equations (3.1) to equation (3.9) and the results is shown in figure 4.1.

3.5.3.4 Absorber plate thickness

The thickness of the absorber plate influences the amount of solar radiation absorbed from the atmosphere, to determined the optimal thickness of the absorber plate, The optimisation analysis was carried out and the optimum absorber thickness was calculated from the programme codes developed in MATLAB programming language (appendix G). The effects of varying the absorber plate thickness on the chosen design objective function with is the efficiency of the system was studied and the result is shown on figure 4.3.

3.5.3.5 Number of glass cover

The function of a glass cover in a flat plate collector is to reduce convective losses if not completely eliminated. Researchers such as Holland (2007) carried out work on the effect of number of glass covers on the efficiency of solar collectors. Convective losses often occur between the absorber plate and the glass cover as the temperature of the plate increases. This is known as energy loss of the first kind. These losses can be reduced by using more covers. Multiple covers is associated with energy loses of the second kind resulting from absorption. The optimisation analysis was carried out and the optimum number of glass cover was calculated from the programme codes developed in MATLAB programming language (appendix H) from equations (3.15) to equation (3.25) and the results is shown in figure 4.4.

The optimisation analysis was carried out and the optimum number of glass cover was determined and it is shown in figure 4.10.

3.5.3.6 Collector absorber plate distance from the glazing material

The mode of transfer of heat from two parallel plates inclined at an angle to the horizontal is by convection and radiation. The distance between the absorber plate and glass cover is a parameter which is of great importance to minimise heat losses.

The distance between absorber plate and the glass cover affects heat loss by convection, Koutoheras (1999) after several studies concluded that the exact solution governing free convection in enclosed spaces have proved to be a difficult task. However, Saygh(2000) on the other hand based on his researches recommended a range of 4cm and 7cm as the best. Holland (2007) in his study of some problems recommended 5cm as the exact value of the distance between absorber plate and the glass cover, for this work the 5cm distanced was adopted for the design of the solar collector.

3.5.3.7 Shading

Shading is another factor which affects performance of solar collectors. Researches by Hottel and Woertz (2004) indicate that when the sun is at normal incidence to the collector, some of the side walls that support the glass cover will cast shadow on the absorber plate while those on the opposite side will add extra radiation to the other edge of the absorber plate. They recommended that the side walls should be painted white, and the outside black. For this work Aluminium sheet was used for the inside wall.

3.6 Design Consideration

The following factors were considered in the design of the solar water heater for a block of postgraduate hostel of Ahmadu Bello University, Zaria;

1. Collector tilt angle
2. The volume of hot water required.
3. Temperature of hot water attained.
4. Amount of solar radiation which is that of August.

Primary considerations are given to the cost of energy to be delivered in the design and fabrication of the solar collector. These are design cost, choices of materials, cost of construction and other necessary costs needed to build the solar collector.

Generally in design theory, in most cases where there are alternative materials meant for the same purpose, it is advisable to choose the cheaper materials so as to minimised cost and maximise profit while achieving what is required (Henry, 2010). In this work some of the materials used are such that the design and construction is reasonable and meet the basic requirement for the demand of hot water to be used in the postgraduate block in Sassakawa Hostel of Ahmadu Bello University.

3.7 Design Assumptions

In this analysis the following assumptions were made

1. The collector is in a thermally steady state.
2. The temperature drop between the top and the bottom of the absorber plate is negligible.
3. Heat flow is in one dimension through the covers as well as through the back insulation.
4. The connecting tubes cover only a small area of the collector and provide uniform flow to the tubes.
5. The sky can be treated as though it was a black body source for infrared radiation at an equivalent sky temperature
6. The radiation on the collector plate is uniform.

3.8 Design Calculation

3.8.1 Determination of total solar radiation absorbed by the collector

The formulae and equations used to determine the total solar radiation absorbed by the collector are tabulated in table 3.3.

Table 3.3 Monthly average absorbed solar radiation

INITIAL DATA	CALCULATIONS AND SKETCHES	REMARKS
n=228, Recommended days of the year	**Declination** From Equation. (3.11), the declination angle for the 16th of August, δ, is $\delta = \left(23.45sin\left(2\pi\frac{n+284}{365}\right)\right)$ $\delta = \left(23.45sin\left(2\pi\frac{228+284}{365}\right)\right)$	$\delta = 13.4550^0$
H and H_d metrological Data obtained from TMY	From Equation. (3.1) **Beam Radiation** $\bar{H}_b = \bar{H} - \bar{H}_d$ $\bar{H}_d = 160956 - 084917$	$\bar{H}_d = 76039$**J/m2. day**
$\delta = 13.4550^0$ $\emptyset = 11.2$ the latitude of location	**The Sunset Hour Angle** From Equation. (3.5) $\omega_s = cos^{-1}(-tan\emptyset tan\delta)$ $\omega_s = cos^{-1}(-tan11.2tan13.455)$	$\omega_s = 76.16^0$
$\omega_s = 76.16^0$ $\delta = 13.4550^0$ $\emptyset = 11.2$ Gsc=1367: solar constant	**Extraterrestrial Radiation** From Equation. (3.9) $H_0 = \frac{86400G_{sc}}{\pi}\left(1 + 0.033cos\left(360\frac{n}{365}\right)\right)(cos\emptyset\cos\delta\, sin\omega_s + \frac{\pi}{180}\omega_s \sin\emptyset\sin\delta)$	H_0 =37674K **J/m^2.day**
$\delta = 13.4550^0$ $\emptyset = 11.2$ $\beta = 11.2$ collector angle of inclination	**Ratio of average daily beam radiation on tilted surface to that on horizontal surface** From Equation. (3.4) $\bar{R}_b = \frac{\cos(\emptyset+\beta)\cos\delta\sin\omega_s{}^1 + (\frac{\pi}{180})\omega_s{}^1\sin(\emptyset+\beta)\sin\delta}{\cos\emptyset\cos\delta\sin\omega_s + \frac{\pi}{180}\omega_s\sin\emptyset\sin\delta}$	$\bar{R}_b = 0.9478$
$\bar{R}_b = 0.9478$ $\bar{H}_b = 084917$ $H_d = 76039$ $\bar{H}$ =160956 $\beta = 11.2$ ρ_g= 0.2	**Radiation on tilted surface** From Equation. (3.7) $H_T = (H_b)R_b + H_d\left(\frac{1+Cos\beta}{2}\right) + \bar{H}\rho_g\left(\frac{1-Cos\beta}{2}\right)$	$H_T = 24316K$**J/m2. day**

$\overline{H}$ =160956 $H_0 = 37674$	**Monthly Average Clearness Index** From Equation. (3.10) $$\bar{K}_T = \frac{\bar{H}}{\bar{H}_0}$$	$\bar{K}_T$ =0.4272
ρ_d = α =0.98:plate absorbtance	***Transmittance-Absorptance Product*** From Equation. (3.) $$(\overline{\tau\alpha})_{eff} = \frac{\overline{\tau\alpha}}{1-(1-\alpha)\rho_d}$$	$(\overline{\tau\alpha})_{eff}$ =0.9124
$\bar{R}_b = 0.9478$ $\bar{H}_b = 084917$ $H_d = 7604$ $\overline{H}$ = 160956 $\beta = 11.2$ ρ_g= 0.2 $(\overline{\tau\alpha})_{eff}$ =	***Monthly Average Absorbed Radiation*** From Equation. (3.8) $$S = (H_b)(\tau\alpha)_b R_b + H_d(\tau\alpha)_d\left(\frac{1+Cos\beta}{2}\right) + H\rho_g(\tau\alpha)_g\left(\frac{1-cos\beta}{2}\right)$$	S =12481000 **J/m².day**

3.8.2 Design calculation of heat loss in the collector

The formulae and equations used to determine the total heat loss by the collector are tabulated in table 3.4.

Table 3.4: Heat loss in the collector

Initial Data	Calculation	Remarks
K = 0.045W/mK	**Back Loss Coefficient (U)** From Equation. (3.20), $U_b = \frac{1}{R} = \frac{K}{L}$	Calculation: Appendix B
K $= 0.045W/mK$	**Collector Edge Loss Coefficient(U)** From Equation. (3.), $U_e = \frac{2Kt(L+b)}{A_c L_i}$	Calculation: Appendix B
	From Equation. (3.17), $f = (1 + 0.089h_w - 0.1166h_w\varepsilon_p)(1 + 0.07866N_G)$ $C = 520[1 - 0.000051\beta^2]$ $e = 0.430\left(1 - \frac{100}{T_{pm}}\right)$	Calculation: Appendix B
E_p=0.96;plate emmittance	**Collector Top Loss** From Equation. (3.16),	Calculation: Appendix B

E_g=0.88;glass emmittance N=1 ;number of coverglass	$U_{top} = \frac{1}{\frac{N_G}{\frac{C}{T_{pm}}\left[\frac{T_{pm}-T_a}{N_G+f}\right]^e + \frac{1}{h_w}}} + \frac{\left[\sigma({T_{pm}}^2 + {T_a}^2)\right]\left[T_a + T_{pm}\right]}{\frac{1}{\varepsilon_p + 0.00591 N_G h_w} + \frac{2N_G + f - 1 + 0.133\varepsilon_p}{\varepsilon_g} - N_G}$	
$A_b = A_t$	**Overall Heat Loss(Q_L)** From Equation. (3.), $Q_L = U_b A_b + U_e A_e + U_t A_t$ $Q_L = U_b A_b + U_t A_t$ $Q_L = A_t (U_b + U_t)$	Calculation: Appendix B Results:Table 4.4
	Collector useful energy From Equation. (3.22), $Q_u = A_C\left[S - U_L\left(T_{pm} - T_a\right)\right]^+$ OR $Q_u = F_R[S - U_L(T_i - T_a)]^+$	Calculation: Appendix B Results:Table 4.4
	Energy Absorbed By A Fluid Moving In The Tube From Equation. (3.23), $Q_u = \dot{m} C_p (T_L - T_i)$	Calculation: Appendix B Results:Table 4.4
	Collector Area From Equation. (3.25), $A_C = \frac{\dot{m} C_p (T_L - T_i)}{\left[S - U_L\left(T_{pm} - T_a\right)\right]^+}$	Calculation: Appendix B Results:Table 4.4
	Collector Fluid Mass Flow Rate From Equation. (3.29), $m = \sqrt{\frac{U_L}{K\delta}}$	Calculation: Appendix C
	Standard Fin Efficiency For Straight Fins From Equation. (3.28), $F = \frac{tanh\left[\frac{m(W-D_i)}{2}\right]}{\frac{m(W-D_i)}{2}}$	Calculation: Appendix C
	Collector Efficiency Factor From Equation. (3.27), $F' = \frac{1/U_L}{W\left[\frac{1}{U_L[D_i + (W-D_i)F]} + \frac{1}{C_b} + \frac{1}{\pi D_i h_{fi}}\right]}$	Calculation: Appendix C

3.8.3 Heat transfer through the storage tank component

The formulae and equations used to determine the total heat transferred through the storage tank component are tabulated in table 3.5.

Table 3.5: Heat transfer through the storage Tank

Initials Data	Calculations	Remarks
	Coefficient of Heat Loss throughinsulation of the surfaces (U_s). From Equation. (3.32), $U_s = \frac{1}{R} = \frac{K}{L}$	Calculation: Appendix D
	Resistance due to convection Between Outer cylinder and the sky(R_2) From Equation. (3.33), $R_2 = \frac{1}{h_w}$	Calculation: Appendix D
	Top loss from cylinder U_t From Equation. (3.34), $U_t = \left\{ \frac{1}{\frac{1}{R_2} + \frac{1}{R_3}} \right\}^{-1}$	Calculation: Appendix D Results: Table 4.5
	Total loss from storage Tank From Equation. (3.5), Heat loss through Curved Surfaces Heat loss through bottom or top surface Total heat loss through insulation is $U_T = U_t + U_s$	Calculation: Appendix D Results: Table 4.5

3.9 Simulation and Validation of the Solar Water Heater

Simulation is very vital in the design of any solar device. TRNSYS (Transient System Simulation) is used to model and simulate the performance of the solar water heating system.

A model is always a simplification of the complex reality of natural phenomena. This simplification has the merit of representing the reality in all its extents. However, the constructed system model may not be capable of producing a response that is entirely in

line with the behaviour of the observed phenomenon (Julien *et al.*, 2013). The system schematic model used for simulation is shown in figure 3.3

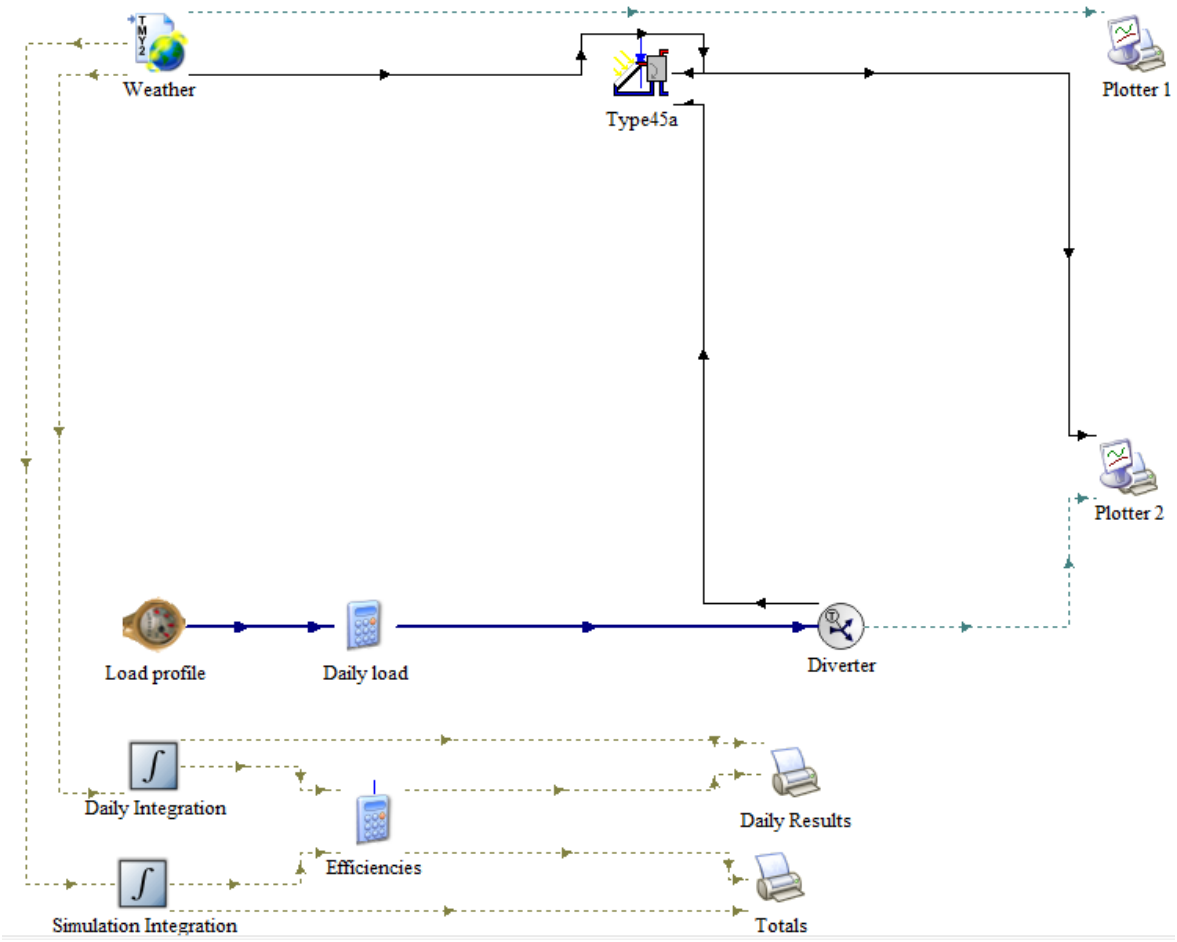


Figure 3.3 Schematic model of simulation studio

The performance of the solar water heating system was numerically simulated by TRNSYS 16 software using the Typical Meteorological Year (TMY) weather data of Zaria.

The flow chart for the simulation of the performance of the thermosyphon water heating system in a TRNSYS software simulation studio is shown in figure 3.4.

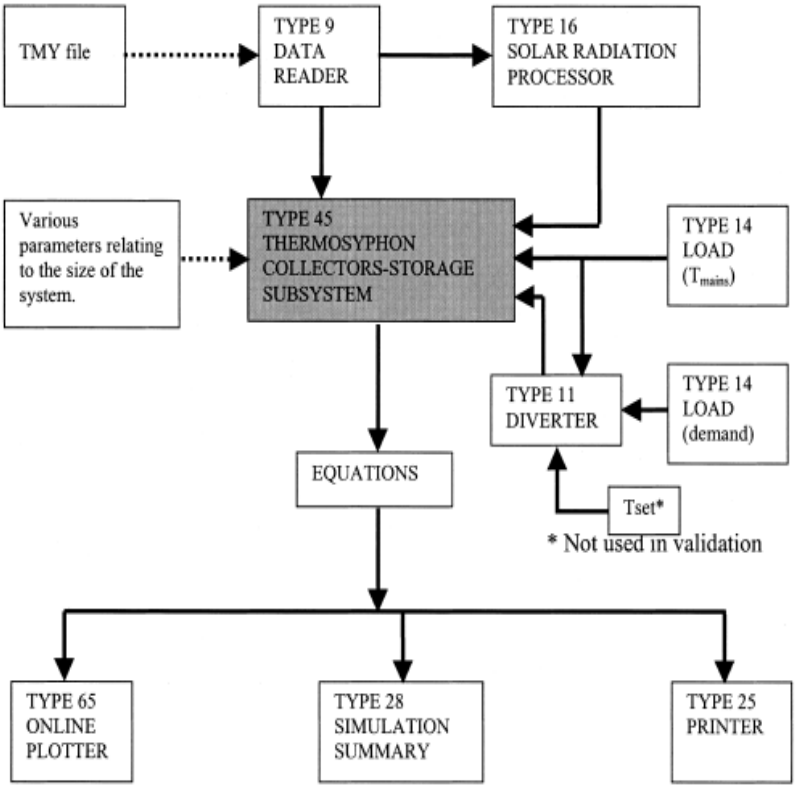


Figure.3.4: Information flow diagram for the simulation of the thermosyphon solar water heating system. (Soteris and Christos 2000)

The optimization of the system component was also conducted using TRNSYS 16, the software simulate and predict the system performance (load temperature) using different system component sizes as shown in table 3.6. the weather data output was connected to the collector input as shown in table 3.7 and the software used has the graphical ability to visualise the effect of varying the components sizes on the objective function (load temperature) and show the result on the plotter as shown in table 3.8 . The set of components sizes and system design parameters which meet system design load (load temperature) after simulation were chosen as the final adopted system component size as presented in Table 4.7.

When the preliminary viability were established, it was necessary to evaluate system performance to generate more precise engineering data and economic analysis. The result of the simulation is shown in figure 4.5

Table 3.6: Parameters for the Collector

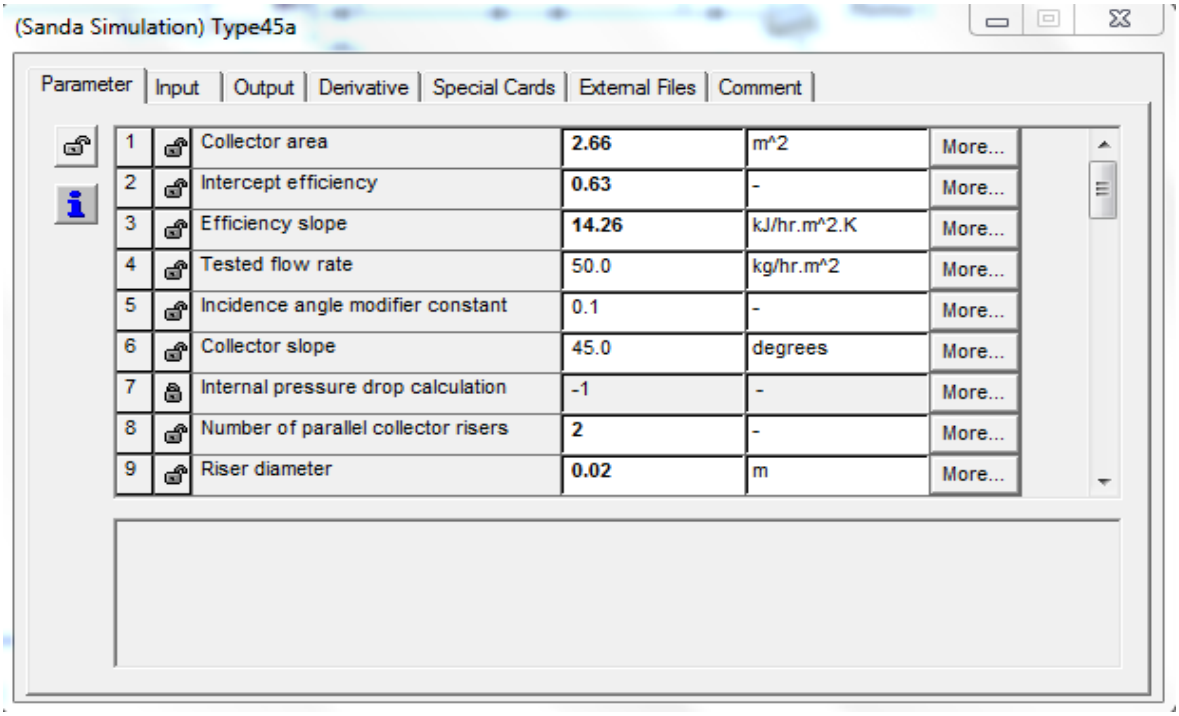


Table 3.7: Connection of the weather data with input of collector

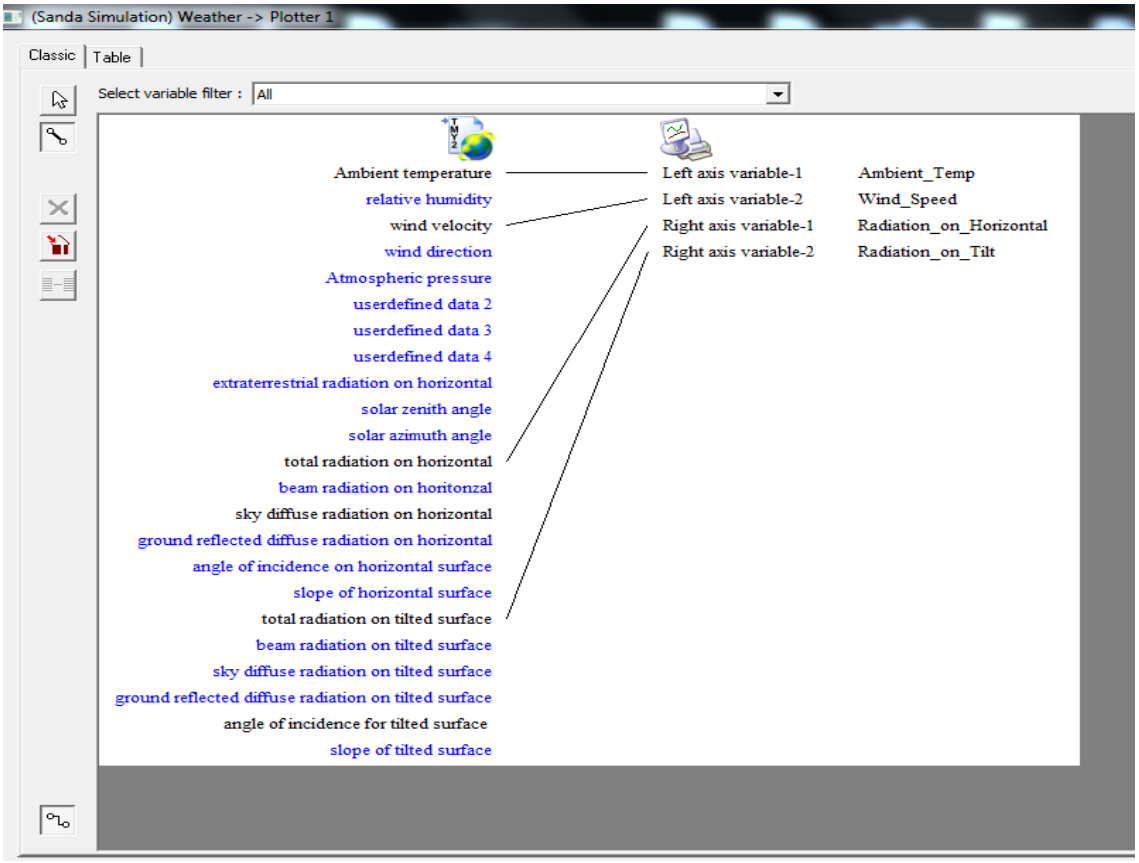
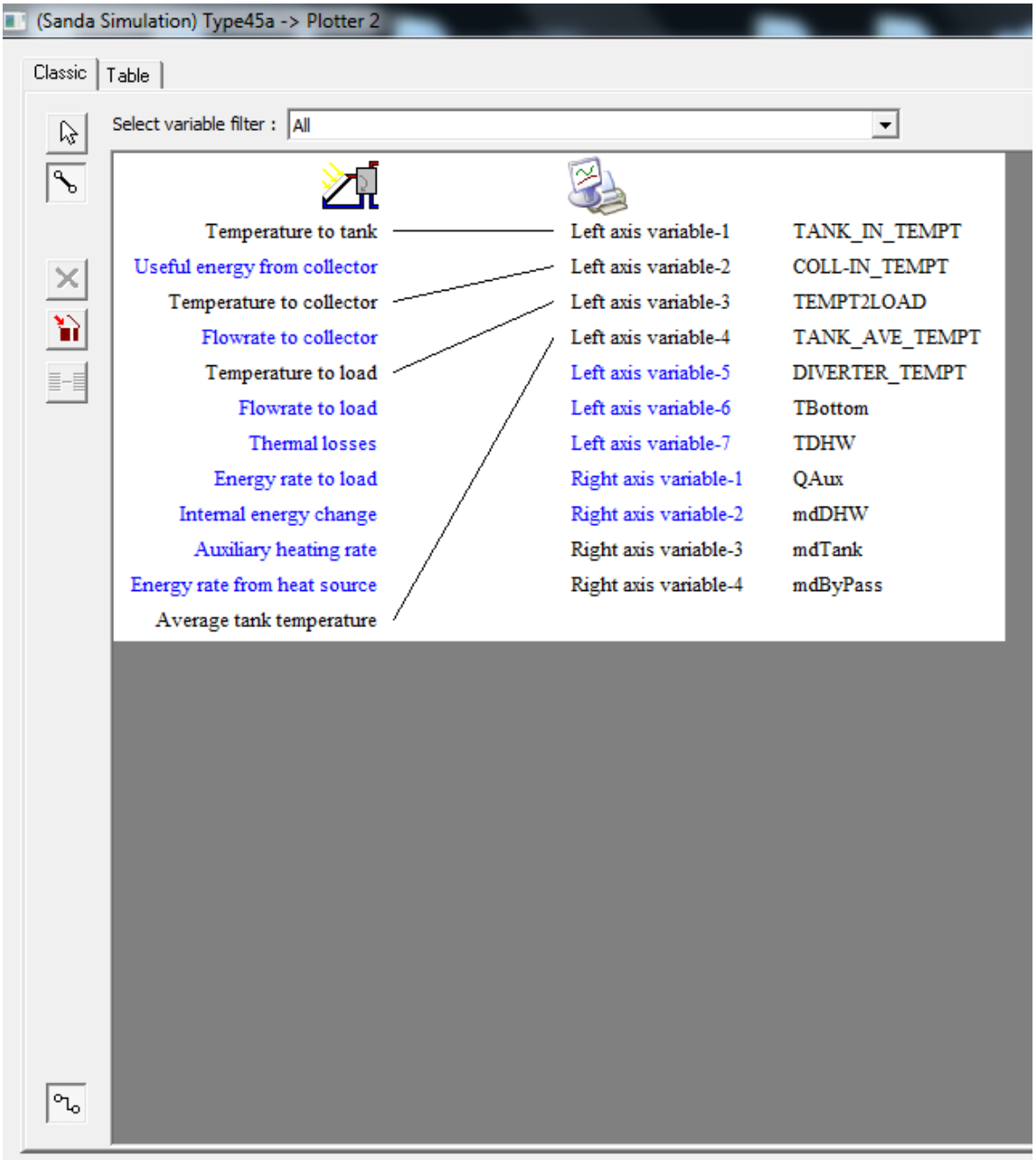


Table 3.8: Connections of the output of collector with the plotter.



3.10 Fabrication, Costing and Testing.

The solar water heater was made up of fourteen (14) 20mm radius copper pipe risers connected to two (2)20mm radius copper pipe (headers).Based on the preliminaries experiment carried out as recommended by (Zwalnan, 2015) the system performance is much better when the copper tubes are placed on the absorber plate as shown in appendix L. The copper tubes absorb heat directly from the sun and also from the absorber plate and

transport the water to the storage tank. Riser pipes are placed together vertically with a spacing of 100mm and each was connected to the lower and upper header pipes which are on the lower sides and upper sides of the riser pipes, as shown in appendix K. This assembly was fixed rigidly to an Aluminium plate of thickness 3mm and placed in a wooden housing, the assembly was insulated with 50mm thick layer of fibre glass(Fibre glass has density of 32kg/m and a thermal conductivity 0.0002kW/mC) (Holland 2007). The top of the housing is covered with 4.00mm thick clear glass serving as glazing.

3.10.1 Fabrication

The construction of the Solar water heater can be divided into

1. The heating system
2. The collector box
3. The storage tank

3.10.1.1. The heating system

The heating system consist of the following

i. A 700mm x 600mm absorber plate
ii. Copper pipes of 20mm external diameter and 600mm long(Riser pipes)
iii. Two copper pipes of 20mm external diameter and 800mm long (Header pipes)
iv. Fibre glass insulation below the copper plate
v. Cover glass to minimise heat loss by convection

The two header pipes were cut to the length of 700mm and 20mm diameter holes were drilled on one side of each of the header pipes at an interval of 100mm. The fourteen risers' pipes were fitted into 20mm holes on the two header pipes. The pipes were all brazed together and placed on a 3mm alluminium plate (700mm x 600mm).

3.10.1.2. The collector box

A 700mmx 600mm box was made of 50mm thick plywood; it was constructed with an open top. Fibre glass was placed on the bottom inner surface of the box and the collector plate/pipe assembly was placed on top of the insulation. A glass was placed on top of the box as glazing.

Cold water enters the piping assembly and is heated by the system and the hot water is taken to the storage unit. The arrangement was in such way that the inlet pipe is connected to one header pipe at one end and the outlet pipe to the other header pipe diagonally. The other ends of the header pipes were sealed. The rubber pipe that passes the hot water to the storage tank was insulated with fibre glass to reduce heat losses.

3.10.1.3. Storage tank

The storage tank consists of two concent.ric cylindrical tanks. The smaller one is enclosed in the bigger one. An insulation material was placed between the two tanks to reduce heat losses to the surroundings. Fibre glass is used as the insulation material. Two 12mm radius PVC pipes are fitted at the top of the tank from the collector and the other one is used to extract hot water from the tank. At the base of the inner tank is another pipe of the same dimension. This is to convey cold water to the collector. This arrangement is done because the cold water will always be at the bottom of the tank and the hot water on the top. The inner tank is made of polyvinyl chloride (PVC) and outer tank is made of galvanised steel. The capacity of the storage tank is 200 litres. The solar water heater was constructed in accordance to optimal system size and dimension whose characteristics and configurations are as described in Figure 3.1, Tables 4.3 and Table 4.4, the different component where constructed in Department of Mechanical Engineering, Workshop, Ahmadu Bello University Zaria. The component where assembled on the rooftop of the Block K of

Sassakawa Postgraduate hostel as shown in the working and assembly drawings (appendix K). The constructed thermosyphon solar water heating system was installed on Block K rooftop of Sassakawa hostel. The tilt of the collector with respect to the horizontal plane is 11.2^{o} towards south. A picture of the setup is shown in Plate 12 of appendix F. The experiments were carried out on the rooftop of the Hostel.

3.10.2 Cost of Solar Water Heater

One of the major objectives of this work is to reduce the cost of fabrication to the minimum taking efficiency into consideration. However, different factors affect the cost of fabrication. These factors include: quality of materials, size of materials used and cost of labour overheads. In selecting materials a balance was struck between optimum efficiency and economic costs, dimensions of materials required have already been determined, and so the actual amounts of material required are known. This involves pipe spacing, plate dimensions, tank dimension etc. Variations in these parameters results into increase or decrease in cost, performance efficiency and capacity. Thus, reasonable spacing, materials and costing were made.

The costs of materials used in fabrication are given in table 3.5.

Table 3.9: Details of costs of material used in fabricating the solar water heater

Materials	Amount Required		Cost(N)	
	Dimensions	Quantity	Unit Price N	Total Price N
Plywood	2mmX1200mmX2000mm	2	1000	2000
Glass materials	4mmX1595mmX1195mm	1	8000	8000
fiber glass	Roll	1	15000	15000
Angle Iron	1550 mm long,	4	1500	6000
Copper tubes	15mmDia5mmX1595mmX	2	5000	10000
Aluminum sheet	1195mm5mmX1595mmX	2	1500	3000
;Galvanized Steel	1195mm 2000mm long,	2	4000	8000
Paint	15mm	2	1500	3000
Thinner	Tin	3	1000	3000
Nut and Bolt	Tin		600	600
Asbestos			1000	1000
Plastic pipes		5	700	3500
Pvc Tank	Pipes	2	5000	10000
Pvc Gum	Drum	2	300	600
Wood	Tin	2	1100	2200
Silicon Gum	2mmX1200mmX2000mm	3	1000	3000
Aradyle gum	Tube	2	300	600
Acytelene Gas	Tube		2000	2000
Cobalt			2000	2000
Pvc fittings			3000	3000
Gas hose			2000	2000
Ball valve		2	500	1000
Clips		10	50	500
Workmanship				20000
Miscellaneous				10000
Total				**115,900.00**

3.10.3 Testing of solar water heater

During the test period, experiment was started and completed by measuring the inlet and outlet water temperatures of the solar collector and the solar radiation at one hour intervals

3.10.3.1 Test rig and instrumentation

The instruments and components used are as follows: A digital thermometer, six (6) Thermocouple wires, and one (1) solarimeter. The parameters measured were the ambient temperature, collector inlet, and outlet temperature. The ambient air was measured. The energy received from the sun on the collector as incident global solar radiation expressed in Joule per square metre. Day, was obtained using a solarimeter. Figure 3.5 shows the experimental setup of the solar water heater.



Figure 3.5: Experimental setup of the solar water heater

3.10.3.2 Test Procedure

During the test period, solar radiation intensity, ambient temperature, collector inlet and outlet temperatures, were measured at hourly intervals for the performance analysis of the solar water heater. The testing was done in the month of August for three days. The solar water heater was placed outside with the collector facing the direction of the sun.

The general layout of the experiment consisted of the following:

- The flat plate collector facing south and set to the required angle of latitude (11.2 N). This is the latitude of Zaria, the location where the experiments were carried out.
- The outlet of the 200litres tank was connected to the inlet of the collector through tubes while the outlet of the collector was connected back to the inlet of the tank. The system was run for three days from 8.00 am to 5.00pm daily. The instrumentation included thermocouple, mercury-glass-thermometer, solarimeter and Infra-red Thermometer which was used to measure the daily water temperatures for the collector inlet and the collector outlet water and also the ambient temperature. A hygrometer was used for the relative humidity as well as the surrounding air temperature

3.11 Validation of simulation with the experimented

The validity of the theory adopted in this study is further fortified by comparing the simulated and experimental storage tank inlet and outlet temperatures. The standard deviations (SD), relative errors (RE)and Nash-Sutcliffe Coefficient of Efficiency (NSE) between simulated and experimental storage tank inlet and outlet temperatures are defined below.

The Standard deviation was used to determine the level of deviation of the predicted results from the actual results. The Standard Deviation measures the quality of fit between the actual data and the predicted model (Julien *et al.*, 2013).

The Standard Deviation of a model prediction with respect to the estimated variable X_{model} is defined as the square root of the mean squared error (Neil, 2010).

$$SD = \sqrt{\frac{\sum_{i=1}^{n}(X_{obs,i} - X_{model,i})^2}{n}} \qquad (3.38)$$

Where

X_{obs} is observed values

X_{model} is modelled values

The lower the Mean Absolute Error or the Bias Percentage value, the better the performance of the model (Neil, 2010).

Furthermore, the Nash-Sutcliffe Coefficient of Efficiency (NSE) defined as follows:

$$NSE = 1 - \frac{\sum_{i=1}^{n}(X_{obs,i} - X_{model})^2}{\sum_{i=1}^{n}(X_{obs,i} - \overline{X_{obs}})^2}, \quad (3.39)$$

Where:

X_{obs} is observed value

X_{model} is modelled value

NSE is generally used to quantitatively describe the accuracy of model outputs. Nash-Sutcliffe efficiencies can range from -∞ to 1. An efficiency of 1 (NSE = 1) corresponds to a perfect match between model and observations. An efficiency of 0 indicates that the model predictions are as accurate as the mean of the observed data, whereas an efficiency less than zero (-∞< E < 0) occurs when the observed mean is a better predictor than the model (Julien *et al.*, 2013).

And also the Relative Error is defined as:

$$RE = \left| \sum_{i=1}^{N}[\boldsymbol{X_{Model}} - \boldsymbol{X_{Obs}}]^2 \right| \ / \ \sum_{i=1}^{N}[\boldsymbol{X_{Model}}] \times 100\% \quad (3.40)$$

Where:

X_{obs} is observed value

X_{model} is modelled value

RE is a statistical tool which is use to determine the accuracy or the error between two compared parameters

CHAPTER FOUR

4.0 RESULTS AND DISCUSSION

4.1 Meteorological and Simulated Solar Data for Zaria and Solar Water Heater Design Parameter

The meteorological data (monthly average daily weather condition of the recommended days of the year) for Zaria, Nigeria (lat. 11.2^{o} N and Long. 7.8^{o} E) is shown on table 4.1. The data was used for the system design calculations.

Table 4.1 Zaria Meteorological data

MONTH	**Recommended days(n)**	**H(J/m^2.day)**	**H_b(J/m^2.day)**	**T_{MAX}(^{0}C)**	**T_{MIN}(^{0}C)**	**T_a(^{0}C)**	**V(m/s)**
JAN	17	22.6584	18.4258	38	16	30.8	2.60
FEB	47	24.8544	19.8700	38	16	28.3	2.57
MAR	75	27.0252	21.4865	40	20	30.7	2.70
APR	105	28.2096	19.9061	32	15	31.2	2.31
MAY	135	18.0144	12.5005	35	22	26.9	2.80
JUNE	162	23.6448	12.2875	32	29	29.1	3.50
JULY	198	18.1250	10.8131	26	18	22.4	2.91
AUG	228	16.0956	08.4917	28	18	24.9	3.08
SEPT	258	24.3108	11.3271	32	20	26.9	1.56
OCT	288	22.2516	14.8025	36	20	27.0	2.57
NOV	318	21.5352	17.2977	35	18	26.4	3.39
DEC	344	22.2317	17.1816	33	17	26.3	2.00

Source:TYPE 109 of TRNSYS 16 software

The meteorological data tabulated in table 4.1 was evaluated to obtain some important parameters which are used for the design calculations, the results are shown in table 4.2.

Table 4.2 Simulated Solar Data for Zaria

MONTH	$\mathbf{R_b}$	$\mathbf{H_o(J/m^2.day)}$	$\mathbf{H_d(J/m^2.day)}$	**Declination**	h_w **(W/m²k)**	h_{fi} **(W/m²k)**
JAN	1.1499	31415000	4233000	-20.9170	10.6000	153.8247
FEB	1.0956	34167000	4948000	-12.9546	10.5100	154.4486
MAR	1.0329	36695000	5539000	-02.4177	10.9000	151.8872
APR	0.9689	37982000	8304000	09.4149	09.7300	152.8683
MAY	0.9200	37814000	5514000	18.7919	11.2000	151.8872
JUNE	0.8973	37351000	1135700	23.0859	13.3000	149.8507
JULY	0.9074	37404000	7312000	21.1837	11.5300	150.5406
AUG	0.9478	37674000	7604000	13.4550	12.0400	151.8872
SEPT	1.0073	36967000	1298400	02.2169	07.4800	153.1898
OCT	1.0748	34747000	7449000	-9.5994	10.5100	152.8683
NOV	1.1354	31963000	4238000	-18.9120	12.9700	216.7242
DEC	1.1660	30477000	5056000	-23.0496	08.8000	152.2170

Source: Calculated by the Researcher

Table 4.3. shows the energy received on the surface of the collector and also the parameters that's are used to determine the design month, from the table it is shown that the month of August has the lowest clearness index which means it has the least among of solar radiation and also the energy ratio of the month of august is the least, therefore from the results of these parameters August was used as the design month.

Table 4.3 Monthly average daily system design for determination of design month

MONTHS	S_R(J/m^2.day)	H_T(J/m^2.day)	H_o(J/m^2.day)	Q_{LOAD}(J/m^2.day)	K_T	R_E
JAN	20679000	25423000	31415000	11061600	0.7213	2.2983
FEB	21799000	26754000	34167000	11061600	0.7274	2.4186
MAR	22667000	27731000	36695000	10056000	0.7365	2.7577
APR	22338000	27566000	37982000	14078400	0.7427	1.9580
MAY	13716000	16996000	37814000	12570000	0.4764	1.3521
JUNE	17762000	22319000	37351000	14078400	0.6330	1.5854
JULY	13677000	17088000	37404000	17095200	0.4846	0.9996
AUGUST	12481000	15611000	37674000	16089600	0.4272	0.9702
SEPT	19403000	24316000	36967000	14078400	0.6576	1.7272
OCT	18872000	23330000	34747000	12067200	0.6404	1.9333
NOV	19468000	23879000	31963000	12570000	0.6738	1.8997
DEC	20357000	25083000	30477000	13575600	0.7296	1.8476

Generated from the appendix A-E by the researcher

Table 4.4 shows the system monthly average daily design load Q_{load} , the system monthly average daily design energy loss Q_{LOSS} (J/m^2.day), system monthly average daily design energy used Q_{use}, and the total collector area Ac require to meet the system monthly average daily design load . from the table 4.4 the month of August has the largest collector Area based on the facts that's it has the least clearest index and energy ratio, therefore the collector area of the month of August was used as the Collector area to assured all year round validity of the system.

Table 4.4 Monthly average daily system design for Determination of Collector Area

MONTHS	S_R(J/m^2.day)	H_T(J/m^2.day)	Q_{LOAD}(J/m^2.day)	Q_{LOSS}(J/m^2.day)	Q_U(J/m^2.day)	A_c
JAN	20679000	25423000	11061600	84295000	12249000	0.9030
FEB	21799000	26754000	11061600	84237000	13375000	0.8270
MAR	22667000	27731000	10056000	85055000	14161000	0.7101
APR	22338000	27566000	14078400	82146000	14124000	0.9968
MAY	13716000	16996000	12570000	83849000	05331000	2.3579
JUNE	17762000	22319000	14078400	84432000	09319000	1.5108
JULY	13677000	17088000	17095200	81670000	05510000	2.5025
AUGUST	12481000	15611000	16089600	82506000	04230000	2.6035
SEPT	19403000	24316000	14078400	80973000	11306000	1.2452
OCT	18872000	23330000	12067200	83684000	10504000	1.1488
NOV	19468000	23879000	12570000	85047000	10963000	1.1465
DEC	20357000	25083000	13575600	81887000	12169000	1.1156
AVERAGE						1.5723093

Source: Generated from the appendix G-J by the researcher.

Table 4.5 shows the system design parameters considering the month with the least energy ratio and clearness index for the solar water heater system to meet all year round hot water load, and it has been established from table 4.3 the month of August has the least energy ratio and clearness index.

Table 4.5 System design parameters

MONTHS	F_R	$\tau\alpha$	U_L(W/m^{2}k)	U_t(W/m^{2}k)	$F_R U_L$	$F_R\,\tau\alpha$
JAN	0.8456	0.9081	84606	0.1303	7.1543	0.7679
FEB	0.8635	0.9107	8.4982	0.1304	7.3382	0.7864
MAR	0.8889	0.9142	8.6581	0.1300	7.6962	0.8126
APR	0.8325	0.9130	8.2176	0.1310	6.8412	0.7580
MAY	0.5863	0.9105	8.1307	0.1298	4.7670	0.5338
JUNE	0.7198	0.9081	8.2851	0.1280	5.9636	0.6536
JULY	0.5058	0.9088	7.8859	0.1295	3.9887	0.4597
AUGUST	0.4356	0.9124	7.9383	0.1290	3.4579	0.3974
SEPT	0.7844	0.9142	8.0244	0.1331	6.2943	0.7171
OCT	0.7938	0.9124	8.3040	0.1304	6.5917	0.7243
NOV	0.7896	0.9107	8.4308	0.1282	6.6570	0.7191
DEC	0.8076	0.9081	8.1485	0.1319	6.5807	0.7334

4.2 Collector Tilt Angle (β)

The tilt angle of the solar collector greatly influences the amount of solar radiation the solar collector received from the sun, fig 4.1 shows that the angle at which this collector received the highest solar radiation is approximately 11.2 ^{0} which is the latitude of Zaria as confirm by (Soteris, 2009); the highest solar radiation is received at angle of the collector equal to the latitude of the location. Therefore for this work the 11.2^0 was used as the optimum collector tilt angle with is the same with the latitude of the location (Zaria).

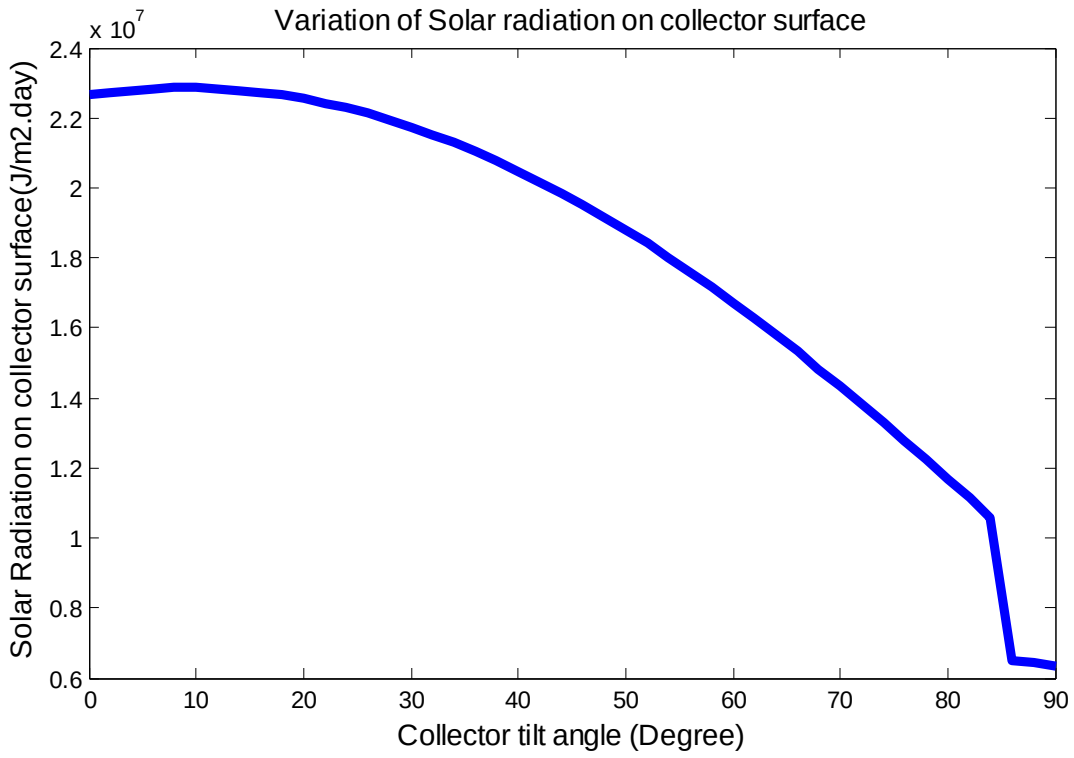


Fig. 4.1 The variation of collectors tilt angle on the absorption of solar radiation.

4.3 Collector Tube Diameter and Centre to Centre Distance.

Fig 4.2 shows how varying the center to center distance and the diameter of the collector tubes affects the efficiency of the system, increasing the distance from 0-0.4m affected the efficiency of (05-15mm diameter tubes) diameters of the tubes by decreasing the efficiency and increasing the efficiency of (25-50mm diameter tubes) to the highest efficiency and further increase in the center to center distance from 0.4m to 02m will lead to uniform decrease in the efficiency of the system. For this work the tube 20mm diameter was used because it ability to achieved the desired result and also its availability in the market and a center to center distance of 0.1m because it corresponded to the point where the maximum efficiency of the 20mm tube is achieved.

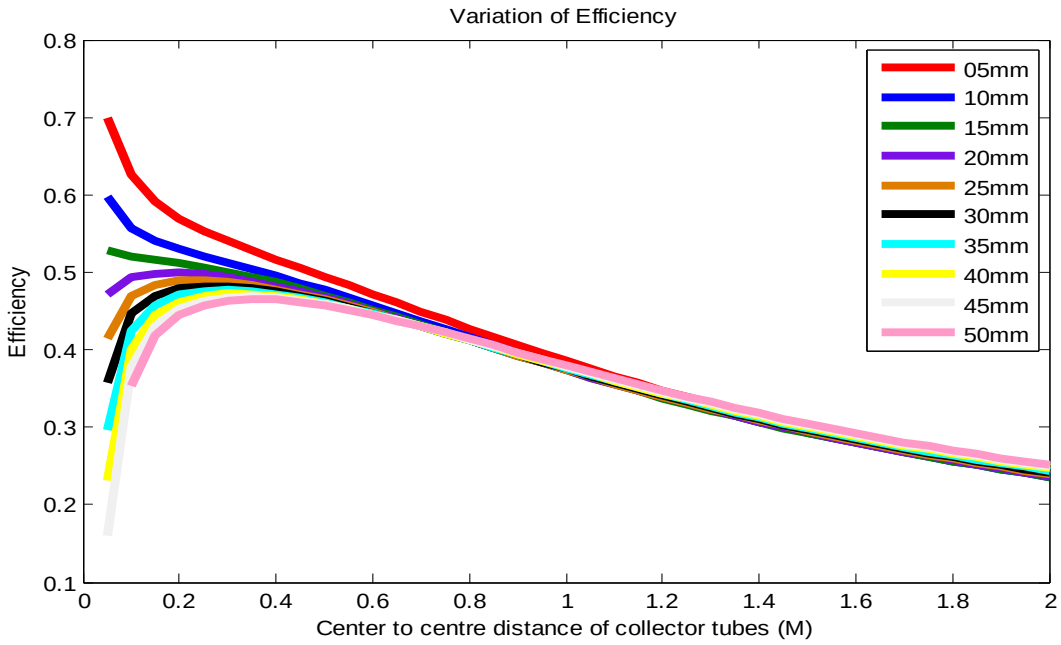


Fig. 4.2 The variation of center to center distance and the diameter of the collector tubes on the system efficiency

4.4 Collector Absorber Plate Thickness

Fig 4.3 shows how varying the collector absorber plate thickness affects the efficiency of the system, increased in thickness of the absorber plate leads to increase in efficiency to a point where it reaches the maximum point, from that point the efficiency approximately remain constant despite the increment of the thickness of the absorber plate, for optimum absorber plate a thickness of 0.003m was used for this work due to its availability and cost but not at the expenses of the efficiency of the system.

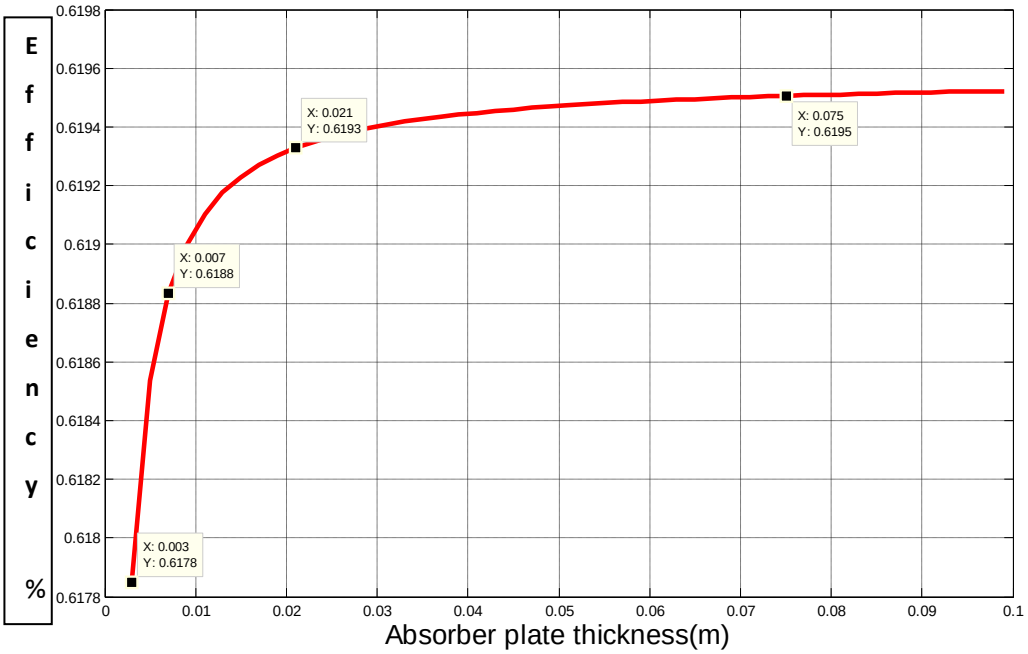


Fig. 4.3 The variation of the Absorber Plate Thickness of the collector with the system efficiency.

4.5 Collector Number of Glazing

Fig 4.4 shows how different number of the collector glazing can affect the performance of the system, from the figure below it is clearly shown that increase in the number of glazing will automatically lead to increase in thermal efficiency of the system and inversely affect the solar radiation absorption of the system, therefore to strike a balance and also considering the cost, a single glazing was used for this work.

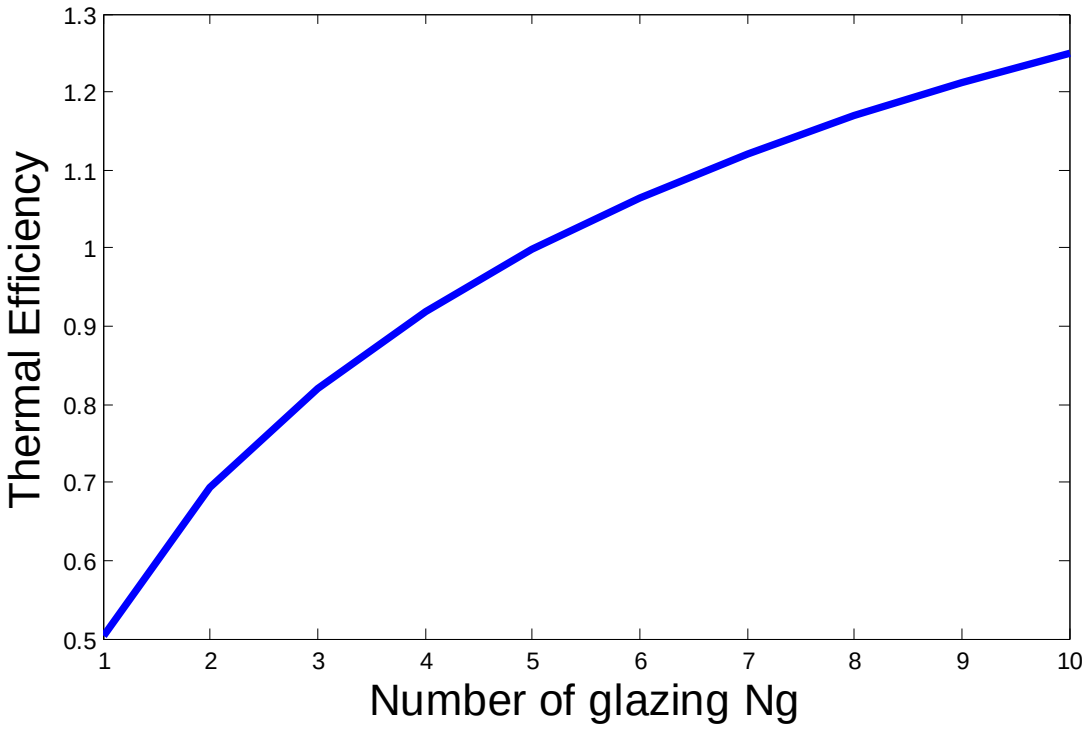


Fig. 4.4 The variation of the number of glazing with the system efficiency.

4.6 System Optimum Parameters and Simulation

Fig 4.5 shows the result of the simulation of the system (Annual variation of hourly solar radiation on a tilted surface) the overall aim of the simulation is to ensure the validity of the system, from fig 4.5 it is shown that the system is valid and the desired temperature will achieved in almost all the month in the year, less auxiliary energy is required to

compliment the desired temperature only for months like August and July..

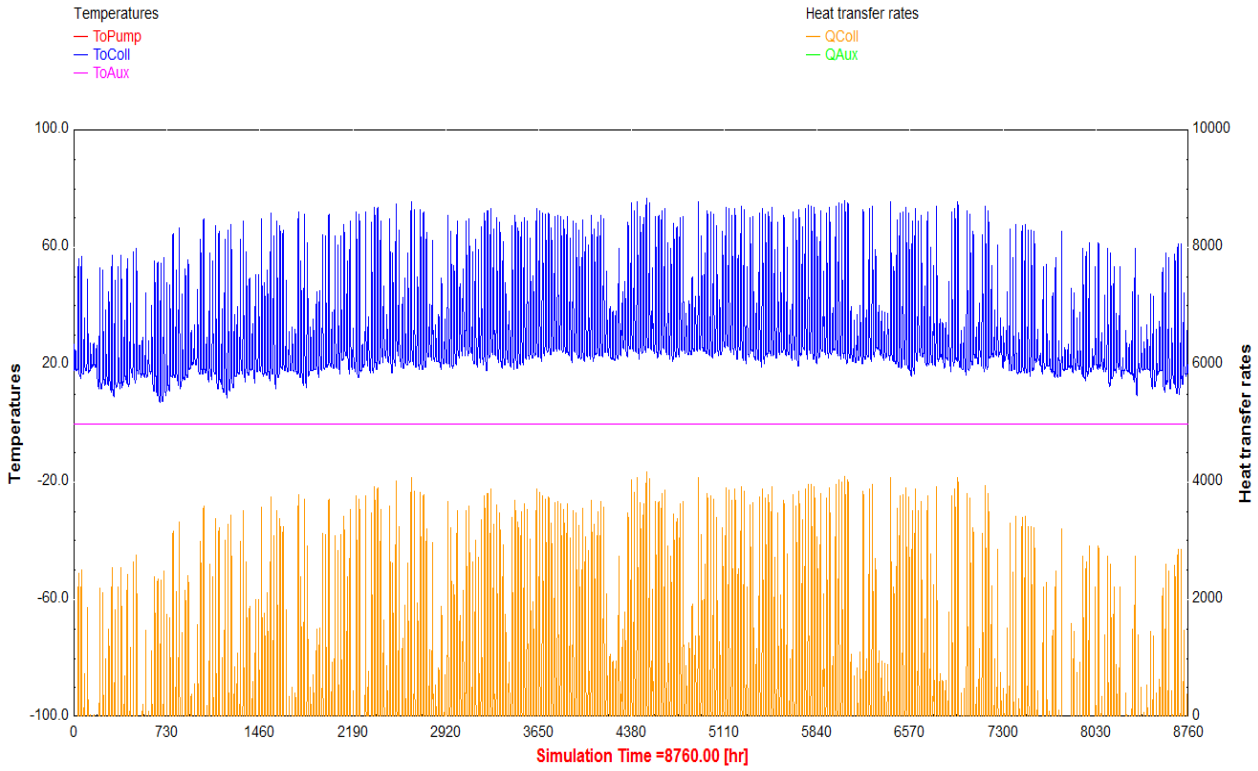


Fig 4.5a Annual variation of hourly Solar Radiation on a tilted surface with tilt angle of $11.2^{0.}$

The final system characteristics and design parameters adopted for the system performance simulation using TRNSYS 16 software are shown in Table 4.6 and Table 4.7.

Table 4.6: System characteristics

Description	**Value/Type**
Storage tank capacity	200L
Number of riser	14
Riser tubes material	Copper
Total aperture area	2.66 m^2
Absorber surface	Painted matt black
Glass type	4 mm low iron glass
Collector insulation	50 mm fibre glass thick for both sides and back insulation.

Table 4.7: System final optimum design parameters and components size.

Parameter	Description	Values
A_C	Collector area (m^2)	2.66
$F_R(\tau\alpha)_n$	Intercept of the efficiency vs. (Ti-Ta)/I_T curve	0.63
$F_R U_L$	Negative of the slope of the efficiency vs. (Ti-Ta)/I_T (kJ/h m^2 C)	14.26
β	Collector slope (degrees)	12.0
N_R	Number of parallel collector risers	14
d_R	Riser diameter (m)	0.02
H_d	Header diameter (m)	0.02
H	Header length (m)	1.75
h_c	Vertical distance between collector outlet and inlet (m)	0.40
h_o	Vertical distance between outlet of tank and inlet of collector (m)	0.58
d_i	Diameter of collector inlet pipe (m)	0.02
L_i	Length of collector inlet pipe (m)	2.45
NB_1	Number of right angle bends (or equivalent) in inlet pipe	2
U_i	Loss coefficient of collector inlet pipe plus insulation (kJ/h m^{2o}C)	0.625
L_o	Length of collector outlet piping (m)	1.05
NB_2	Number of right angle bends (or equivalent) in collector outlet piping	2
U_o	Loss coefficient of collector outlet pipe plus insulation (kJ/h m^{2o}C)	0.625
V_t	Tank volume (m^3)	0.200
H_t	Tank height (if vertical) or diameter (if horizontal) (m)	0.60
H_R	Height of collector return to tank above bottom of tank (m)	0.50

4.7 System Performance Evaluation

The performance of the system was evaluated, by comparing the simulated and the experimental collector efficiency. The hourly collector efficiency of 28th August 2015 was calculated from equation (3.31), the experimental result was compared with the simulated

result and the result is shown in Figure 4.8, which shown that experimental collector efficiency deviated from the simulated collector efficiency, due to the fact that the software cannot predict the weather condition exactly because of it random nature. The Figure 4.18 also shows the simulated collector efficiency increases from 16% at 8.00am reaches its highest value of 58% at 11.00am and decreases back to 22% at 5.00pm, on the other hand, the experimental collector efficiency increases from 24% at 8.00am reaches its highest value of 71% at 10.00am and decreases back to 19% at 5.00pm. From figure 4.8 it can be concluded that, the highest collector efficiency is 71% and at 10.00am and the simulated collector efficiency is less than the experimental collector efficiency

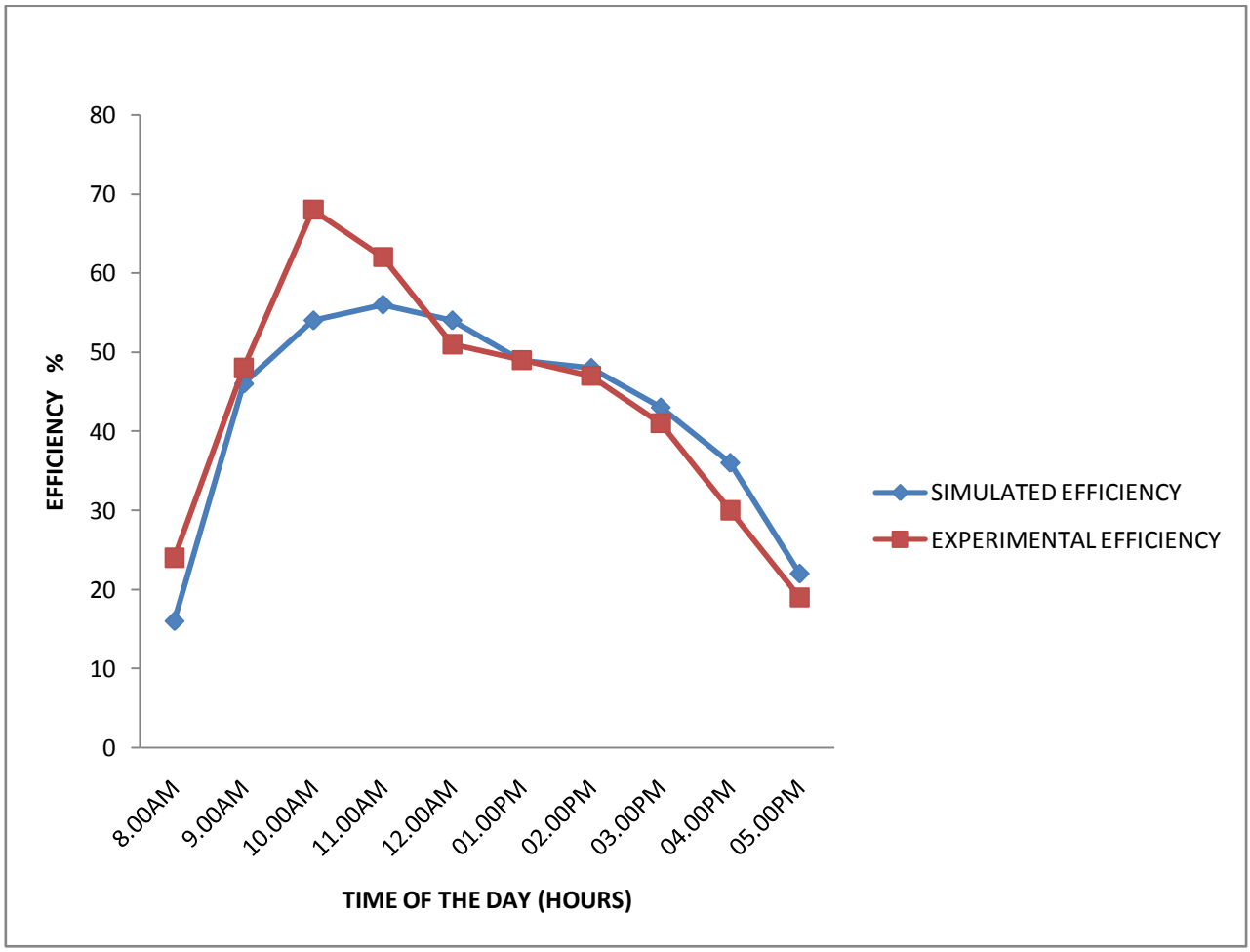


Figure 4.5b: Comparison of solar collector simulated efficiency with experimental efficiency.

4.8 Comparison of experimental results with result obtain from simulation and determining the Authenticity of the simulation software (TRNSYS 16)

The validity of the simulation software used in this study is further fortified by comparing the predicted daily average hourly collector temperature with the experimental daily hourly temperature.

4.8.1 Comparison and Validation of simulated ambient temperature with experimental ambient temperature.

The comparison between the experimental hourly ambient temperature and simulated which was predicted from the model (solar data processor, Type 109 of TRNSYS). Is shown in Figures 4.6, figure 4.7 and figure 4.8. for the three days of the experiment.

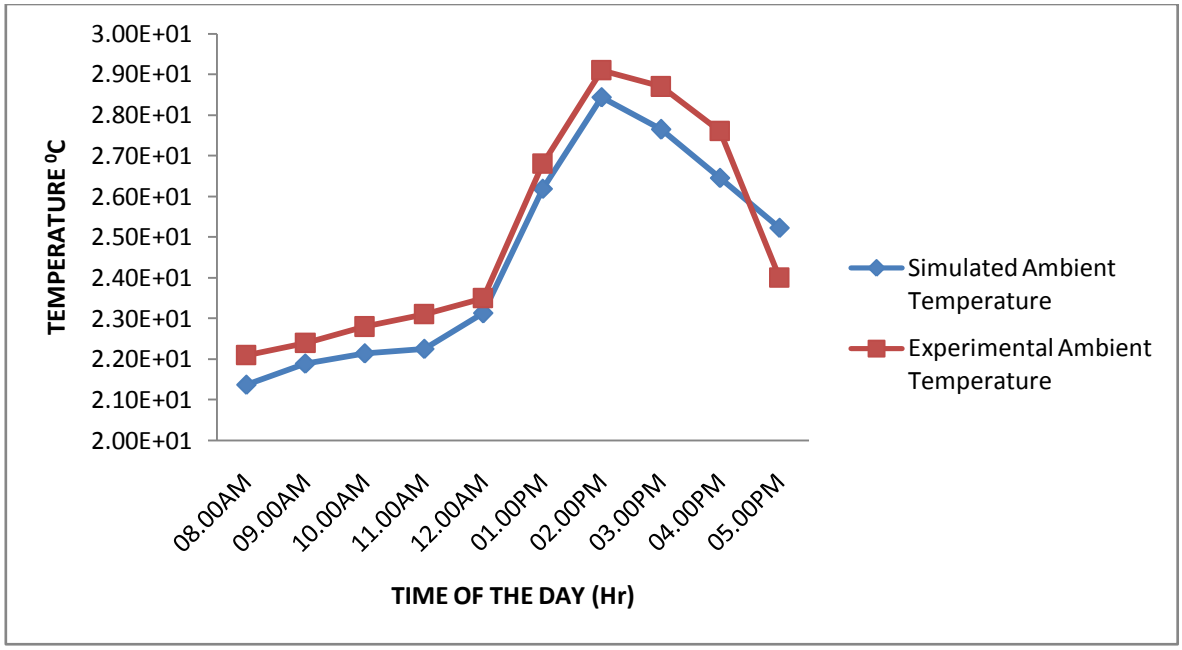


Figure 4.6: Comparison of hourly Ambient Temperature of Zaria obtained during the experiment with the values generated using TRNSYS 16 software. (28 August2015)

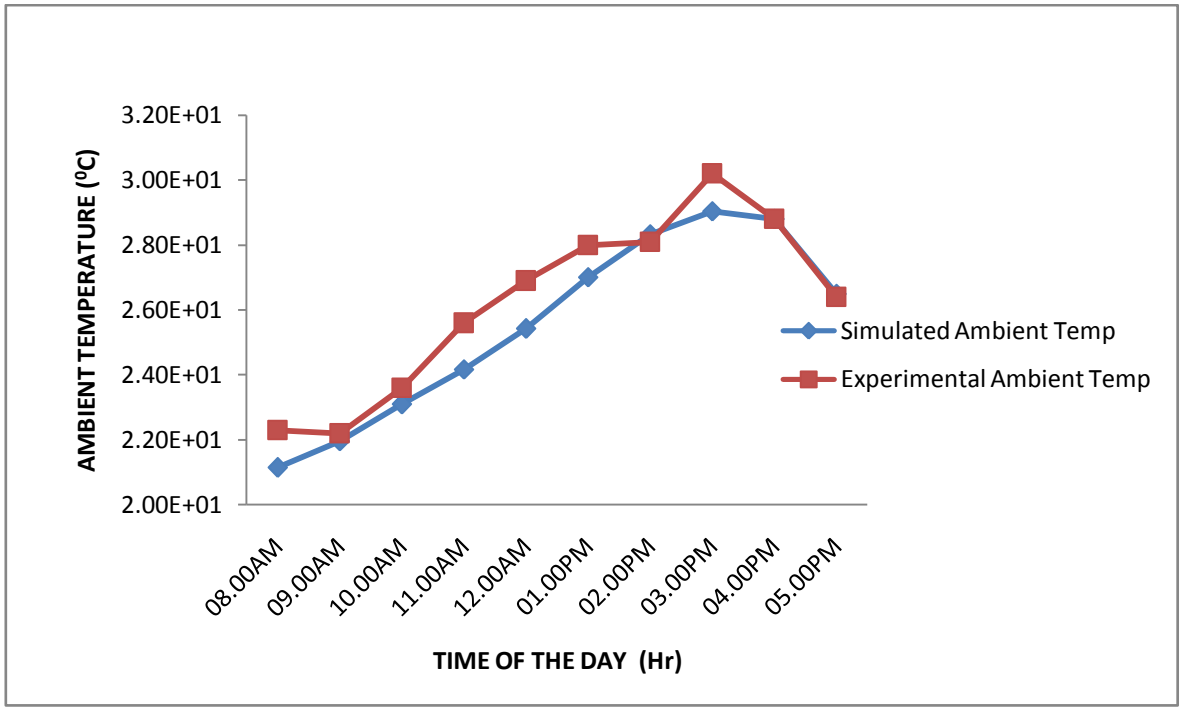


Figure 4.7: Comparison of hourly Ambient Temperature of Zaria recorded during the experiment with the values obtained using TRNSYS 16 software. (29 August, 2015.)

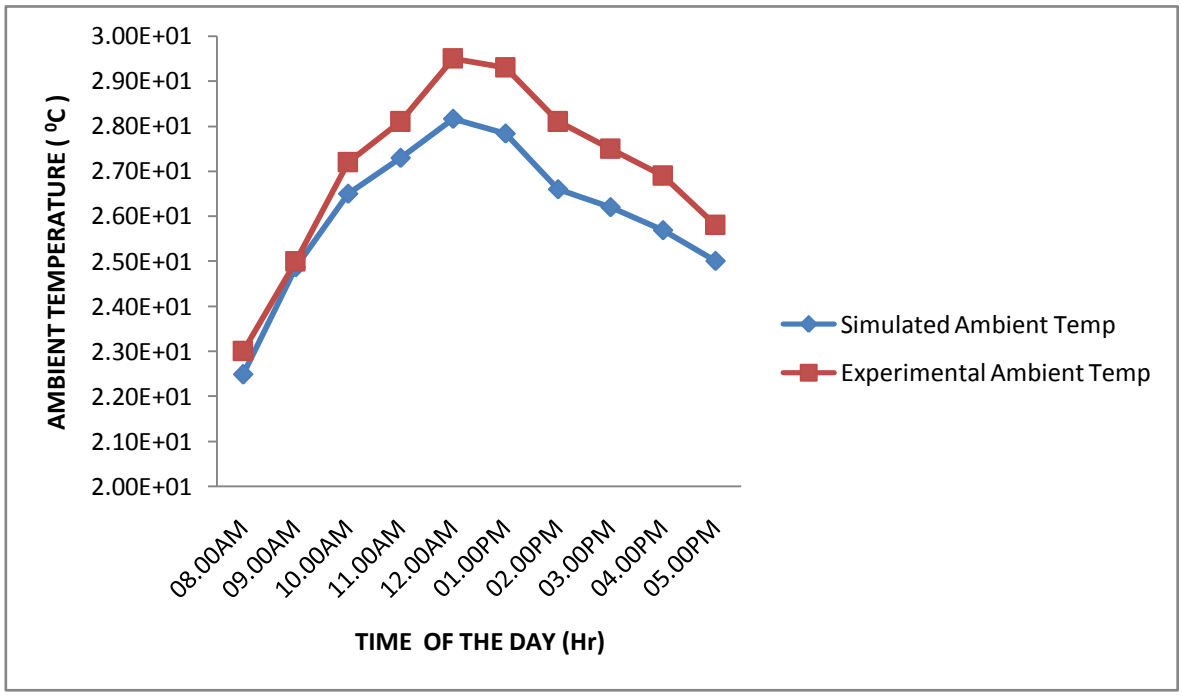


Figure 4.8: Comparison of hourly Ambient Temperature of Zaria recorded during the experiment with the values obtained using TRNSYS 16 software. (30 August, 2015.)

Figures 4.6, figure 4.7and figure 4.8 shows the comparison of the experimental hourly ambient temperature with the predicted result from the model (solar data processor, Type

109 of TRNSYS). The comparison between the experimental and the simulated result shows that the model slightly under estimates the hourly Ambient Temperature for most parts of the day for the location (Zaria) during the three days of experiment the temperature

Increment and decrement follow a similar pattern

Table 4. 8: Validation of simulated Ambient Temperature result with experimental result of 28 August 2015 using the standard deviation, relative error and NSE statistical tools.

TIME	AMSim	AMexp	AMsim - AMexp	$(AMsim-AMexp)^2$	$(AMexp - AMexp)^{-}2$
08.00AM	20.4	24.7	4.33	18.7597	068.5631
09.00AM	21.9	24.9	3.01	09.0375	324.0888
10.00AM	22.2	25.5	3.35	11.2224	250.1936
11.00AM	22.3	25.9	3.65	13.3225	188.1698
12.00AM	23.1	26.5	3.37	11.3690	245.5776
01.00PM	24.2	28.0	3.81	14.5206	156.7338
02.00PM	26.4	28.9	2.46	06.0525	440.4748
03.00PM	27.0	29.7	2.65	07.0437	399.8517
4.00PM	26.5	28.6	2.14	04.5727	504.7751
05.00PM	25.2	27.7	2.47	06.0982	438.5566
TOTAL	239.0	270.4		101.9992	3016.9853
AVERAGE		27.04			

$$\text{Standard Deviation} = \sqrt{\frac{\sum_{i=1}^{n}[\boldsymbol{AM_{sim}} - \boldsymbol{AM_{expt}}]^2}{n}}$$

\

$$= \sqrt{\frac{101.9992}{10}}$$

$$= 3.1937^{o}\text{C}$$

$$NSE = 1 - \frac{\sum_{i=1}^{n}[\boldsymbol{AM_{sim}} - \boldsymbol{AM_{expt}}]^2}{\sum_{i=1}^{n}[\boldsymbol{AM_{expt}} - \overline{\boldsymbol{AM}}_{\boldsymbol{expt}}]^2}$$

$$= 1 - \frac{101.9992}{3016.9853}$$

$$= 0.9661$$

$$\text{Relative Error} = \left| \sum_{i=1}^{N}\left[\boldsymbol{AM_{sim}} - / \sum_{i=1}^{N} \boldsymbol{AM_{expt}}\right] \right| / \sum_{i=1}^{N}[\boldsymbol{TM_{expt}}] \times 100\%$$

$$= \frac{239 - 270.4}{270.4} \times 100\%$$

$$= 11.6\%$$

The average values of standard deviations and relative errors for the day are 3.1937^{o}C and 11.6% as shown in table 4.11 this values interpret that average deviation of ambient temperature from the actual value is just 3.1937 ^{o}C and the percentage error between the measured ambient temperature and the simulated ambient temperature is minimal. However the calculated NSE shown that the model is 96.61 % accurate in predicting the actual ambient temperature on 28th August, 2015.

The experiments of 29 August and 30 August 2015 were conducted to ensure that the simulation model is accurate and could be used to predict the system performance continuously.

4.8.2 Comparism and Validation of simulated Solar Radiation with experimental Solar Radiation.

The comparison between the experimental hourly solar radiation and simulated solar radiation which was predicted from the model (solar data processor, Type 109 of TRNSYS). Is shown in Figures 4.9, figure 4.10 and figure 4.11 for the three days of the experiment.

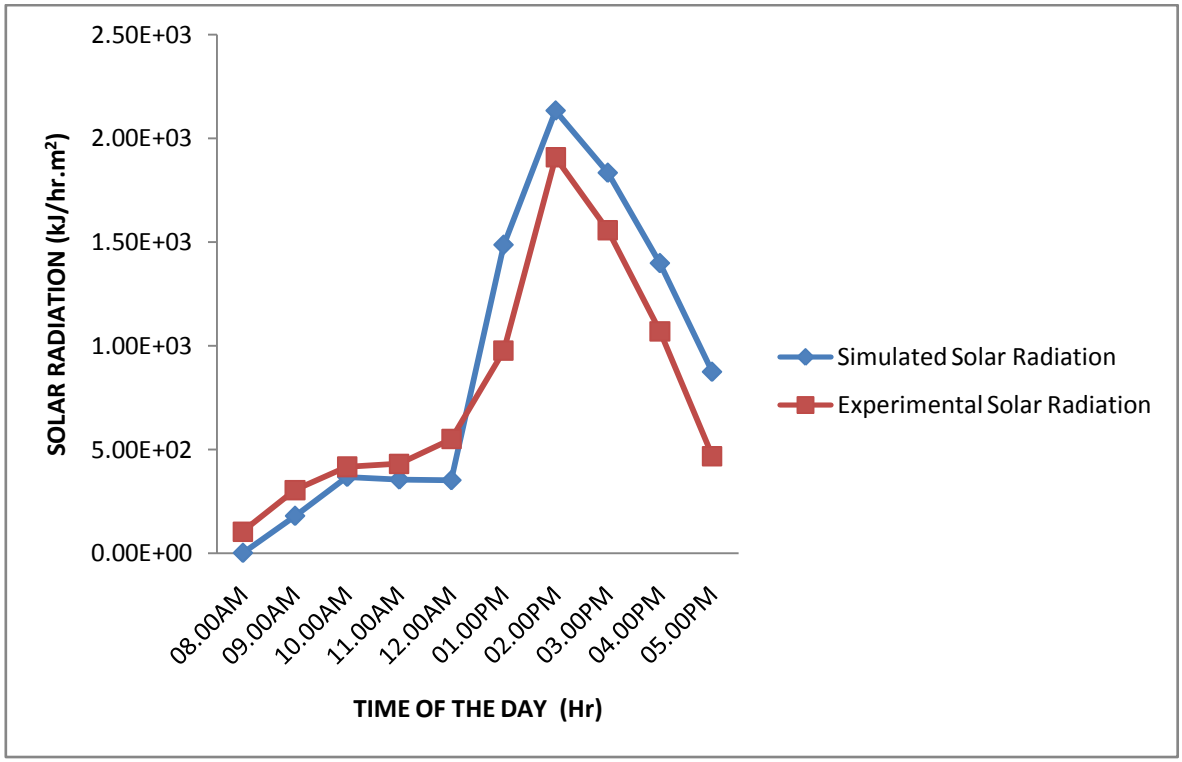


Figure 4.9: Comparison of hourly solar radiation of Zaria recorded during the experiment with the values obtained using TRNSYS 16 software. (28 August, 2015.)

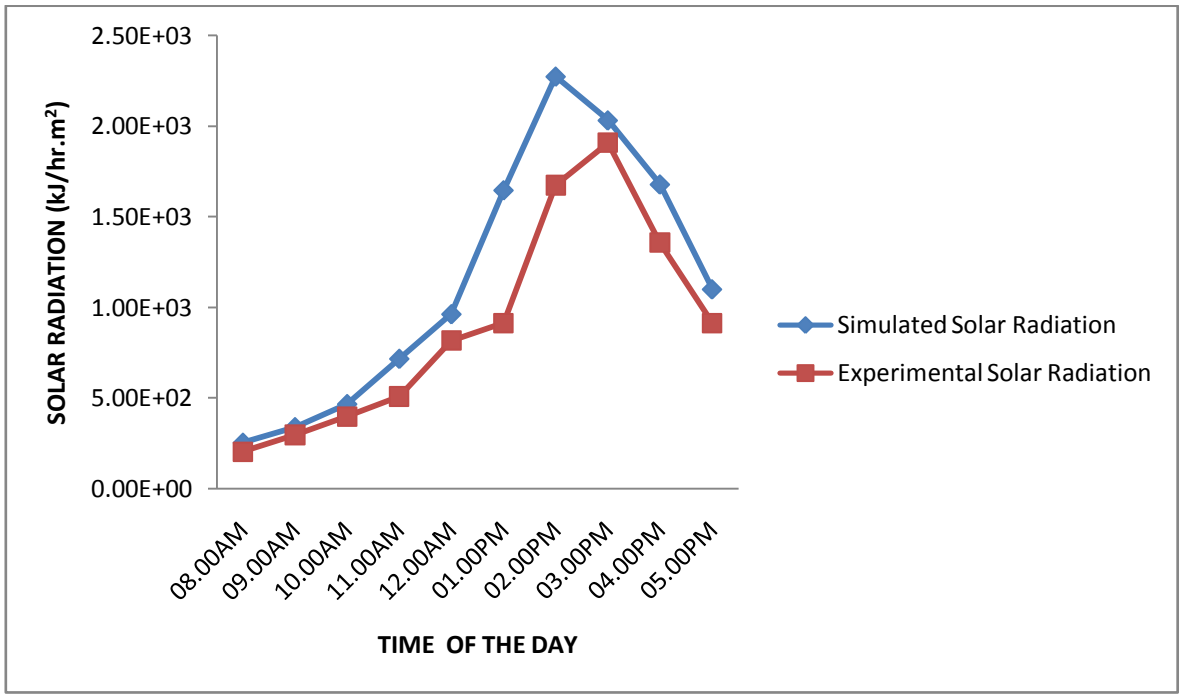


Figure 4.10: Comparison of hourly solar radiation of Zaria recorded during the experiment with the values obtained using TRNSYS 16 software. (29 August, 2015.)

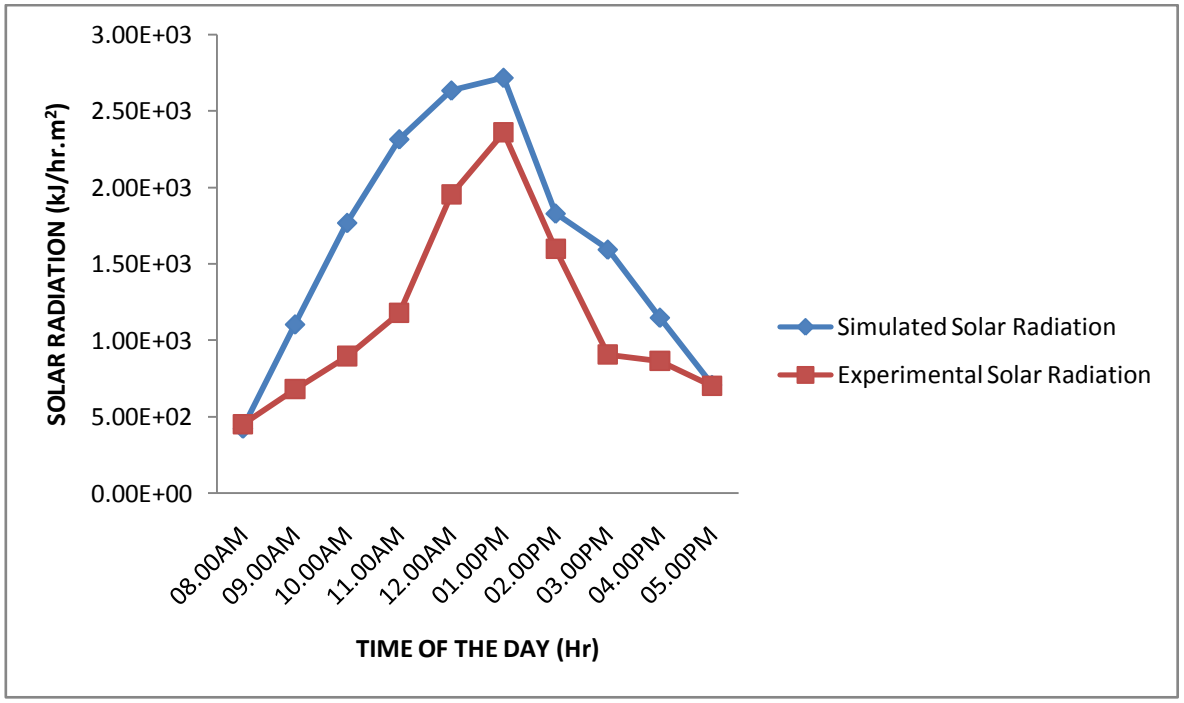


Figure 4.11: Comparison of hourly solar radiation of Zaria recorded during the experiment withthe values obtained using TRNSYS 16 software. (30 August, 2015.)

Figures 4.9, figure 4.10 and figure 4.11 show the comparison of the experimental solar radiation with the predicted solar radiation from the model (solar data processor, Type 109 of TRNSYS). The comparison between the experimental and the simulated result shows that the model slightly over estimates the hourly solar radiation for most part of the day for the location (Zaria) during the three days of experiment the trend of solar radiation increment and decrement follow a similar pattern.

Table 4. 9: Validation of simulated Solar Radiation result with experimental result of 28 August 2015 using the standard deviation, relative error and NSE statistical tools.

TIME	SRSim	SRexp	SRsim - SRexp	$(SRsim - SRexp)^2$	$(SRexp - SRexp)^{-}2$
8.00AM	1.23E+02	103	20.0	0400.0000	166300.84
9.00AM	3.20E+02	303	17.4	0301.1387	256705.6605
10.00AM	4.36E+02	416	20.3	0410.5229	157829.087
11.00AM	4.54E+02	430	23.5	0553.2754	64782.73079
12.00AM	5.69E+02	549	20.3	0413.5915	155400.304
01.00PM	1.01E+03	975	38.7	1494.5150	471577.5836
02.00PM	1.93E+03	1908	23.8	0567.3681	57807.53046
03.00PM	1.63E+03	1557	75.1	5641.8709	23368241.69
04.00PM	1.13E+03	1069	57.5	3300.6945	6214523.336
05.00PM	8.63E+02	768	94.6	8955.6096	66386801.71
TOTAL	8.47E+03	8078		22038.5868	97299970.47
AVERAGE		807.8			

$$\text{Standard Deviation} = \sqrt{\frac{\sum_{i=1}^{n}\left[\boldsymbol{SR_{sim}} - \boldsymbol{SR_{expt}}\right]^2}{n}}$$

$$= \sqrt{\frac{22038.5868}{10}}$$

$$= 46.9453$$

$$NSE = 1 - \frac{\sum_{i=1}^{n}\left[\boldsymbol{SR_{sim}} - \boldsymbol{SR_{expt}}\right]^2}{\sum_{i=1}^{n}\left[\boldsymbol{SR_{expt}} - \overline{\boldsymbol{SR}}_{\boldsymbol{expt_{xpt}}}\right]^2}$$

$$= 1 - \frac{22038.5868}{97299970.47}$$

$$= 0.9998$$

$$\text{Relative Error} = \left| \sum_{i=1}^{N}\left[\boldsymbol{SR_{sim}} - \boldsymbol{SR_{expt}}\right]^2 \right| \Big/ \sum_{i=1}^{N}[\boldsymbol{SR_{sim}}] \times 100\%$$

$$= \frac{8470 - 8078}{8078} \times 100\%$$

$$= 4.8527\ \%$$

The average values of standard deviations and relative errors for the day are 46.9453J/m^2.day and 4.8527% as shown in table 4.13 this values interpret that average deviation of solar

radiation from the actual value is 46.9453 J/m^2.day and the percentage error between the measured solar radiation and the simulated solar radiation is minimal. However the calculated NSE shown that the model is 99.98 % accurate in predicting the actual solar radiation on 28th August, 2015.

The experiments of 29 August and 30 August 2015 were conducted to ensure that the simulation model could be used to predict the accurate system performance with good repeatability

4.8.3 Comparism and Validation of simulated Collector outlet Temperature with experimental Collector outlet Temperature.

The comparison between the experimental hourly collector outlet temperature and simulated hourly collector outlet temperature which was predicted from the model (solar data processor, Type 109 of TRNSYS), is shown in Figures 4.12, figure 4.13 and figure 4.14 for the three days of experiment.

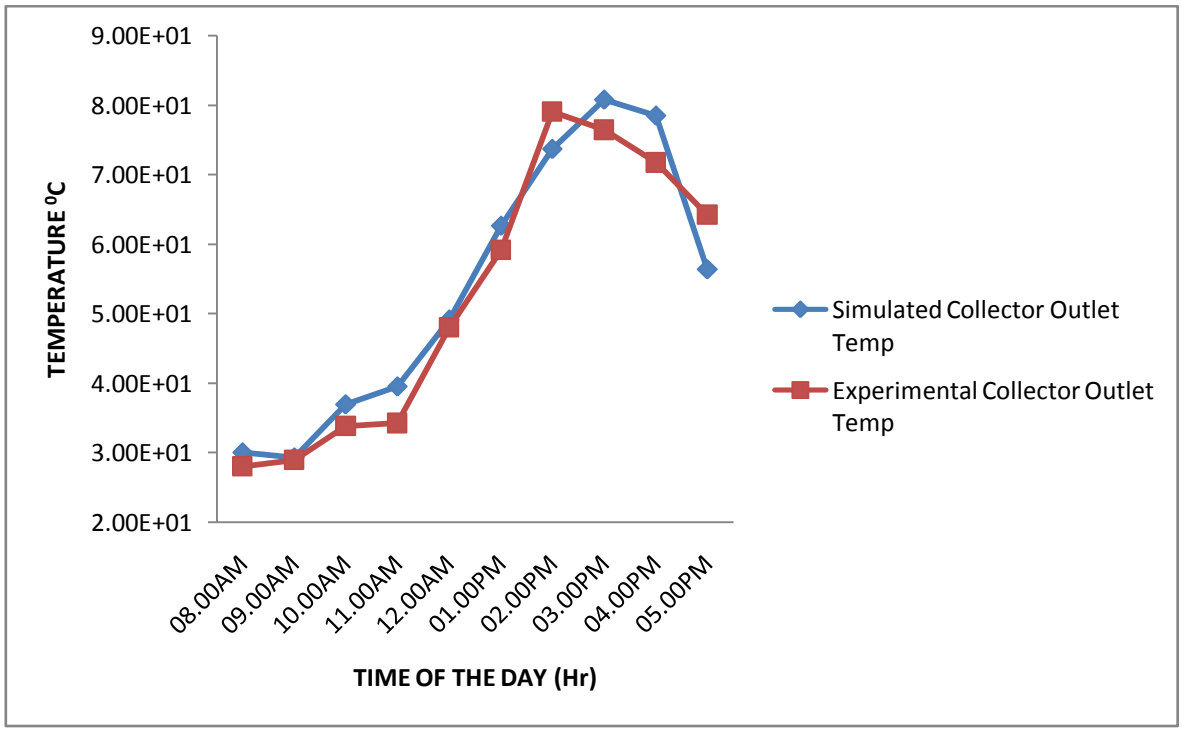


Figure 4.12: Comparison of hourly simulated Collector outlet Temperature collector with experimental results (28 August, 2015)

Figures 4.12, figure 4.13 and figure 4.14 show the comparison of the experimental hourly Collector outlet Temperature with the predicted result from the model (solar data processor, Type 109 of TRNSYS). Figure 4.12 show that the model slightly over estimates the hourly collector outlet temperature for most part of the day for the location on 28 August, 2015.The variation in hourly collector outlet temperature also follows the same orders in Figure 4.13 and figure 4.14. The figure shows an increase in experimental Collector outlet temperature from an initial temperature of 30^{o}C at the start of the experiment at 8.00AM reaching its peak value of 81.5 ^{o}C at 3.00PM. The figure also indicates that the Collector outlet temperature started decreasing after 3.00PM to a value of 55^{o}C at the end of the experiment at 5.00PM.

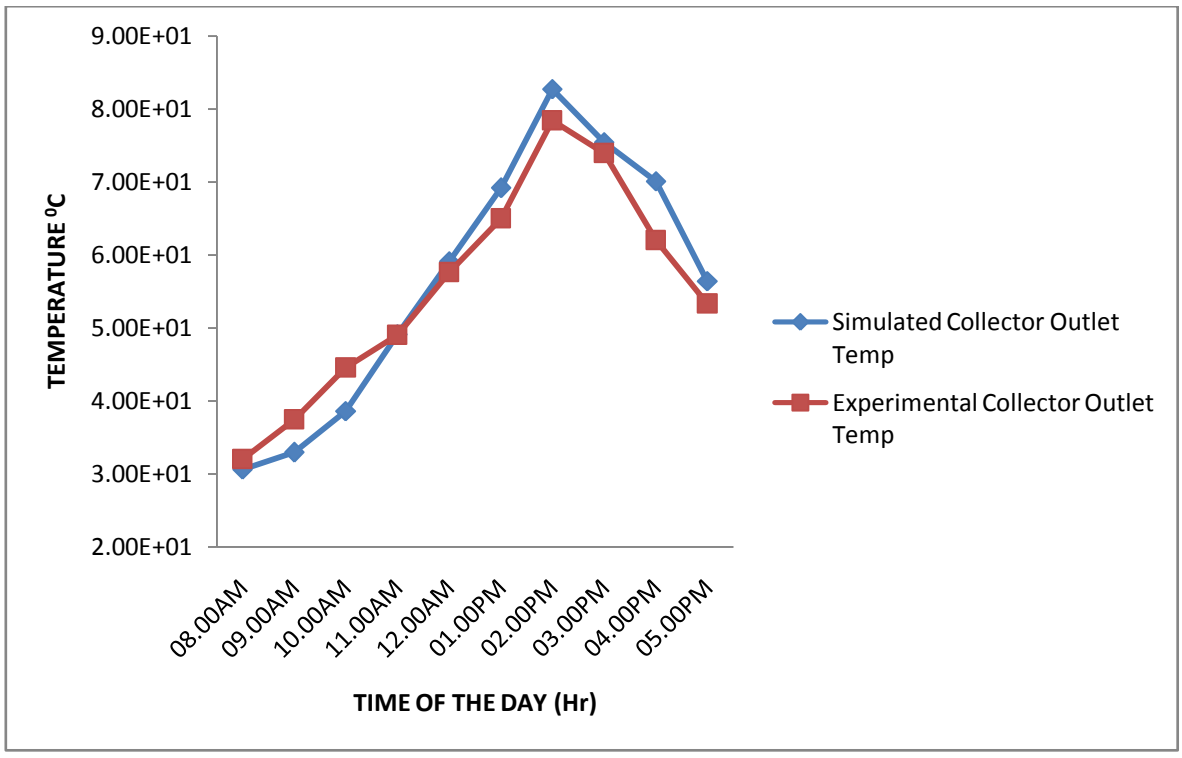


Figure 4.13: Comparison of hourly simulated Collector outlet Temperature with experimental results (29 August, 2015)

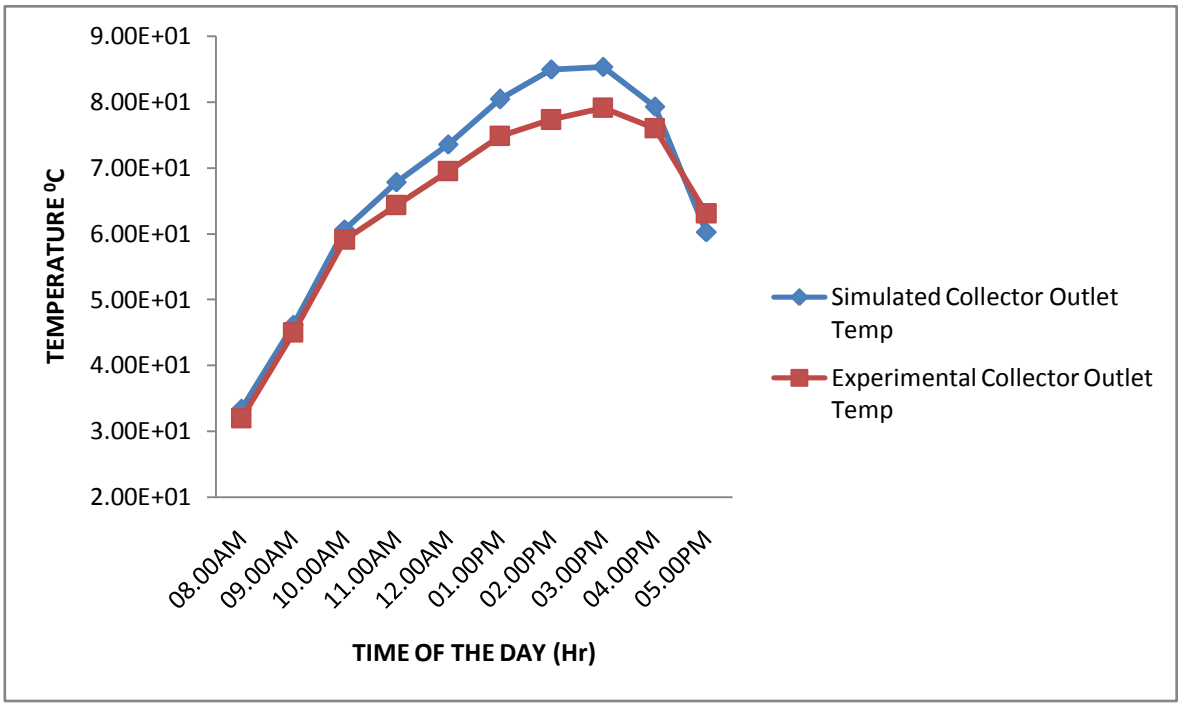


Figure 4.14: Comparison of hourly simulated Collector outlet Temperature with experimental results (30 August, 2015)

Table 4.10: Validation of simulated Collector outlet Temperature result with experimental result of 28 August 2015 using the RMSE and NSE statistical tools.

TIME	TMsim	TMexp	TMsim - TMexp	$(TMsim - TMexp)^2$	$(TMexp - TMexp)^{-}2$
8.00AM	30.0	28	2.00	4.0000	591.9489
9.00AM	29.3	28.9	0.41	0.1637	548.9649
10.00AM	36.9	33.8	3.13	9.7672	343.3609
11.00AM	39.5	34.2	5.30	28.0385	328.6969
12.00AM	49.0	48.0	1.03	1.0647	18.7489
01.00PM	62.6	59.1	3.50	12.2306	45.8329
02.00PM	73.7	79.0	-5.33	28.4149	711.2889
03.00PM	80.7	76.4	4.35	18.9153	579.3649
04.00PM	78.5	71.7	6.75	45.5834	375.1969
05.00PM	56.3	64.2	-7.86E	61.8032	140.8969
TOTAL	537	523.3	13.3	209.9815	3684.301
AVERAGE	53.7	52.33			

$$\text{Standard Deviation} = \sqrt{\frac{\sum_{i=1}^{n}\left[TM_{sim}-TM_{expt}\right]^2}{n}}$$

$$= \sqrt{\frac{209.9815}{10}}$$

$$=4.5824^{o}\text{C}$$

$$NSE = 1 - \frac{\sum_{i=1}^{n}\left[TM_{sim}-TM_{expt}\right]^2}{\sum_{i=1}^{n}\left[TM_{expt}-\overline{TM}_{expt}\right]^2}$$

$$= 1 - \frac{209.9815}{3684.301}$$

$$=-0.9432$$

$$\text{Relative Error} = \left| \sum_{i=1}^{N}\left[TM_{sim} - TM_{expt}\right]^2 \right| \Big/ \sum_{i=1}^{N}\left[TM_{sim}\right] \times 100\%$$

$$=\frac{537-523.3}{523.3} \times 100\%$$

$$= 2.6180\%$$

The average values of standard deviations and relative errors for a day are 4.5824^{o}C and 2.6180% as shown in table 4.14 this values interpret that average deviation of Collector outlet Temperature from the actual value is 4.5824^{o}C and the percentage error between the measured Collector outlet Temperature and the simulated Collector outlet Temperature is very minute. However the calculated NSE shown that the model is 94.32 % accurate in predicting the actual solar radiation on 28th August, 2015.

The experiments of 29 August and 30 August 2015 were conducted to ensure that the simulation model is accurate and could be used to predict the system performance continuously.

4.8.4 Comparison and Validation of simulated Collector Inlet Temperatures with experimental Collector Inlet Temperatures.

The comparison between the experimental hourly Collector inlet Temperatures and hourly simulated Collector inlet Temperatures which was predicted from the model (solar data

processor, Type 109 of TRNSYS). Is shown in Figures 4.15 figure, 4.16 and figure 4.17 for the three days of experiment.

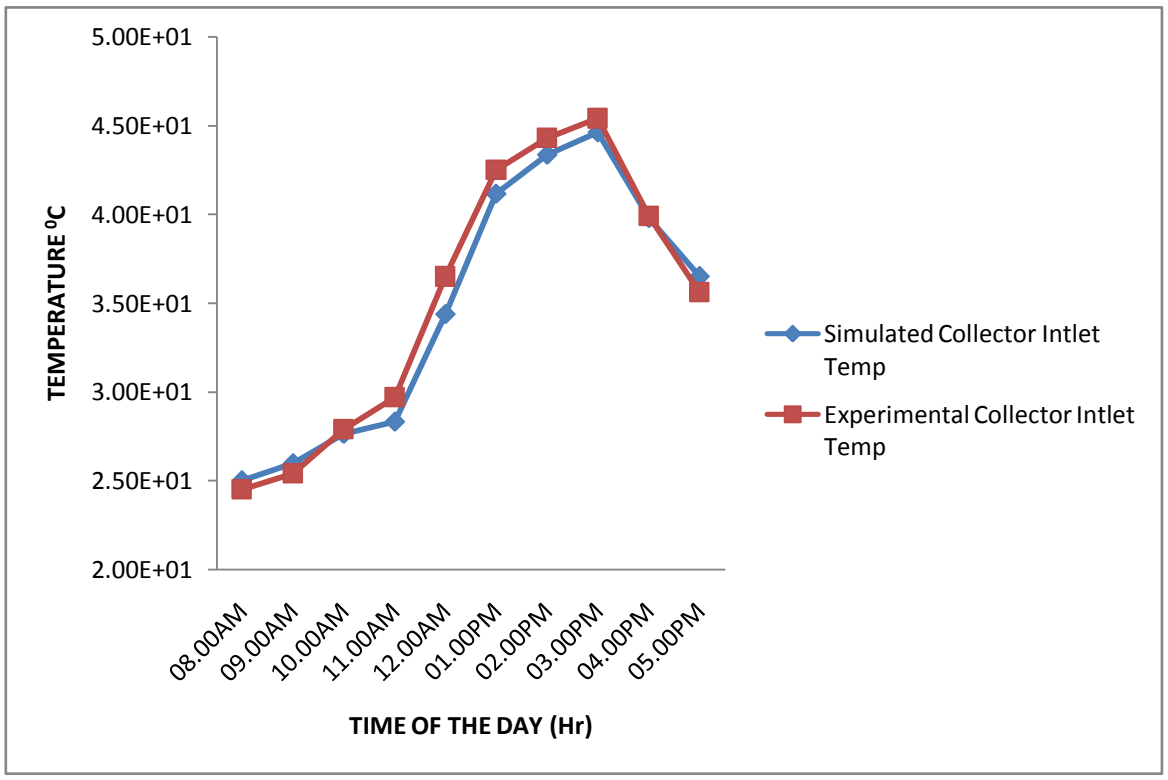


Figure 4.15: Comparison of hourly simulated Collector inlet Temperatures with experimental results (28 August, 2015).

Figures 4.15, figure 4.16 and figure 4.17 show the comparison of the experimental hourly Collector inlet Temperature with the predicted result from the model (solar data processor, Type 109 of TRNSYS). Figure 4.12 shows that the model slightly under estimates the hourly Collector inlet Temperature for most part of the day for the location on 28 August, 2015.The variation in hourly collector inlet temperature also follows the same orders in Figure 4.13 and figure 4.14. The figure shows an increase in experimental Collector inlet temperature from an initial temperature of 24.0^{o}C at the start of the experiment at 8.00PM reaching its peak value of 45.5^{o}C at 3.00PM. The figure also indicates that the Collector inlet temperature started decreasing after 3.00PM to a value of 35.5^{o}C at the end of the experiment at 5.000PM. The temperature increment and decrement follow a similar pattern.

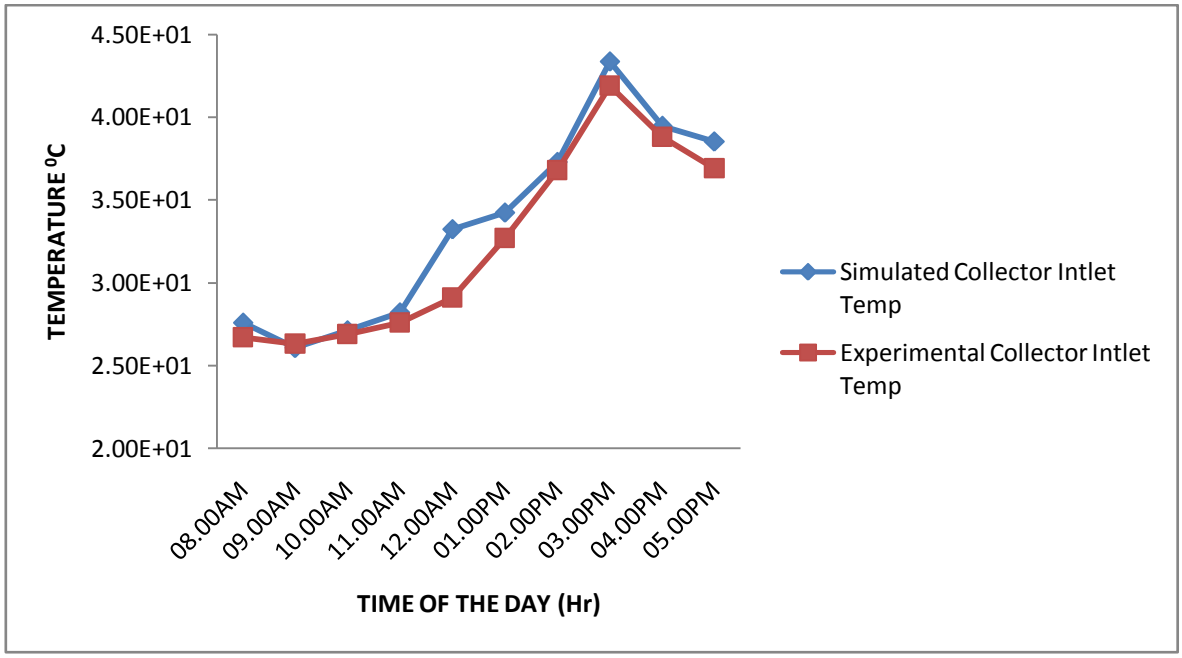


Figure 4.16: Comparison of hourly simulated Collector inlet Temperatures with experimental results (29 August, 2015)

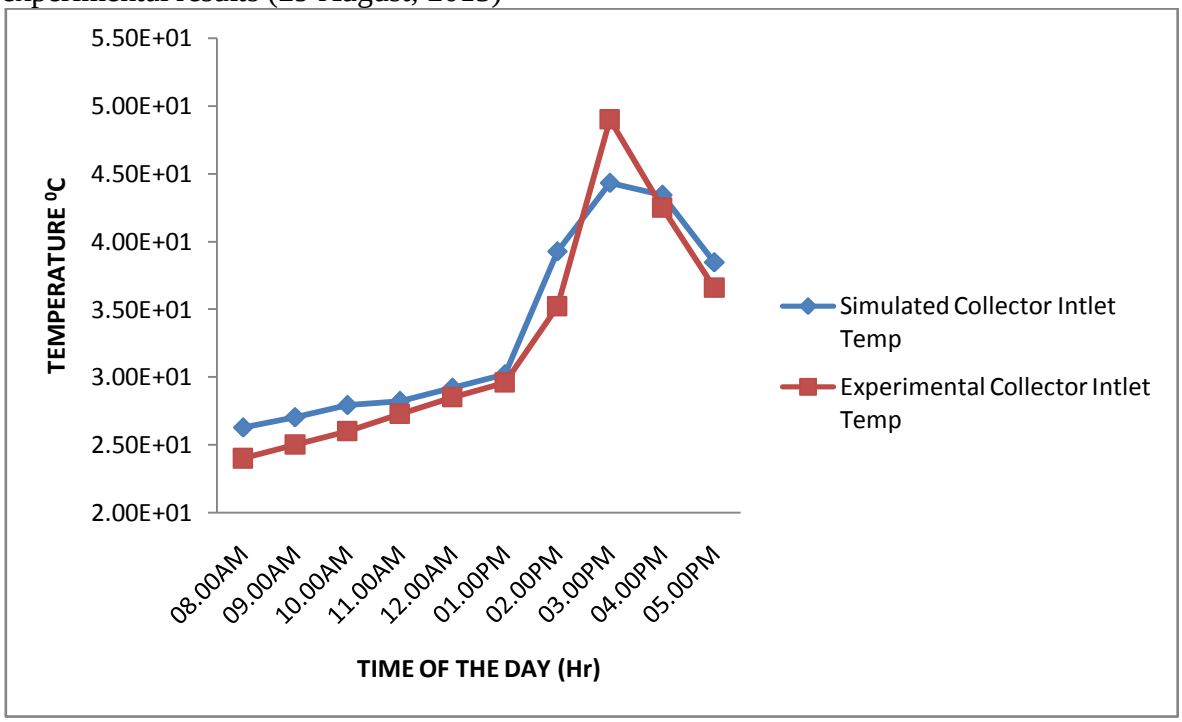


Figure 4.17: Comparison of hourly simulated Collector inlet Temperatures with experimental results (30 August, 2015).

Table 4.11: Validation of simulated result with experimental result of Collector inlet temperature on 29 August 2015 using the RMSE and NSE statistical tools.

TIME	T1sim	T1exp	T1sim - T1exp	$(T1sim - T1exp)^2$	$(T1exp - T1exp)^{-2}$
8.00AM	2.80E+01	-24.5	3.50E+00	12.2500	2178.0889
9.00AM	2.90E+01	-25.4	3.60E+00	12.9600	2244.8644
10.00AM	3.17E+01	-27.9	3.76E+00	14.1184	2355.9802
11.00AM	3.33E+01	-29.7	3.64E+00	13.2814	2275.4278
12.00AM	3.39E+01	-36.5	-2.60E+00	06.7600	1695.7924
01.00PM	4.12E+01	-37.5	3.66E+00	13.4169	2288.3761
02.00PM	4.34E+01	-40.3	3.06E+00	09.3865	1919.0140
03.00PM	4.76E+01	-42.9	4.72E+00	22.2807	3214.9746
04.00PM	4.58E+01	-40.9	4.90E+00	24.0100	3414.0649
05.00PM	4.25E+01	-38.6	3.89E+00	15.1661	2458.7819
TOTAL	3.76E+02	-344.2		143.6303	31701.8972
AVERAGE		-34.42			

$$\text{Standard Deviation} = \sqrt{\frac{\sum_{i=1}^{n}[TI_{sim} - TI_{expt}]^2}{n}}$$

$$= \sqrt{\frac{143.6303}{10}}$$

$$= 3.7899^{o}\text{C}$$

$$NSE = 1 - \frac{\sum_{i=1}^{n}[T1_{sim} - TI_{expt}]^2}{\sum_{i=1}^{n}[TI_{expt} - \overline{TI}_{expt}]^2}$$

$$= 1 - \frac{143.6303}{31701.8972}$$

$$= 0.9955$$

$$\text{Relative Error} = \left| \sum_{i=1}^{N}\left[TI_{sim} - TI_{expt}\right]^2 \right| \Big/ \sum_{i=1}^{N}[TI_{sim}] \times 100\%$$

$$= \frac{376 - 344.2}{344.2} \times 100\%$$

$$= 9.2388\ \%$$

The average values of standard deviations and relative errors for a day are 3.7899^{o}C and 9.2388% as shown in table 4.15 these values interpret that average deviation of Collector inlet

Temperature from the actual value is 4.5824^{o}C and the percentage error between the measured Collector inlet Temperature and the simulated Collector intlet Temperature is negligible. However the calculated NSE shown that the model is 94.32 % accurate in predicting the actual solar radiation on 28th August, 2015.

The experiments of 29 August and 30 August 2015 were conducted to ensure that the simulation model could be used to predict the system performance with good repeatability

CHAPTER FIVE

5.0 SUMMARY, CONCLUSION AND RECOMMENDATIONS

5.1 Summary

The design simulation fabrication and performances test of a thermosyphon solar water heater was carried out successfully for a block in Postgraduate hostel of Ahmadu Bello University Zaria, Which has the ability to heat 200liters of water to a temperature of 45 degree centigrade the design was purposely for students to use the water for bathing in order to totally discourage the use of electric heating devices in the hostel which on several occasions has been the reason of fire outbreaks in the hostel.

The system factors such as costs and sizing were taken into consideration which assisted in the choice of materials and the design drawings. The average solar radiation data was obtained from typical meteorological year (TMY) of Zaria which was used to determine the month with the least solar radiation, from the analysis of the typical meteorological year (TMY) of Zaria the month of August has the least energy ratio which point it out as the month with the least solar radiation and it was used as the design month.

The optimization of the system component was also carried out to determine the optimum system size MATLAB was used for the system optimization.

Finally, the solar water heater conditions were simulated using TRNSYS programme. Typical meteorological year (TMY) solar data of Zaria obtained from www.solaranalytical.com was processed to obtain the monthly average daily solar resources of Zaria using the solar radiation and weather data processor TYPE 109 component of TRNSYS 16 software.

After the fabrication of the system the system performance was evaluated by comparing the simulation result obtained from the model (solar data processor, Type 109 of TRNSYS) and the result obtained from the experiment using Microsoft Excel and also statistical tools where used to validate the predictive power of the model.

5.2 Conclusion

- The optimal system size was determined using MATLAB which ascertained the characteristics of component materials with respect to system efficiency and after which the trynsys was used to obtained the system components sizes.
- The solar water heater was simulated using trynsys to predicted the system performance before the fabrication, to ensure the efficiency of the system, and also to make all the necessary adjustment so that maximum systems performances will be obtain
- The solar water heater component was fabricated in the mechanical engineering workshop Ahmadu Bello University Zaria, using locally available materials, the components of solar water heater were assembled on the rooftop of Sassakawa postgraduate hostel (Block K)
- The cost of the system was estimated after the solar water heater was fabricated using locally available materials.
- The solar water heater was tested for three days and the result obtained was compared with the simulated result with was used to ascertained the system performance and efficiency.

From the result obtained from the research it can be conclude that the thermosyphon solar water heater of collector area of $2.6m^2$ has the ability to heat 200liter of water to a

temperature of 50^{o}C in the month that has the least solar radiation in Ahmadu Bello University.

The statistical tools used for the validation of the simulation model confirm that the model is valid and can be used in the estimation of the actual characteristics of a real system, which a good accuracy the relative error is very minimal for all the measured parameters and Nash-Sutcliff coefficient shows that the degree of fitting is very high which shows that the simulation model has a high accuracy and also the standard deviation shows that the deviation of the experimental parameters from the simulated is very low and therefore it is negligible.The results show little deviation of predicted values from actual values and also a good level of fit, thereby validating the model used for simulating the solar water system

5.3 Recommendations

- Auto tracking reflectors incorporated into the design will also enhance the efficiency as the effect of shading is minimized due to the shift of the reflector with the movement of the sun; it will redirect sunrays falling at the side of the collector unto the absorber plate.
- It is also recommended that the hot water should be separated from the cold water and devices that can control the flow of cold water and the cold water should be incorporated so as to increase the efficiency of the system.
- The adjusting mechanism for setting the collector to the specified latitude of the area is to be designed to further improve the systems flexibility.

REFERENCES

Ahmad, A. R.(2010) Theoretical Analysis Of Solar Water Heating System. Faculty of Mechanical Engineering University Malaysia Pahang.

Alternative Energy Tutorials. (2012). *Alternative and Renewable energy.* Retrieved July 20,2012 from http://www.alternative-energy-tutorials.com/.

Brandemuehl, M. J. and Beckman, W. A. (1980), "Transmission of Diffuse Radiation through CPC and Flat-Plate Collector Glazings," *Solar Energy*, 24: 511-524,

Crawford, R. H., Treloar G.J. Ilozo B.D. and Love P.E.D (2003), Comparative greenhouse emissions analysis of domestic solar hot water systems. *Journal Building Research & Information*, Volume 31, 34–47.

Christopher A. Homola, P.E . (2010)Solar domestic hot water heating system design, installation and maintenance. Retrieved Jan 20th 2012 at http://www.solar- rating.org

Duffie, J.A. and Beckman, W.A (1991). *Solar engineering of thermal processes*, 2nd Edition, Toronto :John Wiley & Sons.

Dobson, T. (2008) Solar Water Heating Theory. rtd@sun.ac.za

Gulland, J.(2012) "Heating water with a wood stove". *woodheat.org*. Wood HeatOrganizationInc.. Retrieved 29 March 2012.

Govind, N.K., Shireesh, B.K., and Santanu, B. (2008). Design of solar thermal systems utilizing pressurized hot water. *Solar Energy, 82* (23), 686–699.

Henry, H. D. (2010) Design and construction of a solar water heater for the microbiological laboratory sick bay. Unpublished B.Eng Degree Project Report.Department of Mechanical Engineering.Ahmadu Bello University, Zaria. Nigeria.

Holland , K.G.T (2005) Free convection in solar collectors.Progress in Energy and Combustion Science 30:231–295 Retrieved January 27, 2013 from http//:www.elsevier.com/locate/pecs.

Hottel H.C and Woertz, B.B (2004) Performance of flat plate ASME pg 91-104 Feb. 2004

.Taherian .H ,RezaniaH.Sadeghi .A, Ganji D.D (2011) Experimental validation of dynamic simulation of the flat plate collector in a closed thermosyphon solar water Energy Conversion and Management 52: 301–307 Retrieved February 27, 2013 from http//:www.elsevier.com/locate/enconman

Institute Sustainable Technologies (2001) "Solar Thermal Systems and Components"

ISO 9459-3:1997(E). (1997). *Performance tests for solar plus supplementary systems. international standards organization*, Geneva, Switzerland

Ityona .A (2003): design a compact solar water heater for domestic and small scale industrial application. Unpublished B.Eng Degree Project Report.Department of Mechanical Engineering. Ahmadu Bello University, Zaria. Nigeria.

Jae-Mo, K. (1999). *Development of a flat plate solar collector design programme*. (Doctoral dissertation, University of Wisconsin). Retrieved March 13, 2011 from http://sel.me.wisc.edu/theses

Jagadash, B.S (2006) Optimum tilt for the flat plate collector.Energy 35: 3156-2169 Retrieved March 27, 2012. fromhttp//:www.elsevier.com/locate/energy

Julien, G. A, Emmanuel, L., Clément, A., Rufin, O. A., and Brice, A. S. (2013). Modeling Solar energy transfer through roof material in Africa Sub-Saharan Regions. *ISRN Renewable Energy 34(7), 632-645*.

Koffi P.M.E, Andoh H.Y., Gbaha P., Toure S., Ado G. (2008). Theoretical and experimental study of solar water heater with internal exchanger using thermosiphon system. Energy Conversion and Management 49 (2008) 2279–2290 Retrieved February 27, 2013 from http//: www.elsevier.com/locate/energy

Klein, S.A. et al., 2004. TRNSYS Version. 16, Solar Energy Laboratory, University of Wisconsin-Madison, Website: <http://sel.me.wisc.edu/ trnsys>.

Kalogirou, Soteris (2009) Solar energy engineering : processes and systems / Soteris Kalogirou.—1st ed. Printed in the United States of America.

Koutoheras, (1999) Convection heat transfer between the collector plate and the glass cover Energy Conversion and Management,49:2279–2290 Retrieved February 27, 2013 from http//: www.elsevier.com/locate/energy

Mudashir.L.J(2008) Design, Contruction and testing of a solar water heater with 50 litres storage tank. Department of Mechanical Engineering. Ahmadu Bello University, Zaria. Nigeria.

Marken C. (2009) Solar collectors – behind the glass. *Homepower magazine* 133,70–76 76"National Renewable Energy Laboratory (NREL) Home Page". Nrel.gov. 6 February 2012. Retrieved 10 February 2012.

Neil, J. S.(2010). *Encyclopedia of research design*. Online ISBN: 9781412961288 | Publisher: SAGE Publications, Inc.

Norton, Brian (2013*). Harnessing Solar Heat. Springer. ISBN 978-94-007-7275-5.* Publisher: SAGE Publications, Inc

Papamarcou(2000) studied thermosyphon solar water heater consisting of two plate collectors of total aperture area of 2.7 m^2 and 150 liter storage tank is modeled using TRNSYS Renewable Energy 21 (2000) 471±493 Retrieved February 27, 2013 from http//:www.elsevier.com/locate/energy.

Rai, G.D. (2008). Solar energy utilization: *A text book for engineering students* 5th Edition, Delhi, Khanna.

Retscreen Internatinal. (2004). *Solar water heating project analysis*. Retrieved January 20,2012 from http//:www.redscreen.net

Rhushi, P.R., Byregowda, H.V., Gangavati, P.B., andShankaran K. P. (2011). Performance analysis of a solar water heater with flat plate collector using computer program. *European Journal of Scientific Research, 53* (23), 67-79. Retrieved Jan 20th 2012 from http://www.eurojournals.com/ejsr.htm

Rodríguez I, Cònsul R, Cadafalch J. and Oliva A. (2010) Numerical Studies of Thermosyphon Solar Heaters. Energy 35: 3156-2169 Retrieved February 27, 2013 From http//:www.elsevier.com/locate/energy.

Soteris A.(2004). Environmental benefits of domestic solar energy systems. Energy

Conversionand Management 45: 3075–3092 Retrieved February 27, 2013 from http//: www.elsevier.com/locate/enconman

Soteris, A. (2012) Solar thermal collectors and applications. Progress in Energy and Combustion Science 30:231–295 Retrieved February 27, 2013 from http//:www.elsevier.com/locate/pecs.

Soteris , A, Christos P. (2000) Modelling of a thermosyphon solar water heating system and simple model validation. Renewable Energy 21: 471-493 Retrieved February 27, 2013 from http//: www.elsevier.com/locate/energy

Saygh, A.A.M (2000) Characteristics of solar radiation.Energy 35: 3156-2169 Retrieved April 30, 2013 fromhttp//:www.elsevier.com/locate/energy

Qin, L . (1998) Analysis modelling and optimum design of solar domestic hot water system. (Phd thesis, University of Wisconsin) Retrieved 13th march 2011 at http://sel.me.wisc.edu/theses

.Tripanagnostopoulos Y, Souliotis M and Nousia T. (1999) Solar ICS systems with two cylindrical storage tanks. *Renewable Energy* Volume 16,665–668.

Taherian H., Rezania A., Sadeghi S. ,Ganji D.D.(2011) studied the dynamic simulation of thermosyphon solar water heater collector considering the weather conditions of a city in north of Iran. Energy Conversion and Management 52 (2011) 301–307 Retrieved October 20, 2012 from http//: www.elsevier.com/locate/enconman

Walker, A. (2012) National Renewable Energy Laboratory ,updated by U.S. Department of Energy Federal Energy Management Program (FEMP)

Young D.Km, Kyaw T, Hitasha K.B., CharanjitS.B.,and Kim C.N. (2012). Thermal analysis and Performance optimization of a solar hot water plant with economic evaluation. *Solar Energy,* 86:1378–1395 Retrieved October 20, 2012 from http//: www.elsevier.com/locate/solener.

Zhani, K, Ben, H, Bacha,T. and Damak, T (2011) Modeling and experimental validation of a humidification and dehumidification. Energy 36: 3159-3169 Retrieved February27, 2013 from http//: www.elsevier.com/locate/energy

Zwalnan, J. (2015): design a compact solar water heater for domestic and small scale Industrial application. Published M.Eng Degree Dissertation Report.Department of Mechanical Engineering. Ahmadu Bello University, Zaria. Nigeria

APPENDIX A

CALCULATION OF RADIATION ON TILTED SURFACE DESIGN PROGRAMME CODES DEVELOPED USING MATLAB

```
N=1.51     %refractive index of glass
Rg = 0.2 %ground reflectance
AB =0.98%plate absorptance
beta=11.2     %collector tilt angle

KL=0.0736 %glass extinction coefficient and length product

LT=11.2     % latitude of location (Zaria)

P=pi/180

n=[17 47 75 105 135 162 198 228 258 288 318 344]
.l

Qd= 59.7-0.1388*beta+0.001479*beta^2 % incident angle of diffuse radiation

Qg= 90-0.5788*beta+0.002693*beta^2 % incident angle of reflected radiation


DLTA =23.45*sin(2*pi*((n+284)/365))%formula for monthly declination

w_s=(acos(-tan(LT*P)*tan(DELTA*P)))*1/P %monthly sunset angle
w_sb=(acos(-tan((LT-beta)*P)*tan(DELTA*P)))*1/P

w_s1=min(w_s,w_sb) %minimum

Rb1=cos((LT-beta)*P).*cos(DELTA*P).*sin(w_s1*P)

Rb2=(pi/180).*w_s1*sin((LT-beta)*P).*sin(DELTA*P)

Rb3=cos(LT*P).*cos(DELTA*P).*sin(w_s*P)

Rb4=(pi/180)*w_s.*sin(LT*P).*sin(DELTA*P)

Rb=(Rb1+Rb2)./(Rb3+Rb4)

 e6

Hd=H-Hb

HT1=H.*(1-(Hd./H)).*Rb+Hd*(1+cos(P*beta))/2

HT2=H.*0.2*(1-cos(P*beta))/2

HT=HT1+HT2
```

Monthly Average Absorbed Radiation

H_b=[18.4258 19.8700 21.4865 19.9061 12.50052 12.2875 10.8131 8.4917 11.3271 14.8025 17.2977 17.1816]'*1e6
H=[22.6584 24.8544 27.0252 28.2096 18.0144 23.6448 18.125 16.0956 24.3108 22.2516 21.5352 22.2371]'*1e6
H_d=H-H_b

beta=11.2 %collector tilt angle

n_d=1.51

A_B=0.98%plate absorbtance

R_g=0.2 %ground reflectance

KL=0.0736 %glass extinction coefficient and length product

Q= [43 41 37.5 38.9 41.2 43.0 42.5 39.5 37.5 39.5 41 43]

n=[17 47 75 105 135 162 198 228 258 288 318 344]

N=1

P=pi/180

m_b=sin(P*Q)

Qr =asin(m_b/ n_d)*(1/P)

R_1=(sin(P*(Qr-Q))).^2./(sin(P*(Q_r+Q))).^2

R_2=(tan(P*(Qr-Q))).^2./(tan(P*(Q_r+Q))).^2

R=(R_1+R_2)/2

T_{R1}=(1- R_2)./(1+(2*N-1)* R_2)

T_{R2}=(1- R_1)./(1+(2*N-1)* R_1)

T_R=(TR_1+ TR_2)/2

T_{Ab}=exp (-N*KL./cos (P*Qr))

T= T_R.*T_{Ab}

TR_B=T*A_B/ (1-(1- A_B)* R_g)

Q_d=59.7-0.1388*beta+0.001479*beta^2 % incident angle of diffuse radiation

$m_d=\sin(P*Q_d)$

$Q_{rd}=\text{asin}(m_d/ n_d)*(1/P)$

$R_{1d}= (\sin(P*(Q_{rd}-Q_d))).\hat{}2. / (\sin(P*(Q_{rd}+Q_d))).\hat{}2$

$R_{2d}= (\tan(P*(Q_{rd}-Q_d))) .\hat{}2 ./ (\tan(P*(Q_{rd}+Q_d))).\hat{}2$

$R_d= (R_{1d}+R_{2d})/2$

$T_{R1d}= (1- R_{2d})./(1+ (2*N-1)* R_{2d})$

$T_{R2d}= (1- R_{1d})./(1+ (2*N-1)* R_{1d})$

$T_{Rd}=(TR_{1d}+ TR_{2d})/2$

$T_{AD}=\exp(-N*KL./\cos(P*Qr))$

$T= T_{Rd.}*T_{AD}$

$TR_d=T*A_B/(1-(1- A_B)* R_g)$

$Q_g=90-0.5788*beta+0.002693*beta\hat{}2$ % incident angle of reflected radiation

$M_g=\sin(P*Q_g)$

$Q_{rg} =\text{asin}(M_g/ n_d)*(1/P)$

$R_{1g}=(\sin(P*(Q_{rg}-Q_g))).\hat{}2./(\sin(P*(Q_{rg}+Q_g))).\hat{}2$

$R_{2g}=(\tan(P*(Q_{rg}-Q_g))).\hat{}2./(\tan(P*(Q_{rg}+Q_g))).\hat{}2$

$R_g=(R_{1g}+R_{2g})/2$

$T_{R1g}=(1- R_{2g})./(1+(2*N-1)* R_{2g})$

$T_{R2g}=(1- R_{1g})./(1+(2*N-1)* R_{1g})$

$T_{rg}=(TR_{1g}+ TR_{2g})/2$

$T_{Ag}=\exp(-N*KL./\cos(P*Q_{rg}))$

$T_g= T_{rg}*T_{Ag}$

$TR_g=T_g*A_B./(1-(1- A_B)* R_g)$

$S_{R1}=H_b.*R_b.*TR_B$

$S_{R2}=H_d* TR_d *(1+\cos(P*beta))/2$

S_{R3}=H.*R_g* TR_g *(1-cos(P*beta))/2

S_R=S_{R1}+S_{R2}+S_{R3}

Calculation of extra terrestrial radiation

Gsc=1367 % solar constant

P=pi/180

n=[17 47 75 105 135 162 198 228 258 288 318 344]' %recommended days of the months

LT=11.2 % latitude of location(Zaria)

DELTA=23.45*sin(2*pi*((n+284)/365))%formula for monthly declination

w_s=(acos(-tan(LT*P)*tan(DELTA*P)))*1/P %monthly sunset angle

A_1=86400*Gsc/pi;

A_2=(1+0.033*cos(360*n*P/365));

A_3=cos(LT*P).*cos(DELTA*P).*sin(P*w_s)+(pi.*w_s*sin(P*LT).*sin(P*DELTA)/180);

Ho=A_1.*A_2.*A_3

Calculation of clearness index

H=[22.6584 24.8544 27.0252 28.2096 18.0144 23.6448 18.125 16.0956 24.3108 22.2516 21.5352 22.2371]'*1e6

K_T= H./H_o

APPENDIX B
SOLAR WATER HEATER COLLECTOR DESIGN PROGRAMME CODES DEVELOPED USING MATLAB

E_p=0.96 %plate emmittance

E_g=0.88 %glass emmittance

N=1 %number of coverglass

B=11.2% collector tilt angle

zegma=5.67e-8 %Boltzman constant
vol = 0.12 %volume of water
density =1000 % density of water
Cp=4190 %specific heat of water
TL=60
K_b=0.04 %thermal conductivity of back insulation mat.
T_b=0.005 %back insulation thickness
SR =12.5
V=[2.6 2.57 2.70 2.31 2.8 3.5 2.91 3.08 1.56 2.57 3.39 2.0]'

Tmax=[38 38 40 32 35 32 26 28 32 36 35 33]'

Tmin=[16 16 20 15 22 29 18 18 20 20 18 17]'

Ta=Tmax
Ta_1=Ta+273
Tpm=Tmax+25
Tpm_1=Tpm+273
hw=2.8+3*V
f=(1+0.089*hw-0.1166.*hw*E_p)*(1+0.07866*N)
C=520*(1-0.000051*B^2)
e=0.430*(1-(100./Tpm_1))
U_{top}1= ((C./Tpm_1).*((Tpm_1-Ta_1)./(N+f)).^e)+1./hw

Ut_{op2}= (N./U_{top1}).^-1+ zegma*(Ta1.^2+Tpm1.^2).*(Ta_1+Tpm_1)

U_{top3}=(1./(Ep+0.00591*N*hw))+((2*N+f-1+0.133*Ep)/Eg)-N
U_{top}=U_{top2}./U_{top3}
U_{back}= K_b/T_b
U_{total}= U_{top}+ U_{back}
mass=density*vol

Qs=mass*Cp*(T_L-Ta)

Qc_loss=U_{total}*12*3600.*(Tpm-Ta)

Qu=SR-U_{tota}l.*12*3600.*(Tpm-Ta)

Ac=(Qs./Qu)

APPENDIX C

REMOVAL FRACTION DESIGN PROGRAMME CODES DEVELOPED USING MATLAB

Di=20/1000 %internal. dia. of collector tube
W=50/1000 %center to center distance of tubes
U_{total} =7.4
Delta_p=5/1000 %plate thickness

Kp=211 %thermal conductivity of plate

m=0.34
C_p=4190
T_{max}=[38 38 40 32 35 32 26 28 32 36 35 33]'
$T_{fm}=T_{max}$
L=2000/1000 %length of collector
density=1001-0.08832*T_{fm}-0.003417*T_{fm}.^2

K_V=((1./(0.5155+0.0192*T_{fm}))-0.12)*1e-6 %kinematic viscocity

K_f=0.557+0.002198*T_{fm}-0.00000708*Tf_m.^2% fluid thermal conductivity

D_V=density.*K_V %dynamic viscocity

Pr=C_p*D_V./K_f

m_o=200/(12*3600)

Re=4*m_o./(pi*D_i*D_V)

if Re>2100

fn=(1.82.*log10(Re)-1.64).^(-2)

K_1=1+1.3*fn

Pr_1=Pr.^0.333
K_2=11.7+(1.8./Pr_1)

N_{uD1}=(fn./8).*Re.*Pr

N_{uD2}=K_1+K_2.*(fn/8).^(1/2).*(Pr.^(2/3)-1)

N_{uD}=N_{uD1}./N_{uD2} %nusset number

Else if Re<2100

N_{uD1}=0.0534*((Re.*Pr.* D_i)./L).^1.15

N_{uD2}=1+0.0335*((Re.*Pr.*D_i)./L).^0.82

$N_{uD}=3.7+(N_{uD1}./N_{uD2})$

Else

$N_{uD}=0$

$h_{fi}=(K_f.*N_{uD})./Di$

$m=((U_{total}./(K_p*Delta_p))).^{0.5}$

$F=\tanh(m*(W-D_i)/2)/(m*(W-D_i)/2)$

$F_{prime1}=1./U_{total}$

$F_{prime2}=W.*(1./((U_{total}.*(D_i+(W-D_i).*F))+1./(pi.*D_i*\ h_{fi}\ )))$

$F_{prime}=F_{prime1}./F_{prime2}$

$F_{R1}=(m_o.*C_p)./(A_c.*U_{total}\ )$

$F_{R2}=\exp(-(A_c.*\ U_{total}.*F_{prime}).(m_o.*C_p))$

$F_R=F_{R1}.*(1-F_{R2})$ % heat removal factor

APPENDIX D

CALCULATION DAILY TANK LOST COEFFICIENT DESIGN PROGRAMME CODES DEVELOPED USING MATLAB

T_{ins_t}=50/1000 % tank insulation thickness

D_T=42/100 %tank diameter.
h=1.2 %height of tank

d=420/1000 %diameter of tank

D_o=25/1000 %ext. dia. of collector tube

vol=0.13 %volume of water

V=[2.6 2.57 2.70 2.31 2.8 3.5 2.91 3.08 1.56 2.57 3.39 2.0]'

hw=2.8+3*V

Kt_{ins}=0.04

A_{st}=1.845*(2+h/D_T)* vol^(2/3)%surface area of tank
U_{T1}=(1/(2*pi*Kt_{ins}))*log(1+2*T_{ins_t}/D_o)
U_{T2}=1./pi*(D_T+2*T_{ins_t}).*hw
U_{st}=(1./(U_{T1}+U_{T2})) % daily tank lost coefficient

APPENDIX E

TILT ANGLE OPTIMISATION DESIGN PROGRAMME CODES DEVELOPED USING MATLAB

```
Gsc=1367
LT=11.2
%recomended days of the months
n1=[228]' % recommended Average day of the year
fori=1:length(n1)
beta=0:2:90
P=pi/180 %factor for the conversion from radian to degree.
DELTA=23.45*sin(2*pi*((n1(i)+284)/365)) %formula for monthly declination
w_s=(acos(-tan(LT*P).*tan(DELTA*P)))*1/P %monthly sunset angle
w_sb=(acos(-tan((LT+beta)*P).*tan(DELTA*P)))*1/P
w_s1=min(w_s,w_sb) %minimum of line 8 and 9.
A1=86400*Gsc/pi;
A2=(1+0.033*cos(360*n1(i)*P/365));
A3=cos(LT*P).*cos(DELTA*P).*sin(P*w_s)+(pi.*w_s*sin(P*LT).*sin(P*DELTA)/180);
Ho=A1.*A2.*A3 %annual average extraterestrial solar radiation of location
H=[22.6584]*1e6 %annual average solar radiation of location
KT= H./Ho
g=0
Hd1=0.775+0.00606*(w_s-90)
Hd2=(0.505+0.0045*(w_s-90)).*cos((115*KT-103)*P)
Hd=(Hd1-Hd2).*H
Hb=H-Hd
Rb1=cos((LT+beta)*P).*cos(DELTA*P).*sin(w_s1*P)
Rb2=(pi/180)*w_s1.*sin((LT+beta)*P)*sin(DELTA*P)
Rb3=cos(LT*P)*cos(DELTA*P)*sin(w_s*P)
Rb4=(pi/180)*w_s*sin(LT*P)*sin(DELTA*P)
Rb=(Rb1+Rb2)/(Rb3+Rb4)
HT1=(H.*(1-(Hd./H)).*Rb+Hd.*(1+cos(P.*beta))/2)'
HT2=(H.*0.2.*(1-cos(P*beta))/2)'
HT=(HT1+HT2)'
plot(beta,HT,'linewidth',2)
xlabel('Collector tilt angle (Degree)','fontsize',12)
ylabel('Solar Radiation on collector surface(J/m2.day)','fontsize',12)
title('Variation of Solar radiation on collector surface','fontsize',12)
hold on
end
hold off
```

APPENDIX F

OPTIMISATION OF COLLECTOR TUBE DIAMETER AND TUBE CENTRE TO CENTRE DISTANCE. DESIGN PROGRAMME CODES DEVELOPED USING MATLAB

```
Ti=28
Ta=28
S_R=12.481
H_T=15.611
Cp=4190  %specific heat of water
k_p=211
u_L=7.938
delta_p=0.004
 Di=[0.5/100:0.5/100:5/100]'
H_fi=151.8872
mdot=0.0035
 AC=(1.8)
fori=1:length(Di)
 W=(5/100:5/100:200/100)'
 m1=((u_L./(k_p*delta_p))).^0.5
 f1=(tanh(m1*(W-Di(i))/2)./(m1.*(W-Di(i))/2))
 f_prime1=1./u_L
 f_prime2=(W.*(1./((u_L.*(Di(i)+f1).*(W-Di(i)))+1./(pi.*Di(i).* H_fi ))))
f_prime=f_prime1./f_prime2
f_R1=(mdot.*Cp)./(AC.*u_L )
f_R2=(exp(-(AC.* u_L.*f_prime)./(mdot.*Cp)))
f_R=(f_R1.*(1-f_R2))
eff1=u_L*(Ti-Ta)
eff2= S_R -eff1
eff3=f_R*eff2
eff= eff3/H_T
plot(W,eff,'r','linewidth',2)
xlabel('Center to centre distance of collector tubes (M)')
ylabel('Efficiency')
title('Variation of Efficiency')
hold on
end
g=0
```

APPENDIX G

OPTIMISATION OF ABSORBER PLATE THICKNESS DESIGN PROGRAMME CODES DEVELOPED USING MATLAB

```
Ti=28
Ta=28
S_R=12.2
H_T=15.225
Cp=4190
k_p=211
u_L=7.4
  Di=0.5/100
H_fi=113.13
mdot=0.0035
AC=(1.8)
delta_p=(5/1000:5/1000:40/1000)'
fori=1:length(delta_p)
 W=(5/1000:5/1000:20/1000)'
 m1=((u_L./(k_p*delta_p(i)))).^0.5
 f1=(tanh(m1*(W-Di)/2)./(m1.*(W-Di)/2))
 f_prime1=1./u_L
 f_prime2=(W.*(1./((u_L.*(Di+f1).*(W-Di))+1./(pi.*Di.* H_fi ))))
f_prime=f_prime1./f_prime2
f_R1=(mdot.*Cp)./(AC.*u_L )
f_R2=(exp(-(AC.* u_L.*f_prime)./(mdot.*Cp)))
f_R=(f_R1.*(1-f_R2))
eff1=u_L*(Ti-Ta)
eff2= S_R -eff1
eff3=f_R*eff2
eff= eff3/H_T
plot(W,eff,'linewidth',2)
xlabel(' Absorber Plate Thickness(m)')
ylabel('Thermal efficiency')
title('Variation of efficiency')
hold on
end
```

APPENDIX H

OPTIMISATION OF NUMBER OF GLASS COVERS DESIGN PROGRAMME CODES DEVELOPED USING MATLAB

```
Ti=28
Ta=28
 u_L=7.4
 S_R=12.2
 H_T=15.225
 % det of optimum number of glass
 Eg=0.88  %glass emmittance
 K_p=211   %thermal conductivity of plate
 Delta_p=5/1000 %plate thickness
 Cp=4190  %specific heat of water
 Kb=0.04 %thermal conductivity of back insulation mat.
 tb=50/1000 %back insulation thickness
 Ke=0.04  %thermal conductivity of edge insulation mat
 t_e=40/1000%edge thickness
 k_p=211
 Di=1.5/100
 hfi5=113.13
 mdot=0.0035
 AC=(1.8)
 Ae5=0.511
 abst=0.90
 rho_g=0.2
 beta5=11.2
 hw5=10.4
 V5=2.4
 Tpm5=70+273
 Ta5=311
 Ep=0.95
 zegma=5.67e-8
 W=10/100
 Ng=(0:1:10)'
 f5=(1+0.089*hw5-0.1166*hw5*Ep )*(1+0.07866*Ng)
 C =520*(1-0.000051*beta5^2)
 e=0.430*(1-100/Tpm5)
 U_top51=((C./Tpm5).*((Tpm5-Ta5)./(Ng+f5)).^e)+1./hw5
 U_top52=(Ng./U_top51).^-1
 U_top53=zegma*(Ta5.^2+Tpm5.^2).*(Ta5+Tpm5)
 U_top5=(1./(Ep+0.00591*Ng*hw5))+((2*Ng+f5-1+0.133*Ep)/Eg)-Ng
 U_topp=U_top52+U_top53./U_top5
 U_back=Kb/tb
 U_e5=Ke*Ae5./(t_e*AC)
 U_L5=U_topp+U_e5+U_back
 m5=((U_L5./(K_p*Delta_p))).^0.5
 F5=tanh(m5.*(W-Di)./2)./(m5.*(W-Di)./2) %fin efficiency
 F_prime51=1./U_L5
```

```
F_prime52=W.*(1./((U_L5.*(Di+(W-Di).*F5))+1./(pi.*Di* hfi5 )))
F_prime5=F_prime51./F_prime52
F_R51=(mdot.*Cp)./(AC.*U_L5 )
F_R52=exp(-(AC.* U_L5.*F_prime5)./(mdot.*Cp))
F_R5=F_R51.*(1-F_R52) % heat removal factor
eff1=u_L*(Ti-Ta)
eff2= S_R -eff1
eff3=F_R5*eff2
eff= eff3/H_T
plot(Ng,eff,'linewidth',3)
xlabel('Number of glazing Ng','fontsize',18)
ylabel('Thermal Efficiency','fontsize',18)
g=0
```

APPENDIX I

```
Ta=[38 38 40 32 35 32 26 28 32 36 35 33]'

 Ti=[38 38 40 32 35 32 26 28 32 36 35 33]'


Temp=(0/10/100)'
 Tem=Ta-Ti

 S_R=12.2

 delta_p=5/1000 %plate thickness
W=10/100

Di=1.5/100

H_T=15.225
Cp=4190
k_p=211
u_L=7.4
H_fi=113.13
mdot=0.0035
 AC=(2.6)
m1=((u_L./(k_p*delta_p))).^0.5
 f1=(tanh(m1*(W-Di)/2)./(m1.*(W-Di)/2))
 f_prime1=1./u_L
 f_prime2=(W.*(1./((u_L.*(Di+f1).*(W-Di))+1./(pi.*Di.* H_fi ))))
f_prime=f_prime1./f_prime2
f_R1=(mdot.*Cp)./(AC.*u_L )
f_R2=(exp(-(AC.* u_L.*f_prime)./(mdot.*Cp)))
f_R=(f_R1.*(1-f_R2))
eff1=u_L*Tem
eff2= S_R -eff1
eff3=f_R*eff2
eff= eff3/H_T
plot(Tem,eff,'linewidth',2)
xlabel(' Temperature (C^o)')
ylabel('Thermal efficiency')
title('Variation of efficiency')
hold on
```

APPENDIX J

PHOTOGRAPHS OF CONSTRUCTION AND THE ASSEMBLY OF THE SYSTEM COMPONENTS



Plate 1:Construction and Insulation of the Hot water Tank



Plate 2: Constructed Solar Water Tank



Plate 3: Coupling of Solar Collector Frame



Plate 4: Insulating the Solar Collector



Plate 5: Assembling the Solar Collector



Plate 6: Fitting the component of the Solar Collector.



Plate 7: Assembling the Solar Collector Stand at an Angle of the Location



Plate 8: Assembling the Complete Solar Water heating system



Plate 9: Side View of the Solar Water Heating System



Plate 10: Glazing The Solar Water heater



Plate 11: Connecting the Solar Water Heater to the University Water Supply



Plate 12: Connecting the Solar water heater to the bathrooms of the block of Sassakawa Postgraduate Hostel



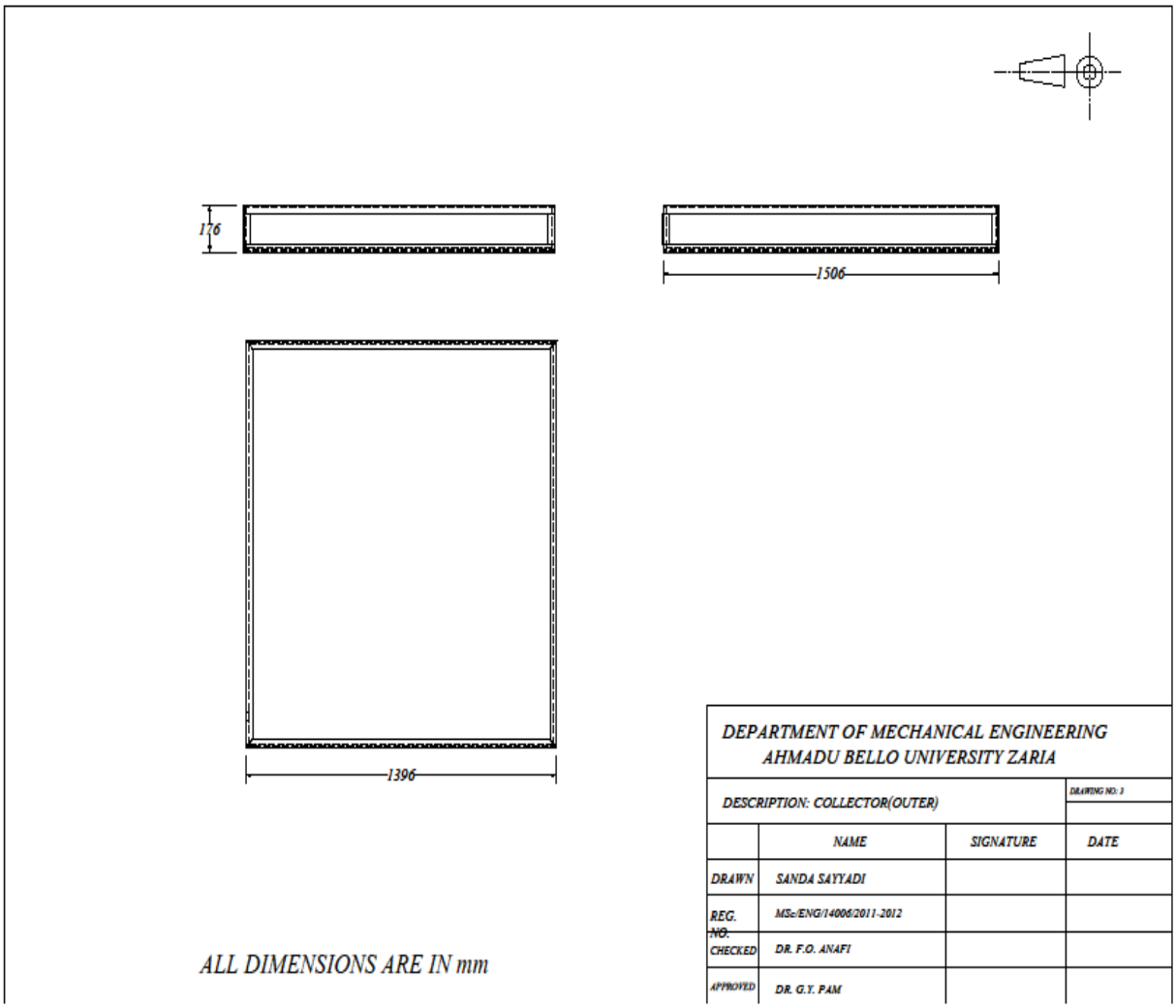
Plate 13 Side View of the Solar system from down

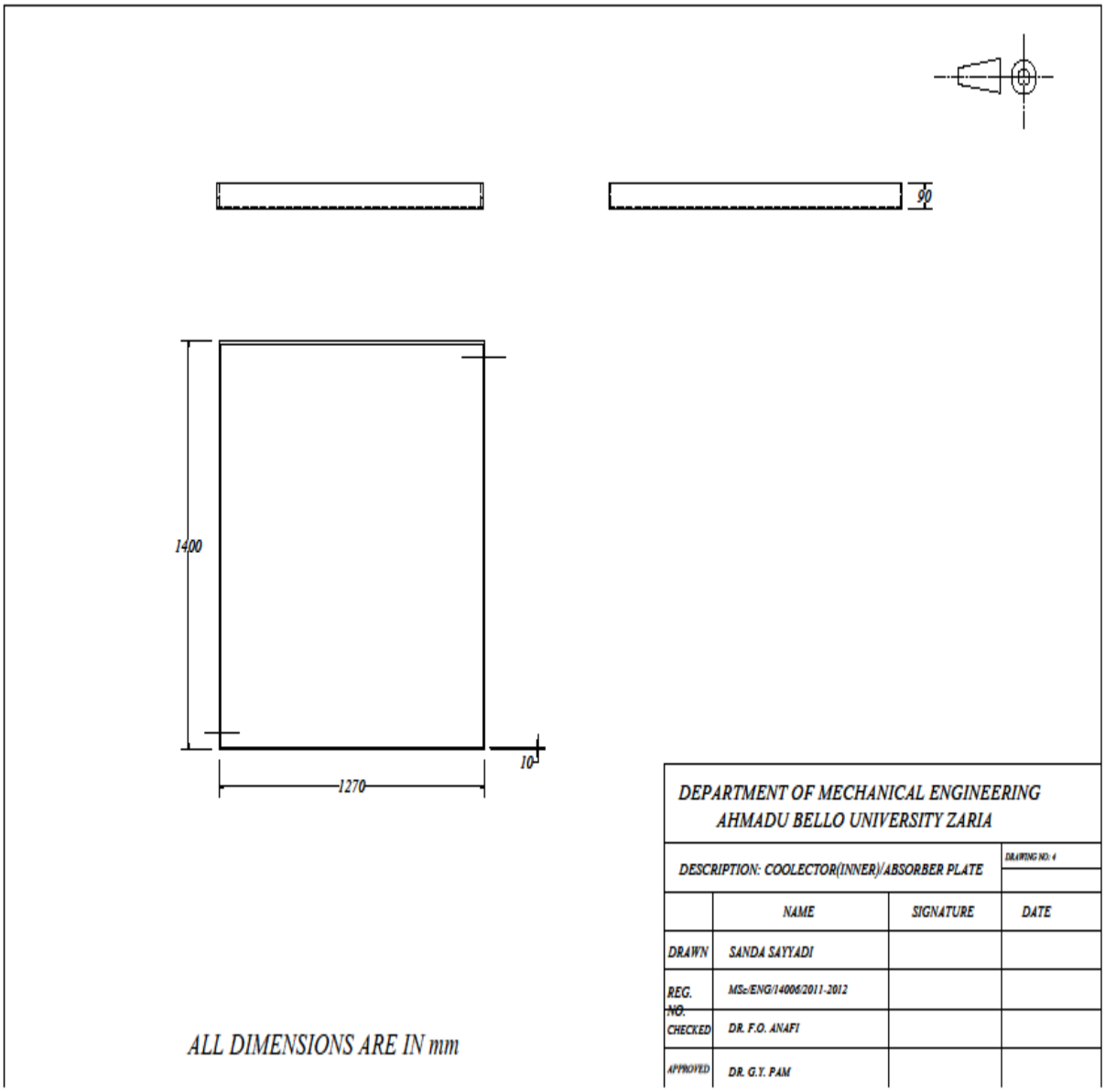


Plate14: Side View of the Postgraduate Hostel

APPENDIX K

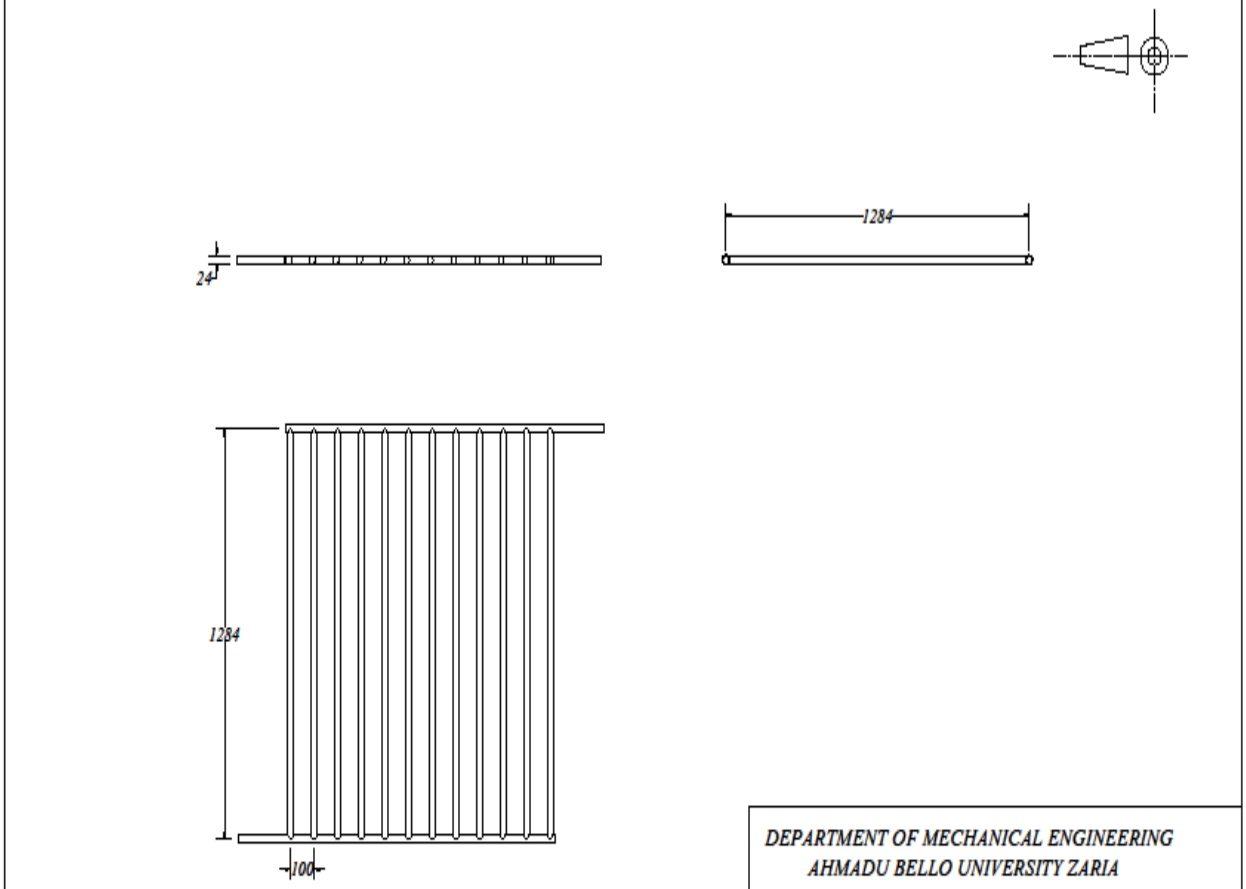
THE ASSEMBLY AND WORKING DRAWINGS OF SOLAR WATER HEATER





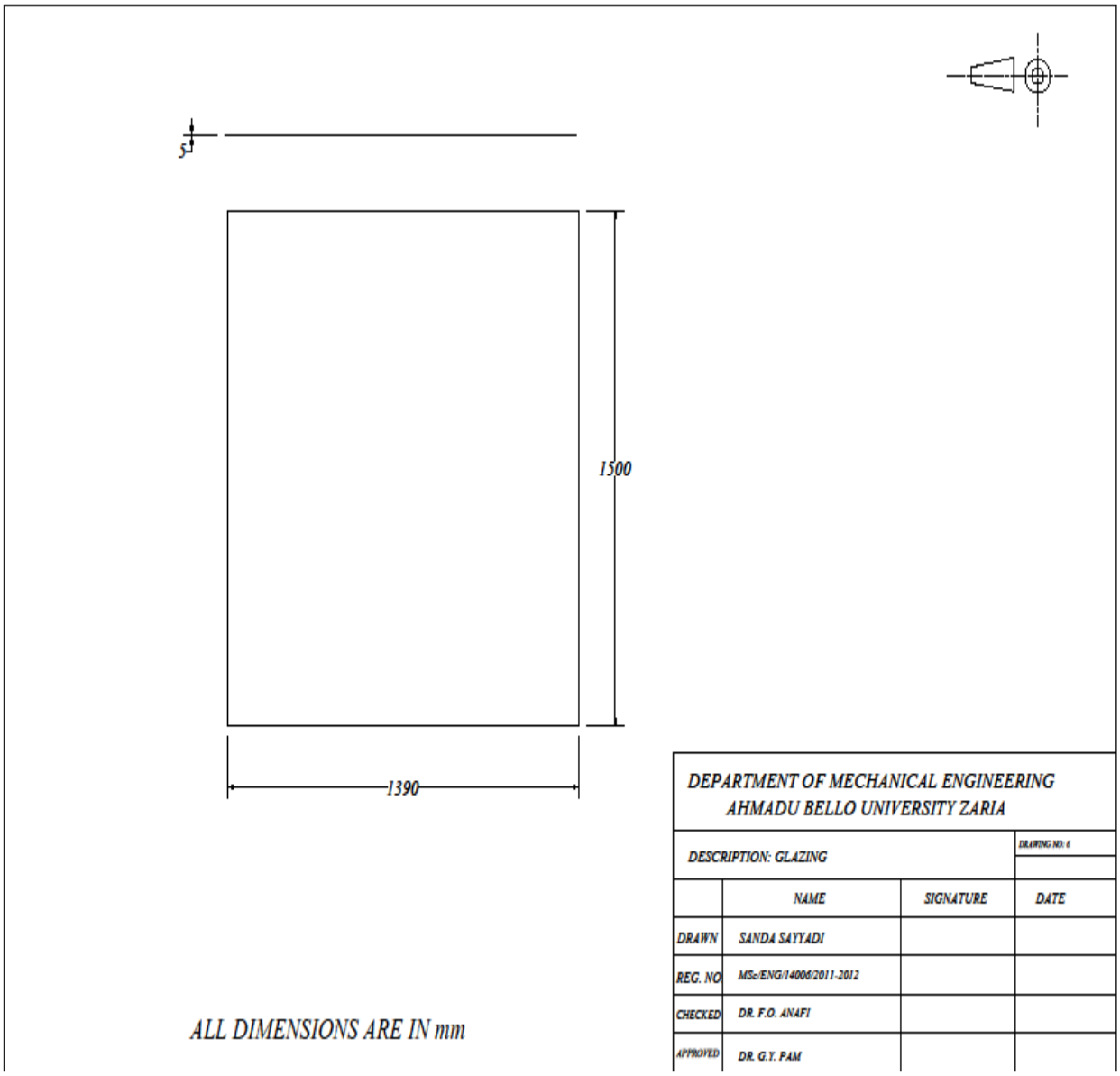
ALL DIMENSIONS ARE IN mm

DEPARTMENT OF MECHANICAL ENGINEERING AHMADU BELLO UNIVERSITY ZARIA			
DESCRIPTION: COOLECTOR(INNER)/ABSORBER PLATE			DRAWING NO: 4
	NAME	SIGNATURE	DATE
DRAWN	SANDA SAYYADI		
REG. NO.	MSc/ENG/14006/2011-2012		
CHECKED	DR. F.O. ANAFI		
APPROVED	DR. G.Y. PAM		



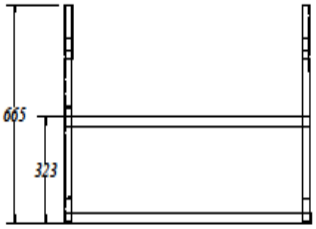
ALL DIMENSIONS ARE IN mm

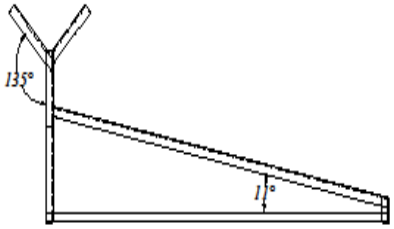
DEPARTMENT OF MECHANICAL ENGINEERING AHMADU BELLO UNIVERSITY ZARIA			
DESCRIPTION: COPPER PIPES			DRAWING NO: 5
	NAME	SIGNATURE	DATE
DRAWN	SANDA SAYYADI		
REG. NO.	MSc/ENG/14006/2011-2012		
CHECKED	DR. F.O. ANAFI		
APPROVED	DR. G.Y. PAM		

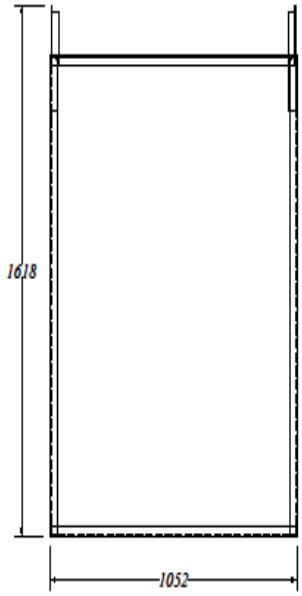


ALL DIMENSIONS ARE IN mm

DEPARTMENT OF MECHANICAL ENGINEERING AHMADU BELLO UNIVERSITY ZARIA			
DESCRIPTION: GLAZING			DRAWING NO: 6
	NAME	SIGNATURE	DATE
DRAWN	SANDA SAYYADI		
REG. NO	MSc/ENG/14006/2011-2012		
CHECKED	DR. F.O. ANAFI		
APPROVED	DR. G.Y. PAM		





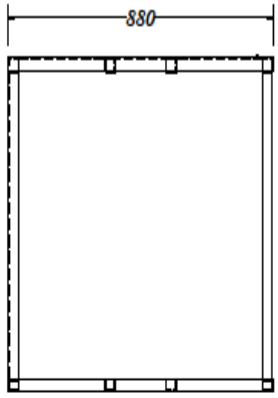


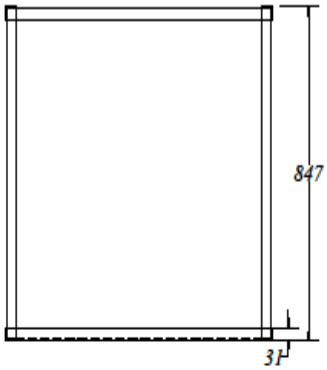
ALL DIMENSIONS ARE IN mm

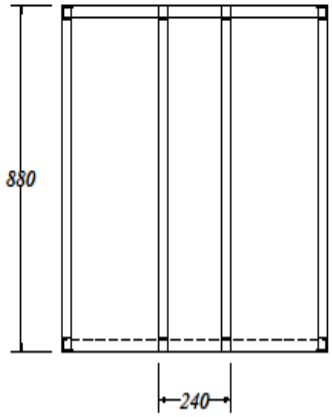
DEPARTMENT OF MECHANICAL ENGINEERING
AHMADU BELLO UNIVERSITY ZARIA

DESCRIPTION: HOT WATER TANK/COLLECTOR STAND — DRAWING NO: 10

	NAME	SIGNATURE	DATE
DRAWN	SANDA SAYYADI		
REG. NO.	MSc/ENG/14006/2011-2012		
CHECKED	DR. F.O. ANAFI		
APPROVED	DR. G.Y. PAM		

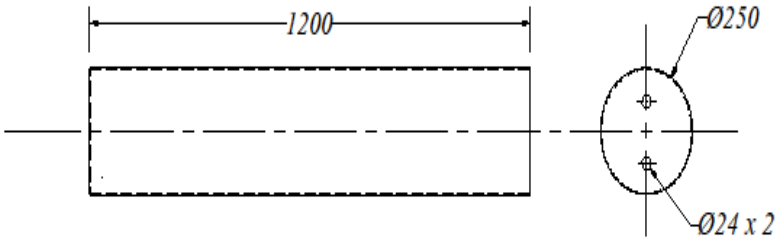






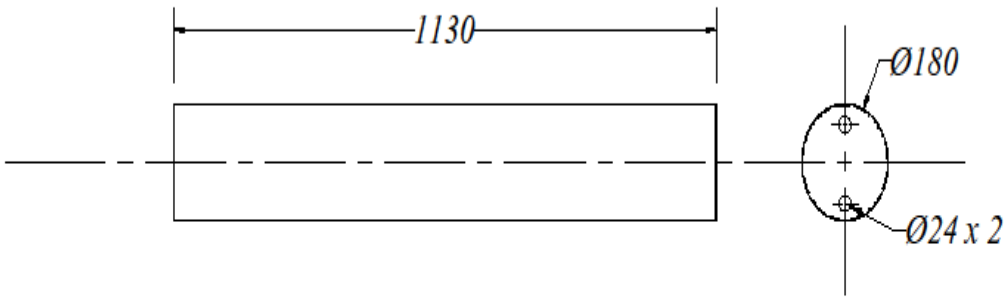
ALL DIMENSIONS ARE IN mm

DEPARTMENT OF MECHANICAL ENGINEERING AHMADU BELLO UNIVERSITY ZARIA			
DESCRIPTION: COLD WATER TANK STAND			DRAWING NO: 9
	NAME	SIGNATURE	DATE
DRAWN	SANDA SAYYADI		
REG. NO	MSc/ENG/14006/2011-2012		
CHECKED	DR. F.O. ANAFI		
APPROVED	DR. G.Y. PAM		



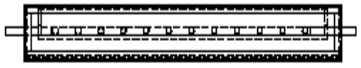
ALL DIMENSIONS ARE IN mm

DEPARTMENT OF MECHANICAL ENGINEERING AHMADU BELLO UNIVERSITY ZARIA			
DESCRIPTION: HOT WATER TANK(OUTER)			DRAWING NO: 7
	NAME	SIGNATURE	DATE
DRAWN	SANDA SAYYADI		
REG. NO	MSc/ENG/14006/2011-2012		
CHECKED	DR. F.O. ANAFI		
APPROVED	DR. G.Y. PAM		

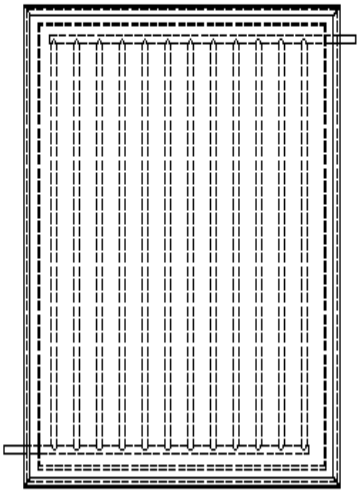


ALL DIMENSIONS ARE IN mm

DEPARTMENT OF MECHANICAL ENGINEERING AHMADU BELLO UNIVERSITY ZARIA			
DESCRIPTION: HOT WATER TANK(INNER)			DRAWING NO: 1
	NAME	SIGNATURE	DATE
DRAWN	SANDA SAYYADI		
REG. NO	MSc/ENG/14006/2011-2012		
CHECKED	DR. F.O. ANAFI		
APPROVED	DR. G.Y. PAM		

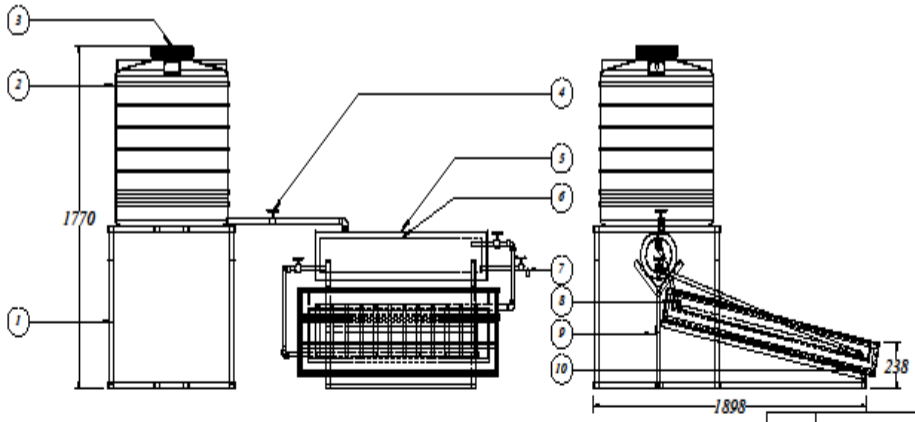


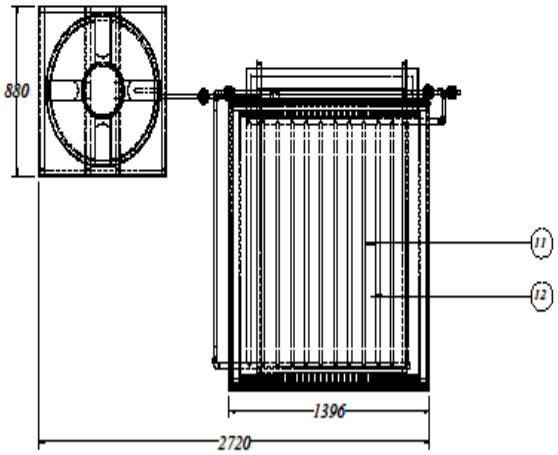




ALL DIMENSIONS ARE IN mm

DEPARTMENT OF MECHANICAL ENGINEERING AHMADU BELLO UNIVERSITY ZARIA			
DESCRIPTION: COLLECTOR SUB-ASSEMBLY			DRAWING NO: 2
	NAME	SIGNATURE	DATE
DRAWN	SANDA SAYYADI		
REG. NO.	MSc/ENG/14006/2011-2012		
CHECKED	DR. F.O. ANAFI		
APPROVED	DR. G.Y. PAM		





ALL DIMENSIONS ARE IN mm

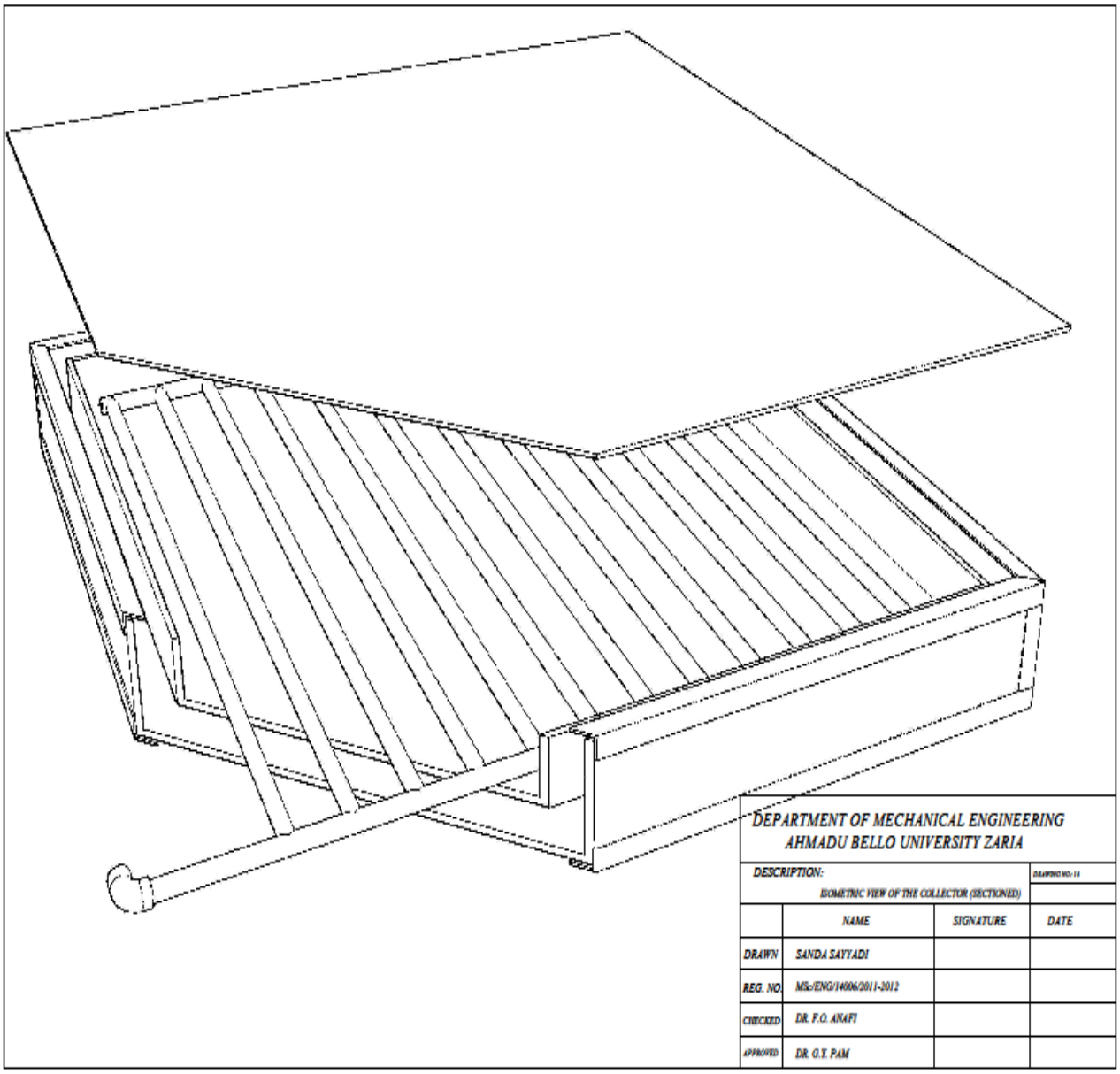
S/N	COMPONENT	QTY	MATERIAL	REMARK
12	GLAZING	1	GLASS	FABRICATED
11	COPPER PIPES	14	COPPER	FABRICATED
10	COLLECTOR CASING(OUTER)	1	WOOD/MILD STEEL	FABRICATED
9	COLLECTOR/TANK STAND	1	MILD STEEL	FABRICATED
8	COLLECTOR CASING(INNER)/ ABSORBER PLATE	5	WOOD/ALUMINUM	FABRICATED
7	WATER COLLECTION TAP	1	PLASTIC	STANDARD
6	HOT WATER TANK(INNER)	1	PLASTIC	FABRICATED
5	HOT WATER TANK(OUTER)	1	PLASTIC	FABRICATED
4	VALVE	3	PLASTIC	STANDARD
3	TANK LID	1	PLASTIC	STANDARD
2	COLD WATER TANK	1	PLASTIC	STANDARD
1	COLD WATER TANK STAND	1	STEEL	FABRICATED

DEPARTMENT OF MECHANICAL ENGINEERING
AHMADU BELLO UNIVERSITY ZARIA

DESCRIPTION:
ASSEMBLY VIEW OF THE THERMOSYPHON WATER HEATER

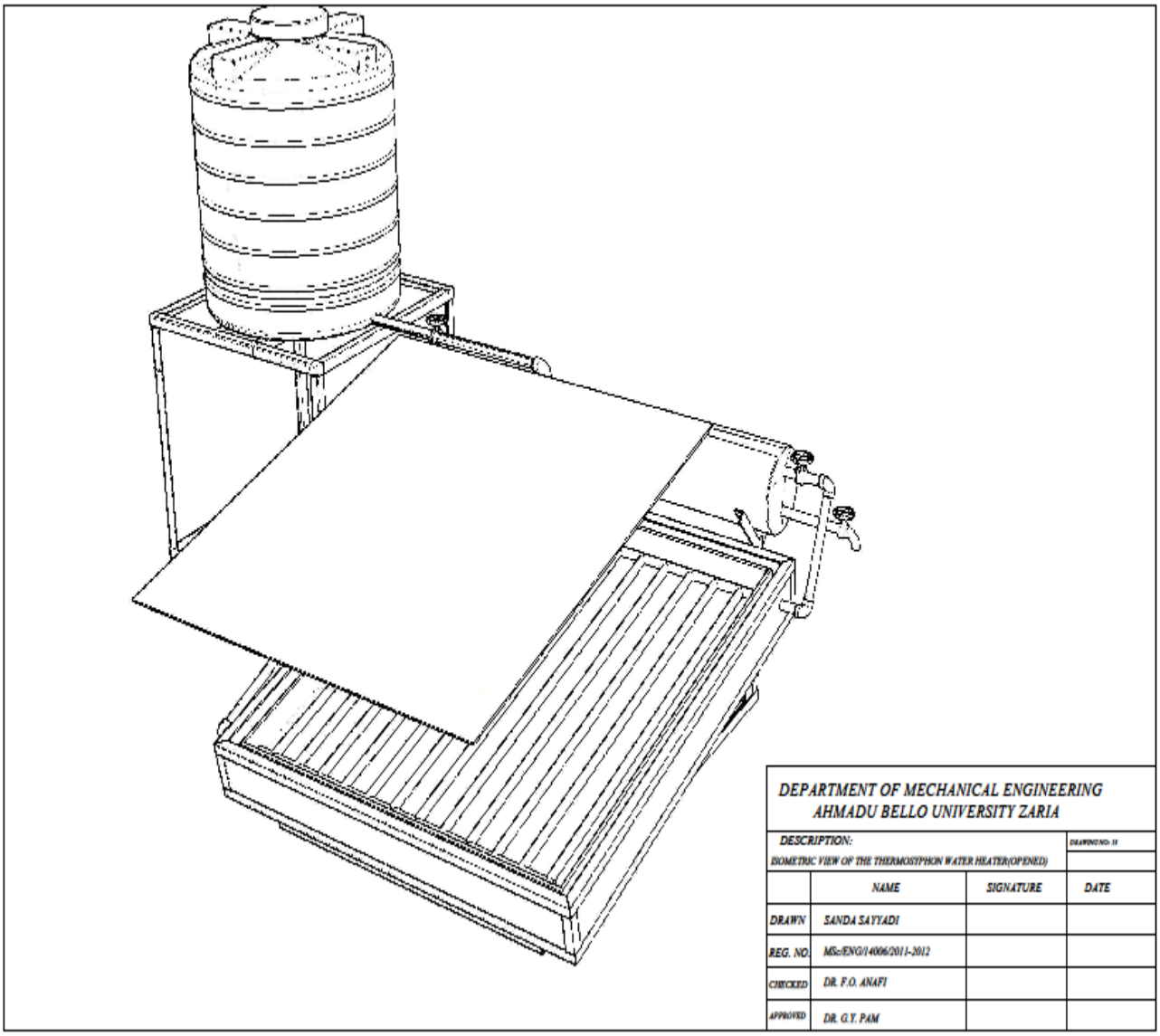
DRAWING NO: 1

	NAME	SIGNATURE	DATE
DRAWN	SANDA SAYYADI		
REG. NO.	MSc/ENG/14006/2011-2012		
CHECKED	DR. F.O. ANAFI		
APPROVED	DR. G.Y. PAM		



DEPARTMENT OF MECHANICAL ENGINEERING
AHMADU BELLO UNIVERSITY ZARIA

DESCRIPTION: ISOMETRIC VIEW OF THE COLLECTOR (SECTIONED)			DRAWING NO: 14
	NAME	SIGNATURE	DATE
DRAWN	SANDA SAYYADI		
REG. NO.	MSc/ENG/14006/2011-2012		
CHECKED	DR. F.O. ANAFI		
APPROVED	DR. G.T. PAM		

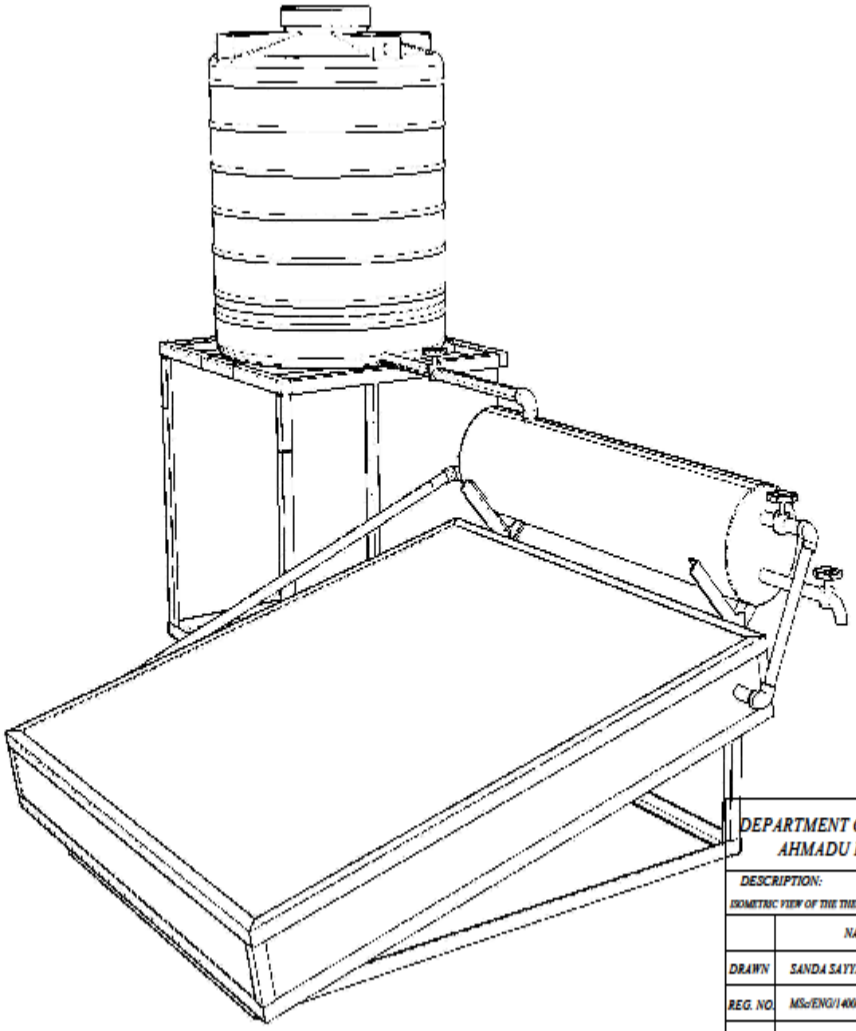


DEPARTMENT OF MECHANICAL ENGINEERING
AHMADU BELLO UNIVERSITY ZARIA

DESCRIPTION:
ISOMETRIC VIEW OF THE THERMOSYPHON WATER HEATER(OPENED)

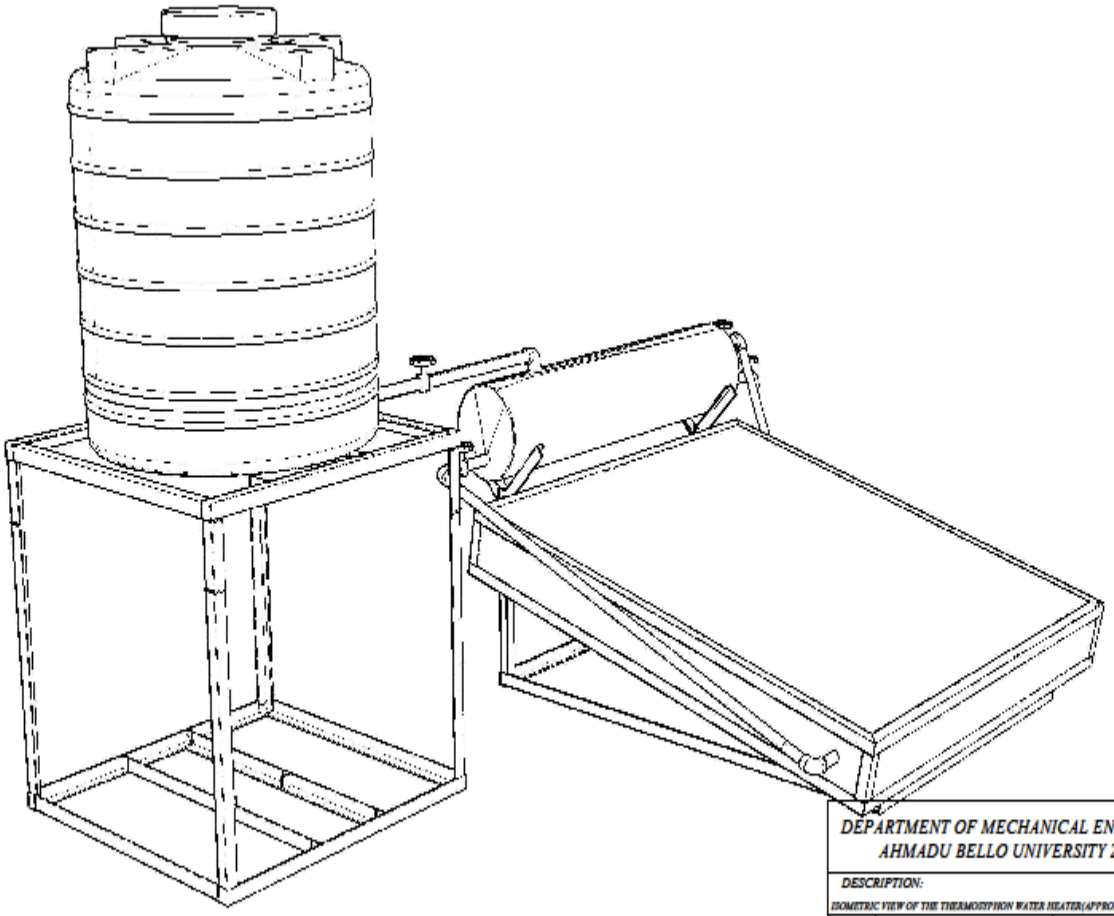
DRAWING NO: 10

	NAME	SIGNATURE	DATE
DRAWN	SANDA SAYYADI		
REG. NO.	MSc/ENG/14006/2011-2012		
CHECKED	DR. F.O. ANAFI		
APPROVED	DR. G.Y. PAM		



DEPARTMENT OF MECHANICAL ENGINEERING
AHMADU BELLO UNIVERSITY ZARIA

DESCRIPTION: ISOMETRIC VIEW OF THE THERMOSYPHON WATER HEATER(ADJACENT VIEW)			DRAWING NO: 12
	NAME	SIGNATURE	DATE
DRAWN	SANDA SAYYADI		
REG. NO.	MSc/ENG/14006/2011-2012		
CHECKED	DR. F.O. ANAFI		
APPROVED	DR. G.Y. PAM		



DEPARTMENT OF MECHANICAL ENGINEERING
AHMADU BELLO UNIVERSITY ZARIA

DESCRIPTION: ISOMETRIC VIEW OF THE THERMOSYPHON WATER HEATER(APPROACH VIEW)			DRAWING NO:-11
	NAME	SIGNATURE	DATE
DRAWN	SANDA SAIYADI		
REG. NO	MSc/ENG/14006/2011-2012		
CHECKED	DR. F.O. ANAFI		
APPROVED	DR. G.Y. PAM		